Estimation of uncertain dynamical systems and related properties. Application to health-monitoring.

Carine Jauberthie

Habilitation à diriger des recherches

présentée devant

l'Université Toulouse 3, Paul Sabatier

par

Carine JAUBERTHIE
Docteur de l'Université de technologie de Compiègne
Maître de conférences à l'UPS

Estimation of uncertain dynamical systems and related properties.
Application to health-monitoring.

préparée au LAAS-CNRS

Soutenue le 18 Octobre 2016 devant le jury composé de :

Rapporteurs :	Abdelatif EL BADIA	Professeur Université de technologie de Compiègne.
	Luc JAULIN	Professeur Université de Bretagne Occidentale.
	Michel KIEFFER	Professeur Université Paris Sud.
Examinateurs :	Michel COMBACAU	Professeur Université Toulouse 3, Paul Sabatier.
	Lilianne DENIS-VIDAL	Maître de Conférences HdR Université de technologie de Compiègne.
	Françoise LE GALL	Chargée de recherche CNRS (LAAS).
	Didier MAQUIN	Professeur Université de Lorraine.
Garant :	Louise TRAVÉ-MASSUYÈS	Directeur de recherche CNRS (LAAS).

Acknowledgments

Les travaux présentés dans ce manuscrit constituent la synthèse de 11 années d'activité au sein du Laboratoire d'Analyse et d'Architecture des Systèmes (LAAS-CNRS). Je tiens donc tout d'abord à remercier Monsieur Malik Ghallab, Directeur du LAAS-CNRS lors de mon recrutement, pour m'avoir accueillie au sein de cet établissement.

Je tiens à remercier Monsieur Didier Maquin d'avoir accepté de présider mon jury de soutenance ainsi que pour les échanges que nous avons eus au cours de la soutenance.
Je remercie Messieurs Abdellatif El Badia, Luc Jaulin et Michel Kieffer d'avoir accepté de rapporter sur ce manuscrit. Je les remercie pour le temps consacré à sa relecture, leurs conseils et propositions d'améliorations.
Je tiens également à remercier Madame Lilianne Denis-Vidal qui fut ma formidable directrice de thèse lilloise durant trois ans, qui m'a toujours soutenue, encouragée et qui a accepté d'examiner mes travaux. Merci à elle de m'avoir donné ce goût pour le métier que je fais et qui me satisfait pleinement!
Mes remerciements vont également à Monsieur Michel Combacau pour avoir accepté d'examiner mon travail. Merci également pour ses encouragements il y a maintenant plusieurs années à poursuivre dans la voie que j'avais choisie.
Mes remerciements vont à Madame Louise Travé-Massuyès, à mes côtés depuis mon recrutement en tant que Maître de Conférences, merci pour tous les moments et échanges que nous avons eus durant ces onze années.
J'exprime ma profonde reconnaissance envers Madame Françoise Le Gall, avec qui je travaille depuis plusieurs années. Je la remercie pour sa relecture soignée du manuscrit, pour ses conseils pleins de bon sens tout au long des moments que nous avons partagés.

Je voudrais également exprimer ma sincère reconnaissance et grande amitié aux collègues universitaires, de différents laboratoires (IRAP, LAAS, Laplace, ...) qui m'ont d'une part très bien accueillie lors de mon arrivée mais également encouragée toutes ces années (pour certains, jusqu'aux derniers instants de préparation de ce manuscrit et soutenance associée : les victimes ne peuvent que se reconnaitre).

Pour finir, je remercie ma famille, mes proches amis pour leur gentillesse, soutien, patience tout au long de ces moments; ils furent pour moi une source d'énergie indispensable.

Contents

List of Figures

Introduction

Providing models representing physical systems is a common concern spread over all scientific and engineering communities. Models are essential to predict the behaviour of systems, or to control them [128]. In my research work, the final aim of modeling concerns diagnosis of physical systems or model-based fault detection. It is known that model-based diagnosis is divided into different axes as for example state or parameter estimation, parity equations or observators. In my work, I consider fault detection and diagnosis relying on state or parameter estimation.

Firstly, fault detection and identification via parameter estimation rely on the principle that possible faults in the monitored system can be associated with specific parameters of the mathematical model of the system given in the form of an input-output relation $y(t) = g(u(t), e(t), \theta, x(t))$, where $y(t)$ represents the output vector, $u(t)$ the input vector and $x(t)$ the state variables which are partially measurable. θ represents the non measurable parameters which are likely to change on the occurrence of a fault and $e(t)$ the modeling error and/or noise term affecting the process. In this approach, parameters of the model are estimated from the input and output measurements of the system. The consistency of this estimation is then checked against parameters computed from a theoretical (possibly faulty) model of the system.

Secondly, fault detection can be based on state estimation (observers or filters) or parity equations. The first method consists in estimating the unknown state variables and the second method consists in eliminating the unknown variables by processing the equations of the model. My research along this line focuses on the second approach in the nonlinear case and the proposed approach is based on the concepts of differential algebra to obtain equations linking inputs, outputs, their derivatives, parameters and faults. These equations are analytical redundancy relations (ARR) and can be used to generate residuals. There are various schemes to formulate residual generation using parity relations. In general, the residual generation filters should be designed to enhance fault isolation so that they exhibit directional or structural properties in response to a particular fault and they also need to maintain robustness to noise, disturbances, or model errors. In [36], the basic concepts of residual generation for both additive and multiplicative faults are developed.

J. Gertler also reviewed the link between the parity relations method and the other two major approaches, observer-based diagnosis and parameter estimation [36].

State and/or parameter estimation problems are usually solved by probabilistic methods [3, 134, 133] when noises and perturbations can be reasonably assumed to be random variables. However, in practice, it is often the case that an explicit characterization of noise and perturbation variables is not available, making difficult to assess proper stochastic hypotheses. An alternative approach consists in assuming that uncertain variable values belong to sets, hence modeling bounded uncertainty. Thus, state and/or parameter estimation problems are now placed into a bounded-error context. Bounded-error approaches permit the characterization of the set of all values of the state/parameter vector that are consistent with the measured data, the model structure and the prior known error bounds. Available methods based on set-membership approaches exist for linear and nonlinear models. Numerous approaches have been investigated for the case of linear models. We can characterize the solution set by a convex polyhedron. But in practice, this set is very difficult to obtain. Thus it may be preferable to compute other geometric shapes, such as for example ellipsoids [33], [65] or zonotopes [40] guaranteed to contain the exact solution set. When the model is nonlinear, the set of values of the state vector to be characterized is usually non convex and may consist of several disconnected components. The previous methods are no longer relevant and other algorithms based on interval analysis have been developed [50].
Actual systems are often described by ordinary differential equations. Interval analysis and an enclosure of the solution of the ordinary differential equation allow to compute guaranteed solutions to the state estimation problem. Then, guaranteed numerical methods for solving the ordinary differential equation are applied. These methods use high-order interval Taylor models [91], [101] to compute intervals which are guaranteed to contain the solution of the ordinary differential equation. More recently a hybrid bounding method based on one of Muller's theorems and a rule based on the signs of some partial derivatives [104] has been developed to compute intervals which are guaranteed to contain the solution of the ordinary differential equation.

Before performing a parameter estimation procedure, it is necessary to analyse identifiability of the model. Identifiability is the property that a mathematical model must satisfy to guarantee an unambiguous mapping between its parameters and the output trajectories. It is of prime importance when parameters are to be estimated from experimental data representing input-output behavior and clearly when parameter estimation is used for fault detection and identification. Surprisingly, the interest for set-membership estimation methods has not been underpinned by investigations about identifiability and only two works can be mentioned. The pioneering paper by [13] outlines that interval based

methods and interval constraint propagation can be used to test for a new definition of global identifiability. In contrast to structural global identifiability [94], the new property no longer allows for the existence of atypical regions in the domain of interest. This is actually a byproduct of using interval methods for testing it. But in this work, what is really an interpretation of identifiability in the set-membership context is only presented as a practical condition. Indeed, instead of imposing parameters corresponding to a given input-output trajectory to be strictly different, they are allowed to be distant by a given ε, which provides a stopping condition to the numerical method. It is only recently that me and co-workers: N. Verdière and L. Travé-Massuyès [46] formalized both the above property and test by introducing two complementary definitions for identifiability of error-bounded uncertain models, namely *set-membership identifiability* and *μ-set-membership identifiability*. The first one is conceptual whereas an instance of the second, called *ε-set-membership identifiability*, can be put in correspondence with interval based parameter estimation methods and the specified stopping condition precision threshold ε.

One of the benefits of set-membership identifiability is that it bypasses standard identifiability and allows one to give (set) estimates of parameters that are unidentifiable in the classical sense. Set-membership identifiability indeed guarantees that there exists a mapping of the parameter space into connected subsets so that every subset can be associated with a distinguishable output behavior. Similarly, before performing a fault diagnosis procedure, it is necessary to analyse diagnosability of the model. In the proposed work, some new definitions of diagnosability are proposed.

Finally, experiment design is important to identify more precisely mathematical models of complex systems. The overall goal is to design an experiment that produces data from which model parameters can be estimated accurately. The conventional approach for experiment design assumes stochastic models for uncertain parameters and measurement errors (see for example [116]). Several criteria for experiment design have been proposed involving a scalar function of the Fisher information matrix. For example the A-optimal experiment minimizes the trace of inverse of the Fisher information matrix, which minimizes, in the linear case, the average variance of the estimates. Another criterion widely used is the D-optimality. The D-optimal experiment minimizes the volume of a confidence ellipsoid. However, some sources of uncertainty are better modeled as bounded uncertainty. This is the case of parameter uncertainties that generally arise from design tolerances and from aging (see for example [124]). Thus in the work I developped with E. Chanthery [44], the optimal input design methodology takes into account some bounded intervals for each parameter to be estimated but uses some statistic information about measurement noise and then an extension of the Fisher matrix has been used.
In a bounded-error context, the experiment design is much less studied and consists in

designing experiments which minimize the estimate parameter volume. In some works such as [100] or [6] for models linear with respect to the input, the worst possible performance of the experiment over the prior domain for the parameters is optimized. In [100], the minimax approach to synthetize the optimal experiment is described, using the Gram matrix of sensitivity functions and specific criteria are developed. These approaches take into account the bounds of the prior domain for the parameters in the search of the optimal experiment but do not take into account the set-membership estimation process which leads to the estimation of a set.
Recently, I with L. Denis-Vidal and Z. Cherfi have shown that the search for an optimal input in nonlinear dynamical systems can be made with the Gram matrix of sensitivity functions in a context of bounded-errors. Prior to this work, we studied the optimization of the initial conditions in the same context but with a different approach [73]. To obtain an explicit expression of the set of parameters to be estimated, the authors in [56] used a centered inclusion function for the model output and they have built an operator involving the parameters to be estimated based on sensitivity functions. Starting from this idea, we build explicitly some criteria to find an optimal experiment in the bounded-error context. In our work, we consider only the optimal input design. The proposed methodology requires a parametrization of the input with a finite number of parameters.

Summarizing, this manuscript deals with identification of bounded error models including the properties of identifiability and diagnosability for such models; fault detection and diagnosis are applications of the presented tools through the manuscript. This document is divided into two parts and it contains seven chapters. The first part is a description of my academic lectures, teachings, supervised projects and contains a detailed curriculum vitae. The second part of the manuscript is devoted to my main research works and reviews some publications that I co-authored like [110, 45, 46, 109, 130, 47, 72]. This part is divided into six chapters. The second chapter concerns the problem formulation and models. In the third chapter, the concepts of identifiability and diagnosability in a set-membership framework are presented. The fourth chapter deals with optimal input design in the bounded error context. In the fifth chapter, some works in the case of mixed uncertainties are proposed. We name "mixed uncertainties" combined stochastic and bounded errors. The sixth chapter concerns the application of the previous tools to diagnosis and fault detection. Finally, the seventh chapter presents perspectives and elaborates my research project for the future.

Part I

Activities synthesis

Chapter 1

Activities synthesis

1.1 Curriculum Vitae

1.1.1 University course

- 2002 : PhD *Université de Technologie de Compiègne* (UTC) in Applied Mathematics, speciality systems control.
  This work was performed at the *Office National d'Etudes et Recherches Aérospatiales* (ONERA) center of Lille, in the Department of *Contrôle des Systèmes et Dynamique du Vol* (DCSD) on the topic: Methodologies of Experiment Design for nonlinear dynamical systems. This work was defended on 19th December 2002 and the committee members were:
  - Mr. Tuong Ha-Duong, *Laboratoire de Mathématiques Appliquées de Compiègne* (LMAC) (President),
  - Mr. Claude Barrouil, Director of the DCSD, ONERA,
  - Mrs. Lilianne Denis-Vidal, *Université des Sciences et Technologies de Lille* (USTL), (Supervisor),
  - Mr. Jacques Henry, *Institut National de Recherche en Informatique et en Automatique* (INRIA) (Referee),
  - Mrs. Ghislaine Joly-Blanchard, LMAC,
  - Mr. Jean-Pierre Richard, *Laboratoire d'Automatique, Génie Informatique et Signal* (LAGIS), *Ecole Centrale de Lille* (Referee)
- 1999-2001 Unregistered student in DEA in UTC: courses on optimization, identification and parameter estimation, decision theory, signal processing, partial differential equations.

- 1999 DEA in Applied Mathematics, USTL. Dissertation on Implementation of GMRES via biorthogonal polynomials under the direction of Professor Claude Brezinski.
- 1998 Master of Mathematics, *Université de Rennes 1*
- 1996-1997 Institut Universitaire de Formation des Maîtres de Rennes
- 1996 Licence in Mathematics, Université de Rennes 1
- 1994-1995 Gap year
- 1994 DEUG A (Mathematics, Physics, Computer Science), Université de Rennes 1

1.1.2 Post doctoral professionnal route

- 2005 — Associate Professor - *Université de Toulouse III* (*Université Paul Sabatier* - UPS)
- 2004-2005 Postdoctoral position : Ecole Centrale de Lille.
  Mathematics teacher : *Ecole des Mines de Douai* and *Institut Supérieur de l'Electronique et du Numérique de Lille*.
- 2003-2004 Assistant Professor : Université des Sciences et Technologies of Lille.
- 2002-2003 Assistant Professor : Université de Technologie de Compiègne.

1.2 Educational activities

1.2.1 Teaching activities (nature and levels of education)

During my teaching years, I have assured more than 2500 teaching hours in first and second graduate levels as well as in engineering schools (Ecole des Mines de Douai, Institut Supérieur de l'Electronique et du Numérique de Lille, UTC).
I participated in the recruitment of engineering students at the Ecole des Mines de Douai. Currently I participate in the recruitment of students at UPS (in Master 2 and Licence 3).
I began teaching in 1999 during my thesis as a teaching assistant at UTC and at USTL. I taught Mathematics and Scientifical Calculus. The description of these teachings are given below. My interventions concerned tutorials and practical works. During the two years of assistant professor, I taught courses, tutorials and practical works in Computer Science and Mathematics. I was firslty a assistant professor at UTC and my researchs were conducted in the LMAC. Then I was a assistant professor at USTL, my researchs

were conducted at *Laboratoire d'Informatique Fondamentale de Lille* in the team Calcul Formel. In 2004, I taught Mathematics at Ecole des Mines de Douai. I lectured students in continuing education and in second year.
Since 2005, I have been an Associate Professor at Université de Toulouse III. These last years, my main teachings concern the domains of Applied Mathematics, Parameter estimation, Probability and Statistical from Licence 3 to Master 2 of the sectors Electronic Electrotechnic and Automatic (EEA) or Physics at UPS.

- From September 2005 at Paul Sabatier University:
  - Courses and tutorials in Mathematics for the students of L3EEA-REL and L3DIM (50 hours).
    The abbreviation REL means *Réorientation for long studies* and DIM means *Diagnosis, Instrumentation and Measures*.
    The DIM formation depends on the Physics Department of UPS.
    These teachings are devoted to:
    -Upgrade,
    -Mathematics tools.
    This module deals with an upgrade in Mathematics (complex numbers, integration, series ...) and introduces the Laplace Transform, Fourier Transform, the expansion in Taylor serie, differential equations, Linear algebra, ...
  - Courses, Tutorials and Practical works for Master 1 SIA students in Introduction to statistical exploitation of data (30 hours).
    SIA means *Signal, Image and Applications*. This module deals with an introduction to manipulations of data. The notions of randomly variables (discrete and continuous), mean, variance, ... parameter estimation (moment method, maximum likelihood, least-squares), properties of estimator (biais, quadratic error, convergences), hypothesis tests (Chi 2 and Kolmogorov-Smirnov) are recalled.
  - Courses, Tutorials and Practical works for M1DIM students in Identification, parameter estimation, hypothesis tests (26 hours). This module is close to the previous one.
  - Courses, Tutorials and Practical works for M2EEA-ASTR students in Detection and diagnosis (10 hours).
    ASTR means *Automatique, Sûreté de fonctionnement et Systèmes Temps-Réel*.
    In this module, I introduce the concepts of supervision, health monitoring, diagnosis and present methods to diagnose dynamical models based on either parameter estimation or observators.

- Courses, Tutorials and Practical works for M2DIM-ICM students in Tools and Technics for Diagnosis (10 hours). This module is close to the previous one.
- Courses, Tutorials and Practical works for M2EEA-SIA students on Identifiability and parameter estimation (20 hours).
- Courses and Tutorials for M2EEA-IRR students on Parameter estimation by least squares method (10 hours). IRR means *Intelligence artificielle, Reconnaissance des formes, Robotique*.
- Practical works for M1EEA-ISTR students entitled Discrete-time linear systems and identification, devoted to parameter estimation by least squares method (12 hours).
  ISTR means *Ingénierie des Systèmes Temps-Réel*.
  These practical works consist in reconstructing an image using the least squares, localising a mobile robot and analysing the periodicity in data where the sampling time is not constant.

• Since September 2005, at Centre National d'Enseignement à distance (CNED), in partnership with UPS, I have been grading papers in Mathematics for the first and second years Licence Ingénierie à Distance as well as proposing the subjects of Probability exams in the second year.

• Since September 2005 in partnership with UPS, I have been teaching Probability, statictics for Signal processing at the Engineering School CESI (10 hours).

• From 2004 to 2005, I taught Mathematics (courses, tutorials and practical works) at Ecole des Mines de Douai :

- Courses and tutorials on Mathematics for Signal processing for 2nd year students (20 hours).
- Courses, tutorials and practical works for 2nd year students on the resolution of numerical problems by using the software Scilab (40 hours).
- Courses for students in continuous formation on Mathematics (48 hours).

• From 2004 to 2005, I taught Modelization, processus Identification at Institut Supérieur de l'Electronique et du Numérique de Lille: courses, tutorials and practical works (20 hours).

• From 2003 to 2004, I was an assistant professor at USTL and I taught:

- Courses, tutorials and practical works in Maple on Scientific calculus for first year students (90 hours),

- Tutorials and practical works in Maple on Modelization, optimisation and graphs for Licence students (53 hours),
- Tutorials on information coding for first year students (36 hours).

• From 2002 to 2003, I assured tutorials in Mathematics at UTC for first year students (192 hours).

• From 1999 to 2002, I taught :

- Tutorials and practical works at UTC in Numercial Analysis for third year students (68 hours),
- Tutorials at UTC in Mathematics for first year students (34 hours),
- Tutorials and practical works at USTL in Modelization, Optimisation and Graphs for Licence students (124 hours),
- Practical works in Maple on Scientific Calculus at USTL for first year students (26 hours).

1.2.2 Teaching responsibilities

Since September 2007, I have been the head of the third year Licence entitled Diagnosis Instrumentation and Measures (DIM)-UPS (of the Physics Department); 20 students are registrated in this training.
I am also in charge of the following teaching modules: Mathematics in L3EEA-REL and L3DIM, Introduction to statistical exploitation of data in M1SIA, Linear time-discrete models and identification in M1ISTR, Detection and diagnosis in M2ASTR and Tools and technics of diagnosis in M2DIM-speciality Instrumentation, Sensors, Measures (ICM).

1.3 Research activities

My research activities will be detailed in the following chapters. These activities concern nonlinear dynamical uncertain models with bounded errors. A large part of my work deals with set-membership identifiability of such models and their set-membership diagnosability. Another part concerns the optimal input design for such models to obtain a "best" estimate of parameters in a sense which is described latter. My works also deal with the application of these tools to diagnose the nonlinear dynamical uncertain models.

- Concerning set-membership identifiability and diagnosability, my research is in collaboration with L. Travé-Massuyès and N. Verdière. In [46], we introduced the

concept of set-membership identifiability and we formalized two complementary definitions for identifiability of uncertain models, namely *set-membership identifiability* and *μ-set-membership identifiability*. We provided operational methods to check the studied properties in set-membership framework. Two methods for checking set-membership and μ-set-membership-identifiability are presented. They take inspiration from well established methods for checking classical identifiability, namely the Taylor Series approach in [95] for the first one, and the differential algebra approach [31, 76, 74, 94] for the second one. The second method, based on differential algebra, is shown to be easily extendable to nonlinear uncertain systems with parameters varying according to polynomial laws. I and co-workers have developped in [109] a method for determining the partitioning of the parameter space in terms of set-membership identifiable sets.
In the same way, we introduced some new definitions on diagnosability in the set-membership framework; links between set-membership identifiability and set-membership diagnosability are exhibited.

- Concerning the optimal input design, my research is in collaboration with L. Denis-Vidal and Z. Cherfi. The aim is to design an experiment that produces data from which model parameters can be estimated accurately in the bounded-error framework.
  In [44], I and E. Chanthery have considered the optimal input design for systems with bounded parameters and some statistic information about measurement noise.
  In the framework of the thesis of Q. Li and in collaboration with L. Denis-Vidal and Z. Cherfi, we showed that the search for an optimal input in nonlinear dynamical systems can be made with the Gram matrix of sensitivity functions in the bounded-error context. We have also studied the optimization of the initial conditions in [73]. We explicitely exhibited some criteria to find an optimized input in the bounded-error context. Our procedure has been applied on different examples (provided from pharmacokinetical domain, aeronautical domain) and it leads to good results in terms of parameter estimation comparatively to results obtained with a non-optimized input.

- A part of my works is devoted to the integration of *mixed uncertainties* which combine stochastic and bounded errors. As said in introduction, some sources of uncertainty are not well-suited to stochastic modeling and are better represented with bounded uncertainties. Hence, combining stochastic and bounded uncertainties may be an appropriate solution. In contrast to stochastic estimation approaches, set-membership estimation advantageously provides a guaranteed solution. However, it does not give any precision about the belief degree and it is often criticized for the

overestimation of its results.
Motivated by the above observations, I consider the modeling and filtering in the case of mixed uncertainties meaning that I consider some bounded uncertainties on parameters and perturbations/noise are modeled through appropriate probability distributions. The literature concerning the filtering problem in case of mixed uncertainties is nowadays expanding: for example a combination of Kalman filter and zonotopes is proposed in [22], a combination of particle filter and intervals is proposed in [10] and my works [137, 138].
In 1997, Chen et al. have developped an extension of Kalman filter considering bounded uncertainties on parameters and gaussian measurement noise by using interval analysis; it is named IKF (Interval Kalman Filter) [19]. An improvement of IKF, named iIKF (improved Interval Kalman Filter) has been developped by J. Xiong during his PhD that I co-supervised with L. Travé-Massuyès [136]. In particular, the approach proposed in [19] does not provide guaranteed results because of the simplification used to avoid interval matrix inversion. The main contribution of J. Xiong's thesis consists in proposing a method to solve the interval matrix inversion problem without loss of solutions while controlling the inherent pessimism of interval calculus.

- Another part of my works concerns fault detection and diagnosis relying on set-membership identifiability, diagnosability, parameter and state estimation in a bounded error context.
  Fault detection via parameter estimation relies on the principle that possible faults in the monitored system can be associated with specific parameters and states of the mathematical model of the system given in the form of an input-output relation. This approach supposes that there exists a relationship between the model parameters p and the physical system parameters. Decision on whether a fault has occurred, is based either on changes in model parameter values or on changes in physical system parameters and tolerances limits. In collaboration with L. Travé-Massuyès and N. Verdière, we have developped an efficient method to estimate faults. This method is based on the polynomials linking inputs, outputs and their derivatives, parameters and faults obtained through variables elimination relying on set-membership identifiability.
  With R. Pons and L. Travé-Massuyès, we have also developped a fault detection method based on state estimation with bounded-errors. It is a simplified version of the method based on Taylor serie expansion in which two parameters η and ζ are introduced. The integer η deals with the number of successive empty intersections between the prediction value of model output and the measure. The integer ζ is used to set the number of iterations between two successive resettings of the prediction

on the measured value. This method has been successfully used in a benchmark proposed in the SIRASAS project developped in Section 1.5.3.

1.4 Supervision activities (PhD and post-PhD)

1.4.1 Theses Supervisor

I have co-supervised two theses (defended in 2013 and in 2015) and I have been co-supervising one thesis since October 2014.

1.4.1.1 Thesis of Jun Xiong

I co-supervised the thesis of Jun Xiong from 1 October 2009 to 9 December 2013. The title was "Set-membership state estimation and application on fault detection".
The commitee members were Patrick Danès (President), Luc Jaulin (referee), Tarek Raïssi (referee), Vicenç Puig (Examinator), Carine Jauberthie (Thesis-Supervisor), Louise Travé-Massuyès (Thesis-Supervisor) and Françoise Le Gall (invited). The co-supervision has been made 50% with L. Travé-Massuyès.
This thesis dealt with the problem of integrating both statistical and bounded uncertainties for discrete time linear systems. Building on the Interval Kalman Filter (IKF) developed by C. Chen in 1997, we proposed significant improvements based on recent techniques of constraint propagation and set inversion which, unlike the IKF algorithm, allow to obtain guaranteed results while controlling the pessimism of interval analysis. The improved filter is named iIKF. The iIKF filter has the same recursive structure as the classical Kalman filter and delivers an enclosure of all the possible optimal estimates and the covariance matrices. Chen's IKF algorithm avoids the interval matrix inversion problem and consequently loses possible solutions. For the iIKF, we proposed an original guaranteed method for the interval matrix inversion problem that couples the SIVIA (Set Inversion via Interval Analysis) algorithm and a set of constraint propagation problems. In addition, several mechanisms based on constraint propagation are implemented to limit the overestimation effect of interval propagation within the filter recursive structure. A fault detection algorithm based on the iIKF is proposed. It implements a semi-closed loop strategy which stops feeding the filter with observation corrupted by the fault as soon as it is detected. Through various examples, the advantages of the iIKF filter are presented and the effectiveness of the fault detection algorithm is demonstrated.

1.4.1.2 Thesis of Qiaochu Li

The second thesis that I have co-supervised is the thesis of Qiaochu Li from 1 October 2012 to 10 November 2015.
The title of this thesis was "Contribution to the experimental design and active diagnosis for nonlinear dynamical systems, application in aerospace and automotive fields".
The committee members were Abdellatif El Badia (President), Luc Jaulin (referee), Michel Kieffer (referee), Floriane Collin (Examinator), Nathalie Revol (Examinator), Zohra Cherfi (Thesis-Supervisor), Lilianne Denis-Vidal (Thesis-Supervisor), Carine Jauberthie (Thesis-Supervisor).
This thesis has been co-supervised (40%) with L. Denis-Vidal 35% and Z. Cherfi 25%.
In this work, we studied the optimal input design for parameter estimation for uncertain dynamical systems. The problems of optimal sampling time and optimal initial states were also considered.
Some set-membership criteria have been proposed to find an optimal input in the bounded-error context. These criteria are based on the Gram matrix of sensitivity functions. They have been used for the search of optimal input and optimal initial states. These criteria allowed to obtain better parameter estimation results. The comparisons are made on different applications: pharmacokinetical domain and aeronautical domain. The obtained results highlight the potential of our proposed methodology. The application to active diagnosis have also be considered; active diagnosis means in this work, to refine diagnosis if this last one is ambiguous. We considered diagnosis by parameter estimation. The obtained results by using our optimal input methodology were very satisfactory.

1.4.1.3 Thesis of Tuan Anh Tran

I have been co-supervising (50%) with F. Le Gall (50%) the thesis of Tuan Anh Tran, since 1 October 2014.
The title of this work is "Unified framework for modeling the stochastic and bounded errors - Application to the fault detection and isolation in uncertain dynamical systems".
In this thesis, several problems are investigated. The first one concerns the definition of a unified theoretical framework for modeling stochastic and bounded uncertainties. The second one deals with the design of filtering algorithms with mixed uncertainties (including generalization of the extended Kalman filter and the particle filter) for nonlinear dynamical models and the last one concerns the study of theoretical properties such stability and convergence.

1.4.2 Post-Doctorate Supervision

I have co-supervised (50%) the post-doctoral position of Laleh Ravanbod-Hosseini from September 2012 to August 2013 with N. Verdière 50% in the project funded by ANR named MAGIC-SPS. This post-doctorate concerned the development of tools and algorithms to analyse set-membership identifiability.

1.5 Participation and coordination of projects

1.5.1 MAGIC-SPS

I was the coordinator of the project MAGIC-SPS (Guaranteed Methods and Algorithms for Integrity Control and Preventive Monitoring of Systems) from 01/10/2011 to 30/09/2015. It was a 3-years joint project funded by the French National Research Agency (ANR) Digital Engineering and Security (INS) year 2011 program, contract number ANR-11-INSE-006,
link: http://projects.laas.fr/ANR-MAGIC-SPS/.
The financial support of the ANR was 380 297 euros and the involved laboratories were LAAS CNRS (Toulouse), Lab ENSEA ECS (Cergy), IMS CNRS (Bordeaux), PRISME (Orléans), LMAH (Le Havre).
MAGIC-SPS aimed at:

- The development of reliable algorithms for system monitoring and integrity control. Current systems must show autonomous capabilities that allow them to remain operational even in a degraded but safe mode when a fault, a failure or any other disturbance occurs. To achieve such an objective, current modern systems often embed software and hardware that allow them to detect in an automatic and autonomous way the need of switching to the degraded mode, and either proceed with the necessary corrective actions to resume normal operational mode or remain in a degraded but safe one. One of the main challenges that must be addressed is how to take into account the uncertainties that act on the embedded system and that may be induced by measurement errors, loose conception, faults, or ageing, ... The first objective of MAGIC-SPS project was to investigate in a thorough manner computational techniques applicable to fault detection and isolation as a means to monitor the systems subject to bounded error uncertainties. This kind of uncertainties remain confined within a bounded set, with known bounds but no additionnal characterization. Both time-continuous and hybrid continuous-discrete dynamical systems with bounded uncertainties are addressed in the project. To do so, modelling approaches, model identification and estimation techniques have been studied in the bounded

error framework.

- The development of set-membership estimation techniques based on interval analysis.
  Set membership techniques, also known as guaranteed methods, for fault detection and isolation have recently benefited from a large number of works and have shown significant progress. Nevertheless, a significant shortcoming remains: the propagation of spurious uncertainty due to over-approximations in set computation, which yields algorithms with exponential complexity hence prohibitive computation time for on-line applications. The MAGIC-SPS project aimed to (1) extend the capabilities of current guaranteed methods for nonlinear continuous reachability computation, hence coming out with scalable methods in presence of bounded uncertainty; (2) develop guaranteed and efficient set membership techniques for hybrid reachability computation in presence of bounded uncertainty; (3) use the above to develop methods for preventive monitoring of both error bounded continuous and hybrid dynamical systems. We also investigated the feasibility of fault prognosis by using set membership state and parameter estimation techniques. Finally, the computational techniques developed within the project are made freely available on the web as an open source toolbox library, to make easier their diffusion and evaluation among the international scientific community.

I was coordinator of the MAGIC-SPS project and I contributed in the workpackage 2 on set-membership identifiability/diagnosability with the analysis of these concepts for uncertain dynamical models. Some methods and algorithms to test set-membership identifiability were developped. In the workpackage 2, we developped a method based on Differential Algebra and a partial-injectivity test. An algorithm allowing to obtain set-membership identifiable sets into the admissible parameter set was given. Some links between the classical definitions of identifiability and diagnosability (without uncertainties) were exhibited. In the bounded-error framework, some new definitions of diagnosability were established; links with set-membership identifiability were also demonstrated.

1.5.2 ADES

I was co-leader of the project ADES (Set Estimation and Detection Applications) with Nacim Ramdani 50% in 2007. ADES was supported by the GDR MACS and brought together four laboratories. It targeted the set-membership methods for the simulation of nonlinear dynamical uncertain systems with bounded uncertainties. The potential application of set-membership methods have been evaluated for the fault detection problem.
The project ADES allowed to construct and propose the project DROCSETA at ANR in

2008, DROCSETA has not been funded but its rewritten into MAGIC-SPS was successfull.
The four involved laboratories were ECS-ENSEA (Cergy), LAAS-CNRS, LAPS-CNRS (Talence), LIRMM (Montpellier).

1.5.3 SIRASAS

From 2007 to 2010, I participated in the french collaborative project SIRASAS (Stratégies Innovantes et Robustes pour l'Autonomie des Systèmes Aéronautiques et Spatiaux), supported by the Fondation de Recherche pour l'Aéronautique & Espace (FRAE) and managed by IMS-Bordeaux.
The overall aim of SIRASAS was to increase significantly the spacecraft autonomy. It addressed the model-based Fault Detection, Identification and Recovery (FDIR) challenges for Guidance and Control. The picture was rather dark : there is a widening gap between the advanced FDIR methods developed by the academic community and those currently in use by the industrial end-users. In fact, the selection of any advanced FDIR solution at a local or global level for space missions or aeronautical systems, necessarily includes a trade-off between the best adequacy of the technique and its implementation level for covering an expected fault profile, as well as its industrialization process with support tools for its design/tuning and validation. Many attractive advanced FDIR algorithmic solutions may not be accepted, and so cannot be adopted, without such industrial framework. The actions undertaken within SIRASAS aimed at overcoming the dead zone between the scientific advanced methods proposed by the academic and research communities and the technological solutions demanded by the aerospace industry, with stringent operational constraints.
Industrial and laboratories involved in this project were IMS, SATIE (ENS Cachan), LAAS-CNRS, CRAN (Nancy), LRI (Université Paris-Sud, Orsay), ONERA Center of Toulouse, CNES, Airbus and Thales Alenia Space France.
My contribution, in collaboration with L. Travé-Massuyès and R. Pons, in SIRASAS project concerned the fault detection and diagnosis for the oscillatory failure cases based on interval analysis with CRAN.

1.5.4 CORAC-EPICE

Through the CORAC-EPICE project (2011-2016) and MICPAC (2011-2015), I have been interested in prognosis using an interval-based approach.
CORAC (Council for Civil Aeronautics Research) brings together all the French players in the airline industry. CORAC offers six demonstrators for the future of aviation.

The group responded to the call for proposals SPICE P6 WP1 Health Monitoring of the number 4 platform technology demonstration SPICE (Propellant Together with Integrated Composites Environment). The project aims to develop a health monitoring application of air sampling system (bleed).
My contribution in the CORAC-EPICE project concerns the monitoring and prognosis based on interval analysis.
In collaboration with L. Travé-Massuyès, R. Pons, P. Ribot and Y. Pencolé, we proposed a two-stages set-membership condition-based monitoring method. The first stage achieves diagnosis and provides an estimation of the system's health status. It takes the form of set-membership parameter estimation using focused recursive partitioning. The second stage concerns prognosis in the form of the estimation of the remaining system's lifespan. It is based on the use of a damaging table. The case study of a shock absorber was used to illustrate the method [124].

1.5.5 MICPAC

The project MICPAC (Interval method for bonded joints characterization and prognosis) was financed by the ANR (JCJC project) from October 2011 to September 2015.
Adhesives and sealants are widely used in many industrial applications, such as in aerospace, automotive and electrical industries. The characterisation, evaluation of their properties and diagnosis is a key-point for the use of these multi-materials: if the usual characterisation techniques allow a good description of the adhesives in the bulk, or their practical adhesion at model interfaces, reliable parameters of thick interphases between the substrates and the adhesives are missing. Then, dielectric spectroscopy is an extremely effective method for characterising the molecular dynamics over a large range of time scales, and a very promising method to study these complex multi-materials. Unfortunately, the resulting curves are very difficult to analyse as many phenomena take place at the same time (or frequency): dipole relaxations, sample conductivity, electrodes polarisation. Then, some modeling has to be done, and the real and imaginary parts of the permittivity have to be simultaneously modelled, which is really rarely done now. As classical tools for the dielectric spectroscopy data fitting are not satisfactory, some new mathematical and simulation tools have been developped.

The interval analysis method takes into account the experimental error of each data point in the measured dielectric spectrum in order to find the suitable number of relaxations, and gives a confidence interval for every parameter of the dielectric function implemented in the software (Set Inversion Via Interval Analysis applied to DiElectric Spectroscopy). The obtained result is guaranteed which means that this algorithm is able to validate or nullify a mathematical model. Then, the number of relaxations in the characterised system, their position and intensity are determined and guaranteed.

On the one hand, this new approach of the polymer and interphase study leads to a better comprehension of the bonded systems, their ageing and to the determination of their Remaining Useful Life. Of course, this fundamental research in molecular dynamic is coupled with a strong experimental work in practical adhesion and interphases study.
On the other hand, the interval analysis and the developed software put into a general use (all kind of fit and peak deconvolution): for example the fit of dynamical mechanical analysis data, or deconvolution of X-Ray diffraction, infra-red spectroscopy, Raman spectroscopy, X-ray photoelectron spectroscopy. Using interval analysis, it is possible to guarantee the number of Gauss or Lorentz type peaks hidden under a common peak
The coordinator of the project MICPAC was M. Aufray (Institut National Polytechnique de Toulouse) and the laboratories involved were CIRIMAT (Toulouse), LAAS-CNRS and LAPLACE (Toulouse).

1.6 Implication in the international community

- Since July 2010, I have been member of the editorial board of the Journal Européen des Systèmes Automatisés.
- In July 2011, I was invited to the Workshop on Experiments for Processes with Time or Space Dynamics in Cambridge (UK). I presented my thesis works and my presentation was entitled Methodology and implementation of optimal input design for parameter estimation.
  http://www.newton.ac.uk/programmes/DAE/daew01.html
- I participated to two selection committees for Assistant Professor:
  - University of Bordeaux 1 in 2012.
  - University of Toulon in 2013.
- I was:
  -a Chair for IFAC European Control Conference 2007 on the Regular Session on Nonlinear Systems,
  -a Co-chair for IFAC Symposium on Nonlinear Control Systems 2013 on the Regular session on Vehicles Control and Mechatronics.
- I was a member of the program committe for JD-JN MACS in 2015 at Bourges, France.
- I am a member of the national organizing committee of World IFAC Congress 2017, technical visits.

- I am a reviewer for international journals and conferences among Aeronautical Journal, AI Communications, American Control Conference, CIFA, European Control Conference, IEEE Transactions on Control Systems Technology, IMA Journal of Mathematical Control and Information, International Journal of Advanced Manufacturing Technology, International Journal of Applied Mathematics and Computer Science, Journal Européen des Systèmes Automatisés, Mediterranean Conference on Control and Automation, Nonlinear Control Systems, SAFEPROCESS, DX, SYSID.
- I was a reviewer for the French National Research Agency in the program Villes et Bâtiments Durables Edition 2012.
- I was a reviewer for doctoral contracts for the Doctoral School SICMA (*Université de Bretagne Occidentale*) from 2008 to 2010.

1.7 Publications

1.7.1 Articles published in International journals

- C. Jauberthie, L. Travé-Massuyès, N. Verdière, Set-membership identifiability of nonlinear models and related parameter estimation properties. To appear in 2016 in the International Journal of Applied Mathematics and Computer Science (AMCS), Vol. 26, No. 4.
- Q. Li, C. Jauberthie, L. Denis-Vidal, Z. Cherfi, M. Maïga. Entrée optimale pour l'estimation de paramètre des systèmes dynamiques non linéaires avec application en aéronautique, (préselectionné aux JD-JN-MACS 2015). To appear in 2017 in Journal Européen des Systèmes Automatisés (JESA).
- Q. Li, C. Jauberthie, L. Denis-Vidal, Z. Cherfi. Optimal Initial State for Fast Parameter Estimation in Nonlinear Dynamical Systems. To appear in 2016 in a Special Issue of Computer Methods and Programs in Biomedicine.
- N. Verdière, C. Jauberthie, L. Travé-Massuyès. Functional diagnosability and detectability of nonlinear models based on analytical redundancy relations, Journal of Process Control, Volume 35, pp.1-10, 2015.
- Q. Li, C. Jauberthie, L. Denis-Vidal, Z. Cherfi. Impact of optimized input on guaranteed parameter and state estimation in a bounded error context for nonlinear dynamical aerospace models. Journal of Multidisciplinary Engineering Science and Technology, Vol.2, pp.217-224, 2015.

- L. Ravanbod, N. Verdière, C. Jauberthie. Determination of set-membership identifiability sets. Mathematics in Computer Science Journal, Vol.8, pp.391-406, 2014.

- C. Jauberthie, N. Verdière, L. Travé-Massuyès. Fault Detection and Identification Relying on set-membership identifiability. Annual Reviews in Control, Vol.37, No.1, pp.129-136, April 2013, http://dx.doi.org/10.1016/j.arcontrol.2013.04.002.

- C. Jauberthie, R. Jauberthie, Y. Mélinge. Indicateurs d'endommagement et durée de vie d'ouvrages d'assainissement, modélisation. MATEC Web of Conferences, Vol.2, September 2012, Item 04002, 8 pages, http://dx.doi.org/10.1051/matecconf/20120204002 (Special issue: Innovation et Valorisation en génie civil et Matériaux de Construction (INVACO 2), Rabat (Morocco), 23-25 November 2011.

- C. Jauberthie, L. Travé-Massuyès. A sufficient condition to test identifiability of a nonlinear delayed-differential model with constant delays and multi-inputs. Automatica, Vol.46, No. 7, pp.1222-1227, 2010.

- C. Jauberthie, F. Bournonville, P. Cotton, F. Rendell. Optimal Input Design for Aircraft Parameter Estimation. Aerospace Science and Technology, Vol.10, No. 4, pp.331-337, 2006.

- L. Denis-Vidal, C. Jauberthie, G. Joly-Blanchard. Identifiability of a nonlinear delayed-differential aerospace model. IEEE Transactions on Automatic Control, vol.51, No. 1, pp.154-158, 2006.

- C. Jauberthie, L. Denis-Vidal, P. Cotton, G. Joly Blanchard. An optimal input design procedure. Automatica, vol.42, No. 5, pp.881-884, 2006.

1.7.2 Articles submitted to international journals

- Q. Li, C. Jauberthie, L. Denis-Vidal, Z. Cherfi. Optimal input design for parameter estimation in a bounded-error context for nonlinear dynamical systems. Submitted to Automatica in July 2016.

- L. Ravanbod, C. Jauberthie, N. Verdière, L. Travé-Massuyès. Improved solutions for ill-conditioned problems involved in set-membership estimation for fault detection and isolation. Submitted to Journal of Process Control.

1.7.3 Articles published in International conferences with proceedings and Committee

- C. Jauberthie, L. Travé-Massuyès, N. Verdière. Set-Membership diagnosability: definitions and analysis. In Proceedings of International Conference on Control and Fault-Tolerant Systems, 6 pages, Barcelona, Spain, 2016.
- T. Anh Tran, F. Le Gall, C. Jauberthie, L. Travé-Massuyès. Two stochastic filters and their extenxions using interval analysis. In Proceedings of IFAC International Conference on Intelligent Control and Automation Sciences, 6 pages, Reims, France, 2016.
- Q. Li, C. Jauberthie, L. Denis-Vidal, Z. Cherfi. Optimal initial state for fast parameter estimation in nonlinear dynamical systems. In Proceedings of IFAC Biological and Medical Systems, pp.556-562, Berlin, Germany, 2015.
- Q. Li, C. Jauberthie, L. Denis-Vidal, Z. Cherfi. A diagnosis scheme for dynamical systems : approach by guaranteed parameter estimation. In Proceedings of International Conference on Informatics in Control, Automation and Robotics, pp 330-335, Colmar, France, 2015.
- J. Blesa, F. Le Gall, C. Jauberthie, L. Travé-Massuyès. State estimation and fault detection using box particle filtering with stochastic measurements. In proceedings of international Workshop on Principles of Diagnosis 2015, pp.67-73, Paris, France, 2015.
- L. Travé-Massuyès, R. Pons, P. Ribot, Y. Pencolé, C. Jauberthie. Condition-Based Monitoring and Prognosis in an Error-Bounded Framework. In Proceedings of Workshop on Principles of Diagnosis, Paris, France, 2015.
- Q. Li, C. Jauberthie, L. Denis-vidal, Z. Cherfi. Guaranteed state and parameter estimation for nonlinear dynamical aerospace models. In Proceedings of International Conference on Informatics in Control, Automation and Robotics, pp.519-527, Vienna, Austria, 2014.
- J. Xiong, C. Jauberthie, L. Travé-Massuyès, F. Le Gall. Fault detection using interval Kalman Filtering enhanced by contraint propagation. In Proceedings of IEEE Conference on Decision and Control (CDC), pp.490-495, Florence, Italy, 2013.
- C. Jauberthie, E. Chanthery. Optimal input design for a nonlinear dynamical uncertain aerospace system. In Proceedings of IFAC Symposium on Nonlinear Control Systems (NOLCOS) 2013, 6p, Toulouse, France, 2013.

- J. Xiong, C. Jauberthie, L. Travé-Massuyès. Improvements in computational aspects of interval Kalman Filtering enhanced by constraint propagation. In Proceedings of IEEE International Workshop Electronics, Control, Measurement, Signals and Their Application to Mechatronics (ECMSM), 6p, Toulouse, France, 2013

- J. Xiong, C. Jauberthie, L. Travé-Massuyès. New computation aspects for existing interval Kalman filtering and application. In Proceedings of IFAC Conference on Control Applications of Optimization (CAO), 6p, Rimini, Italy, 2012

- N. Verdière, C. Jauberthie, L. Travé-Massuyès. Fault detection and identification Relying on SM-identifiability. In Proceedings of IFAC International Symposium on Fault Detection Supervision and Safety of Technical Processes (SAFEPROCESS'2012), pp.1262-1267, Mexico City, Mexico, 2012.

- C. Jauberthie, N. Verdière, L. Travé-Massuyès. Set-membership identifiability and guaranteed parameter estimation for nonlinear uncertain dynamical systems. In Proceedings of IFAC Symposium is System Identification (SYSID), pp.434-439, Brussels, Belgium, 2012.

- C. Jauberthie, N. Verdière, L. Travé-Massuyès. Set-membership identifiability: definitions and analysis. In Proceedings of IFAC World Congress (IFAC), pp.12024-12029, Milan, Italy, 2011.

- R. Jauberthie, Y. Mélinge, C. Jauberthie, R. Bashir. Gestion patrimoniale des systèmes d'assainissement. In Proceedings of Génie Civil et Développement Durable (GCDD 2011), 6p, Tebessa, Algeria, 2011.

- J. Karim, C. Jauberthie, M. Combacau. Model-based fault detection method using interval analysis: application to an aeronautic test bench. In Proceedings of 19th International Workshop on Principles of Diagnosis (DX-08), pp.269-274, Blue Mountains, Australia, 2008.

- R. Pons, C. Jauberthie, L. Travé-Massuyès, P. Goupil. Control surfaces oscillatory failures identification using interval analysis. In Proceedings of 19th International Workshop on Principles of Diagnosis (DX-08), pp.323-330, Blue Mountains, Australia, 2008.

- R. Pons, C. Jauberthie, L. Travé-Massuyès, P. Goupil. Interval analysis based learning for fault model identification. Application to control surfaces oscillatory failures. In Proceedings of 22nd International Workshop on Qualitative Reasoning (QR08), 8p, Boulder, USA, 2008.

- P. Ribot, C. Jauberthie, L. Travé-Massuyès. State estimation by interval analysis for a nonlinear differential aerospace model. In Proceedings of European Control Conference (ECC'07), pp.4839-4844, Kos, Greece, 2007.

- C. Jauberthie, L. Denis-Vidal, G. Joly-Blanchard. Identifiability and estimation of aircraft parameters and delays by using optimal input design. In Proceedings of 44th IEEE Conference on Decision and Control - European Control Conference, 6p, Séville, Spain, 2005.

- C. Jauberthie, L. Denis-Vidal, G. Joly-Blanchard. Identifiability and estimation of aircraft parameters and delays. In Proceedings of Mathematical Theory of Networks and Systems 2004, Leuven, Belgium, in 2004.

- C. Jauberthie, L. Denis-Vidal, L. Belkoura. Aircraft Parameter and Delay identifiability. In Proceedings of European Control Conference ECC, pp.37-40, Cambridge, UK, 2003.

- C. Jauberthie, L. Denis-Vidal, G. Joly-Blanchard. Parameter estimation by using optimal design and linear matrix Inequalities. In Proceedings of System Identification, Rotterdam, The Netherlands, on CD, 2003.

- C. Jauberthie, L. Denis-Vidal, G. Joly-Blanchard. Identifiability Analysis of a Time Delay System. In Proceedings of Applied Mathematics and Applications of Mathematics, Nice, France, 2003.

- L. Denis-Vidal, C. Jauberthie, G. Joly-Blanchard, P. Cotton. Aircraft parameter estimation: successive steps. In Proceedings of IFAC Nonlinear Control Systems, pp.322-327, St. Petersburg, Russia, 2001.

1.7.4 Reports

- Deliverable 2.2: set-membership identifiability and diagnosability: links and methods. C. Jauberthie, L. Hosseini, L. Travé-Massuyès, N. Verdière.
  Contract Report: MAGIC-SPS: ANR-11-INSE-006, in July 2013, 47 pages.

- Diagnosis and prognosis in health monitoring systems. State of art. C. Jauberthie, Y. Pencolé, R. Pons, P. Ribot, L. Travé-Massuyès.
  Contract Report: Coralie Project, in December 2012, 82 pages, No. 12680.

- Deliverable 2.1: set-membership identifiability and diagnosability: definitions. C. Jauberthie, L. Travé-Massuyès, N. Verdière.

Contract Report: MAGIC-SPS: ANR-11-INSE-006, in July 2012, 27 pages, No. 12362.

- Deliverable 1: Project Sirasas, Stratégies Innovantes et Robustes pour l'Autonomie des Systèmes Aéronautiques et Spatiaux. Contrat FRAE. Délivrable 1, WP2. Mars 2009, 289 pages. Laboratoires impliqués : SATIE Cachan, CRAN-ENSEM, IMS Bordeaux, groupe DISCO LAAS-CNRS.

- Project Report ADES: Guaranteed set estimation of dynamical systems and application to the fault detection problem.
C. Combastel, C. Jauberthie, T. Raïssi, N. Ramdani, L. Travé-Massuyès. 08035 LAAS report in January 2008, 21 pages.

- R. Pons, C. Jauberthie, L. Travé-Massuyès. Set-membership detection of oscillatory failure cases. LAAS report 10516, September 2010, 47 pages.

- C. Jauberthie, Recherche d'identifiabilité d'un modèle de comportement en vol d'avion dans la turbulence", "Flight dynamics and system identification ", Scientific Activity, Technical Report TR4/DVIS, ONERA, pp 105-107, February 2001.

- P. Coton, A. Bucharles, C. Jauberthie, T. Le Moing et L. Planckaert, "CAIRE - Identification des dérivées de stabilité dynamique" - ph.2. Rapport technique 1/05650, ONERA, December 2001, (personal contribution : chapter 3 : 25 pages).

- C. Jauberthie, "Optimisation d'essais pour l'estimation de paramètres de modèle de comportement d'avion", Information Processing and Systems, "Scientific and technical activities", Revue ONERA, 2001 (ONERA, versions anglaise et française), pp.4-7.

Part II

Research activities

Chapter 2

Problem formulation and models

2.1 Motivations

As said in introduction, complex systems are often prone to uncertainties that complicate the modeling task. In a stochastic framework, uncertainty is taken into account through appropriate assumptions about noise and model error probability distributions [3, 134]. However, some sources of uncertainty are not well-suited to the stochastic uncertainty assumption and are better modeled as bounded uncertainty. This is typically the case for modeling tolerances on the parameter values, for which the manufacturer provides lower and upper bounds corresponding to the inherent variability of technological processes. Bounded uncertainty hence represents an interesting alternative to stochastic uncertainty and can be advantageously handled with set-membership models whose parameter values are defined by sets. Set-membership methods can be based on interval analysis and several algorithms have been proposed (for example [50, 110, 57]). Other approaches dedicated to linear models include ellipsoid shaped methods ([85, 65]), parallelotope and zonotope based methods [2, 42]. As this work concerns essentially nonlinear dynamical models, we use interval analysis which is very well adapted to the manipulation of these model equations. Thus in this chapter, after having described the model equations, we recall some basic tools of interval analysis and concepts of contractors. Contractors are tools of constraint propagation [48].

2.2 The considered model

We consider the uncertain dynamical parameter models described by the following form:

$$\Gamma_1 \begin{cases} \dot{x}(t,p) = f(x(t,p),u(t),p), \\ y(t,p) = g(x(t,p),p), \end{cases} \tag{2.1}$$

where :

- $x(t,p) \in \mathbb{R}^n$ and $y(t,p) \in \mathbb{R}^m$ denote respectively the state variables and the outputs at time t respectively,
- the time t is supposed to be such that $t_0 \leq t \leq T$ where T is a finite or infinite time bound,
- the initial conditions $x(t_0,p) = x_0$, if any, are supposed to belong to a bounded set $\mathbb{X}_0$,
- $u(t) \in \mathbb{R}^r$ is the input vector at time t; in the case of uncontrolled models, $u(t)$ is equal to 0,
- the vector of parameters p belongs to a connected set P supposed to be included in $\mathcal{U}_\mathcal{P}$ where $\mathcal{U}_\mathcal{P} \subseteq \mathbb{R}^p$ is an a priori known set of admissible parameters,
- the functions f and g are real and analytic[1] on M, where M is an open set of $\mathbb{R}^n$ such that $x(t,p) \in M$ for every $t \in [t_0,\ T]$ and $p \in P$.

In chapter 2, Γ_1^{p,x_0} denotes a specific model of the family of models represented by (2.1), where $p \in P$, $x_0 \in \mathbb{X}_0$ and we assume that $\mathbb{X}_0$ does not contain equilibrium points of the system. We will also introduce models Γ_2 including a stochastic part. These models will be described in the chapter two. Notice that P may be reduced to a single point.

We suppose that there exists a "true" value of parameters p^* such that the N data $z(t_i)$ are described by:

$$z(t_i) = y(t_i, p^*) + v(t_i), \quad i = 1, ..., N. \tag{2.2}$$

We assume that $v(t_i)$ belongs to the real *interval vector* $[\underline{v(t_i)}, \overline{v(t_i)}]$ where $\underline{v(t_i)}$ and $\overline{v(t_i)}$ are known as lower and upper bounds for the acceptable output errors. Such bounds may, for instance, correspond to a bounded measurement noise. The integer N is the total number of sample times.

As said in the motivations of this chapter, the works presented through this manuscript concern essentially the nonlinear uncertain dynamical systems described by the system (2.1); the interval analsis is well adapted to the manipulation of these model equations. Thus, in the following section, the main tools of interval analysis are briefly described.

[1] In particular, they are considered infinitely differentiable. This assumption is important in chapter 2 for the use of differential algebra.

2.3 Basic tools of interval analysis

Interval analysis introduced by R. E. Moore [86] provides tools for computing with sets which are described using outer-approximations formed by union of non-overlapping *boxes*. It is used for many tasks: for example in system robust control [62, 108, 27], in estimation [96, 106] or in computer science [61, 84].

In this section, the basic concepts and definitions of interval analysis are presented. The following results are mainly taken from [50].

2.3.1 Basic definitions

2.3.1.1 Interval

Definition 2.3.1 *A real interval* $[u] = [\underline{u}, \overline{u}]$ *is a closed and connected subset of* $\mathbb{R}$ *where* $\underline{u}$ *(respectively* $\overline{u}$*) represents the lower (respectively the upper) bound of* $[u]$.

The set of all real intervals of $\mathbb{R}$ is denoted $\mathbb{IR}$.

Definition 2.3.2 *The width* $w(.)$ *of an interval* $[u]$ *is defined by* $w([u]) = \overline{u} - \underline{u}$.

Definition 2.3.3 *The midpoint* $m(.)$ *of an interval* $[u]$ *is defined by* $m([u]) = (\overline{u} + \underline{u})/2$.

Definition 2.3.4 *The magnitude of an interval* $[u]$*, noted* $\mid [u] \mid$ *is given by the largest absolute value of* $[u]$ *that means the absolute value of the real with the largest value in* $[u]$*. We have* $\mid [u] \mid = max(|\underline{u}|, |\overline{u}|)$.

Definition 2.3.5 *The mignitude of an interval is* $mig([u]) = min(|\underline{u}|, |\overline{u}|)$ *if* $0 \notin [u]$*, else* $mig([u]) = 0$.

We note that two intervals $[u]$ and $[v]$ are equal if and only if $\underline{u} = \underline{v}$ and $\overline{u} = \overline{v}$.

2.3.1.2 Interval vector

Definition 2.3.6 *An interval vector (or box)* $[x]$ *is a vector with interval components and may equivalently be seen as a cartesian product of intervals:*

$$[x] = [x_1] \times [x_2] ... \times [x_n].$$

The set of $n-$dimensional real interval vectors is denoted by $\mathbb{IR}^n$.

Definition 2.3.7 *The width* $w(.)$ *of an interval vector is the maximum of the widths of its interval components.*

Example 2.3.1 $w([-2,2]\times[1,3])=4.$

Definition 2.3.8 *The midpoint $m(.)$ of an interval vector is a vector composed of the midpoints of its interval components.*

Definition 2.3.9 *The magnitude $\mid(.)\mid$ of an interval vector is a vector composed of the magnitude of its interval components.*

Definition 2.3.10 *The mignitude $mig(.)$ of an interval vector is a vector composed of the mignitude of its interval components.*

Moreover, for an interval vector $[x]$ with components $[x_i]$, the real $\parallel[x]\parallel$ is given by $\parallel[x]\parallel=\max_i(\mid([x_i])\mid)$ (used in Chapter 4).

2.3.1.3 Interval matrix

Definition 2.3.11 *An interval matrix $[A]$ is a matrix with interval components. It can be written as:*

$$[A]=\begin{pmatrix}[a_{1,1}] & \dots & [a_{1,m}]\\ \dots & \dots & \dots\\ [a_{n,1}] & \dots & [a_{n,m}]\end{pmatrix}, \tag{2.3}$$

where the matrix $[A]$ is composed of n lines and m columns.

The set of $n\times m$ real interval matrices is denoted by $\mathbb{IR}^{n\times m}$.

Definition 2.3.12 *The width $w(.)$ of an interval matrix is the maximum of the widths of its interval components.*

Definition 2.3.13 *The midpoint $m(.)$ of an interval matrix is a matrix composed of the midpoints of its interval components.*

Definition 2.3.14 *A square interval matrix $[A]$ is regular if $0\notin det([A])$.*

Remark 2.3.1 *Let $[A]^{-1}$ the inverse interval matrix of $[A]$ which means the narrowest interval matrix enclosing the set of inverse matrices $\{A^{-1}/A\in[A]\}$. Considering the matrix $[I_\epsilon]$ whose entries are $[1-\epsilon,1+\epsilon]$ on the main diagonal and $[0-\epsilon,0+\epsilon]$ outside. Then there exists $\epsilon\in\mathbb{R}^{+*}$ such that $[A]^{-1}[A]\subset[I_\epsilon]$.*

Definition 2.3.15 *An interval matrix $[A]$ is said to be positive definite if each $A\in[A]$ is positive definite (in the classical sense).*

Positive definiteness of symmetric interval matrix is closely related to regularity. A symmetric interval matrix is positive definite if and only if it is regular and contains at least one positive definite matrix [115].

Definition 2.3.16 *The Frobenius norm for an interval matrix* $[A]$ *is denoted by* $\| [A] \|_F$ *and* $\| [A] \|_F = \sqrt{| \mathrm{tr}([\mathrm{A}]^{\mathrm{T}}[\mathrm{A}]) |} = \sqrt{\sum_{i,j} | [a_{ij}] |^2}$ *where* $\mathrm{tr}([\mathrm{B}])$ *is the trace of the interval matrix* $[B]$.

2.3.1.4 Paving and subpaving

Before describing the notions of paving and subpaving, we explain the principle of *bisection*.

Definition 2.3.17 *The bisection of a box* $[x]$ *is an operation that partitions this box into two other boxes* $L[x]$ *and* $R[x]$ *which are:*

$$L[x] = [\underline{x_1}, \overline{x_1}] \times ... \times \left[\underline{x_j}, \frac{\underline{x_j} + \overline{x_j}}{2}\right] \times ... \times [\underline{x_n}, \overline{x_n}], \tag{2.4}$$

$$R[x] = [\underline{x_1}, \overline{x_1}] \times ... \times \left[\frac{\underline{x_j} + \overline{x_j}}{2}, \overline{x_j}\right] \times ... \times [\underline{x_n}, \overline{x_n}], \tag{2.5}$$

where the j*th component of* $[x]$ *is bisected.*

Example 2.3.2 *The bisection of the first component of* $[x] = [-2, 2] \times [1, 3]$ *leads to two boxes:*

$$L[x] = [-2, 0] \times [1, 3] \text{ and } R[x] = [0, 2] \times [1, 3].$$

Definition 2.3.18 *A subpaving* $\mathbb{X}$ *of a box* $[x] \subset \mathbb{R}^n$ *is a union of non-overlapping sub-boxes of* $[x]$ *with non-zero width.*

Definition 2.3.19 *A subpaving of* $[x]$ *is regular if each of its boxes can be obtained from* $[x]$ *by a finite succession of bisections and selections.*

A regular subpaving may be represented as a binary tree [50].

Definition 2.3.20 *A regular subpaving of* $[x]$ *is minimal if it has no sibling leaves.*

Any non-minimal tree representative of a regular subpaving can be made minimal by discarding all sibling leaves so that their parents become leaves.

Definition 2.3.21 *When a subpaving* $\mathbb{X}$ *of a box* $[x]$ *covers* $[x]$ *then it is a paving of* $[x]$.

Example 2.3.3 *In the previous example,* $L[x]$ *and* $R[x]$ *define a paving of* $[x]$.

2.3.2 Interval arithmetic

The mathematical operations allowing to manipulate interval variables (intervals, boxes or matrices) are presented in this subsection. More details can be found in [86, 55, 50].

The classical operations $\{+, -, \times, /\}$ on real numbers can be extended to intervals:

$$[x] \diamond [y] = [\{x \diamond y \mid x \in [x], y \in [y]\}], \tag{2.6}$$

with $\diamond \in \{+, -, \times, /\}$.

Let $[x]$ and $[y]$ two intervals of $\mathbb{IR}$, the result of $[x] \diamond [y]$ is given by:

$$\left\{ \begin{array}{lcl} [x] + [y] & = & [\underline{x} + \underline{y}, \overline{x} + \overline{y}], \\ [x] - [y] & = & [\underline{x} - \overline{y}, \overline{x} - \underline{y}], \\ [x] \times [y] & = & [\min(\underline{x}\underline{y}, \underline{x}\overline{y}, \overline{x}\underline{y}, \overline{x}\,\overline{y}),\ \max(\underline{x}\underline{y}, \underline{x}\overline{y}, \overline{x}\underline{y}, \overline{x}\overline{y})], \\ 1 \,/\, [y] & = & \left\{ \begin{array}{l} [-\infty, \infty] \text{ si } 0 \in [y], \\ [1/\overline{y}, 1/\underline{y}] \text{ otherwise}, \end{array} \right. \\ [x] \,/\, [y] & = & [x] \times 1/[y]. \end{array} \right.$$

Example 2.3.4 *Consider the two intervals of* $\mathbb{IR}$, $[x] = [1, 3]$ *and* $[y] = [-1, 2]$. *We have:*

$$\left\{ \begin{array}{lcl} [x] - [y] & = & [1, 3] - [-1, 2] = [-1, 4], \\ [x] \times [y] & = & [1, 3] \times [-1, 2] = [-3, 6], \\ [x] \,/\, [y] & = & [1, 3] \times 1/[-1, 2] = [-\infty, +\infty] \text{ because } 0 \in [y]. \end{array} \right.$$

An elementary real function f can often be extended to interval context by the following expression:

$$f([x]) = [\inf_{x \in [x]}(f(x)), \sup_{x \in [x]}(f(x))]. \tag{2.7}$$

It is then easy to write down the expressions of different monotonic functions, for example:

$$\left\{ \begin{array}{rcl} \exp([x]) & = & [\exp(\underline{x}), \exp(\overline{x})], \\ \ln([x]) & = & \left\{ \begin{array}{l} [-\infty, \ln(\overline{x})]\ if\ 0 \in [x], \\ \emptyset\ if\ \overline{x} \leq 0, \\ [\ln(\underline{x}), \ln(\overline{x})]\ otherwise, \end{array} \right. \\ [x]^2 & = & \left\{ \begin{array}{l} [0, \max(\underline{x}^2, \overline{x}^2)]\ if\ 0 \in [x], \\ [\min(\underline{x}^2, \overline{x}^2), \max(\underline{x}^2, \overline{x}^2)]\ otherwise, \end{array} \right. \\ \sqrt{[x]} & = & \left\{ \begin{array}{l} \emptyset\ if\ \overline{x} \leq 0, \\ [\sqrt{\underline{x}}, \sqrt{\overline{x}}]\ if\ \underline{x} \geq 0, \\ [0, \sqrt{\overline{x}}]\ if\ 0 \in [x]. \end{array} \right. \end{array} \right. \tag{2.8}$$

Other non monotonic functions need specific analysis.

Example 2.3.5

$$\begin{cases} \exp([0,1]) &= [1,e], \\ \ln([-2,-1]) &= \emptyset, \\ [-2,2]^2 &= [0,4], \\ [-2,2]\times[-2,2] &= [-4,4], \\ \sqrt{[-2,4]} &= [0,2], \\ abs([-2,1]) &= [0,2], \\ \sin([0,\frac{2\pi}{3}]) &= [0,1], \\ \cos([0,\frac{2\pi}{3}]) &= [-\frac{1}{2},1]. \end{cases} \tag{2.9}$$

Let us notice that $[-2,2]^2$ and $[-2,2]\times[-2,2]$ provide different results, which is discussed follows.

2.3.3 Inclusion function

2.3.3.1 Some definitions

Definition 2.3.22 *The interval function $[f]$ from $\mathbb{IR}^n$ to $\mathbb{IR}^m$ is an inclusion function for f if:*

$$\forall [x]\in\mathbb{IR}^n, f([x])\subseteq[f]([x]). \tag{2.10}$$

Providing, for a large class of functions, an inclusion function $[f]$ giving for a box $[x]$ an image $[f]([x])$ not too large and computed reasonably quickly is one of the proposes of interval analysis.

Definition 2.3.23 *An inclusion function $[f]$ for f is thin if, for any punctual real interval vector $[x]=x$, $[f](x)=f(x)$.*

Definition 2.3.24 *An inclusion function $[f]$ for f is convergent if for any sequence of boxes $[x](k)$, we have:*

$$\lim_{k\to\infty} w([x](k))=0 \Rightarrow \lim_{k\to\infty} w([f]([x](k)))=0, \tag{2.11}$$

which implies:

$$\forall [x]\in\mathbb{IR}^n, [f]([x])=f([x]). \tag{2.12}$$

Definition 2.3.25 *The inclusion function $[f]$ for f is minimal if for any $[x]$, $[f]([x])$ is the smallest box containing $f([x])$. In this case, $[f]$ is noted $[f]^*$ and we have:*

$$\forall [x]\in\mathbb{IR}^n, [f]^*([x])=f([x]). \tag{2.13}$$

Definition 2.3.26 *A function $[f]$ is inclusion monotonic if:*

$$[x] \subset [y] \Rightarrow [f]([x]) \subset [f]([y]), \tag{2.14}$$

with $[x]$ and $[y]$ two boxes of $\mathbb{IR}^n$.

2.3.3.2 Natural inclusion function

There exist various methods to find a convergent inclusion function for a given function f, from $\mathbb{R}^n$ to $\mathbb{R}$. The simplest and the most direct way consists in replacing every pointwise number by an interval containing this number and the real elementary functions by their interval extensions. This method provides the *natural inclusion function*.

Theorem 2.3.1 *This theorem is taken from [50].*
Let a function f from $\mathbb{R}^n$ to $\mathbb{R}$ such that $f(x_1, x_2, ..., x_n) = y$ expressed as a finite composition of the operators $+, -, \times, /$ and of elementary continuous functions such that $\sin, \cos, \exp, ...$ A monotonic and thin inclusion $[f]$ for f is obtained by replacing each real variable x_i by an interval variable $[x_i]$ and each operator or function by its interval counterpart. If f involves only continuous operators and continuous elementary functions then $[f]$ is convergent. If moreover, each of the components of x occurs at most once in the formal expression of f then $[f]$ is minimal.

Example 2.3.6 *Consider the function f such that :*

$$f(x) = x^2 + 2x + 1.$$

A natural inclusion function of f is:

$$[f]([x]) = [x]^2 + 2 \times [x] + 1.$$

The evaluation of this function for $[x] = [-1, 1]$ is:

$$[f]([-1, 1]) = [-1, 1]^2 + 2 \times [-1, 1] + 1 = [0, 1] + [-1, 3] = [-1, 4].$$

Notice that the image of $[x]$ by f is $f([-1, 1]) = [0, 4]$, which verifies the inclusion relation (2.10).

Many works ([51, 107]) have proven that natural inclusion functions are rarely minimal. The pessimism is always introduced by the fact that each occurrence of an interval variable is considered as an independent variable with respect to other occurrences of the same variable. A given function has generally different formulations in natural interval arithmetic.

Example 2.3.7 *Consider the function $f : x \to x^2+2x+2$. This function can be rewritten under the following forms:*

$$\begin{cases} f_1(x) &= x(x+2)+2, \\ f_2(x) &= x \times x + 2 \times x + 2, \\ f_3(x) &= x^2 + 2 \times x + 2, \\ f_4(x) &= (x+1)^2 + 1, \end{cases} \tag{2.15}$$

and for $[x] = [-2, 1]$, we have:

$$\begin{cases} [f_1]([x]) &= [x]([x]+2)+2 = [-4, 5], \\ [f_2]([x]) &= [x] \times [x] + 2 \times [x] + 2 = [-4, 8], \\ [f_3]([x]) &= [x]^2 + 2 \times [x] + 2 = [-2, 8], \\ [f_4]([x]) &= ([x]+1)^2 + 1 = [1, 5]. \end{cases} \tag{2.16}$$

$[f_4]$ gives the smallest interval solution and it can be proven to be minimal.

The first observation on pessimism of interval arithmetic is that the evaluation of the function f depends on the number of occurrences of each interval variable in the expression of function f.

To reduce the pessimism introduced by multi-occurrences, the number of occurrences of each variable has to be reduced. If each variable appears just once in the function f, the natural inclusion function is minimal. Unfortunately there is no method which can be used systematically to find the minimal inclusion function. The natural inclusion function is still the simplest way to evaluate an interval function.

An approach to reduce pessimism consists in considering a *centered inclusion function*. This form is based on interval Taylor serie expansion [93, 103].

2.3.3.3 Centered inclusion function

Let f a function from $\mathbb{R}^n$ to $\mathbb{R}$. Assume that f is differentiable over every box $[x]$ in a subset $D \subset \mathbb{R}^n$, then:

$$\forall [x] \subset D, f(x) \in [f]_m([x]) = [f](m) + \left[\frac{df}{dx}\right]^T ([x])\ ([x] - m), \tag{2.17}$$

where m is the midpoint of $[x]$ and $\left[\frac{df}{dx}\right]^T ([x])$ is an inclusion of the gradient of f computed in $[x]$. $[f]_m$ is called the centered inclusion function.

The centered inclusion function gives generally a less pessimistic result compared to the natural inclusion function if $w([x])$ is not too large.

2.3.3.4 Convergence of the inclusion function

The criterion of convergence of inclusion functions was studied by Moore [87]. In his work, the convergence order of an inclusion function is defined as the largest integer α which satisfies:

$$\exists \beta \in \mathbb{R}^+ / w([f]([x])) - w(f([x])) \leq \beta w([x])^\alpha. \tag{2.18}$$

The convergence order of a minimal inclusion function is infinite. It shows that the centered inclusion function is more interesting than the natural inclusion function when the width of intervals is small. But for larger size intervals, it is preferable to use the natural inclusion function.

2.4 Implementation of set computation

To our knowledge, three approaches have been proposed during the last decades to solve linear or nonlinear equation systems. The first one is known as the *set inversion problem* [51], the second one is known as *direct image* [51] and the last one concerns the *constraint satisfaction* [15].

2.4.1 Set inversion problem

Consider the problem of determining a solution set $\mathbb{S}$ for the unknown quantities u, belonging to an *a priori* search set U, defined by:

$$\mathbb{S} = \{u \in \mathrm{U} | f(u) \in [y]\} = f^{-1}([y]) \cap \mathrm{U}, \tag{2.19}$$

where $[y]$ is a priori known and f a nonlinear function not necessarily invertible in the classical sense. (2.19) involves computing the reciprocal image of f and is known as a set inversion problem which can be solved using the algorithm *Set Inverter Via Interval Analysis* (denoted SIVIA). The algorithm SIVIA proposed in [51] is a recursive algorithm which explores all the search space without loosing any solution. This algorithm makes it possible to derive a guaranteed enclosure of the solution set $\mathbb{S}$ as follows:

$$\underline{\mathbb{S}} \subseteq \mathbb{S} \subseteq \overline{\mathbb{S}}. \tag{2.20}$$

The inner enclosure $\underline{\mathbb{S}}$ is composed of the boxes that have been proved feasible. To prove that a box $[u]$ is feasible, it is sufficient to prove that $f([u]) \subseteq [y]$. Reversely, if it can be proved that $f([u]) \cap [y] = \emptyset$, then the box $[u]$ is unfeasible. Otherwise, no conclusion can be reached and the box $[u]$ is said undetermined. The latter is then bisected and tested again until its size reaches a user-specified precision threshold $\varepsilon > 0$.

Such a termination criterion ensures that SIVIA terminates after a finite number of iterations.

Thus the algorithm SIVIA allows to obtain these two subpavings with a required precision ε, based on an inclusion test. The relation between the two subpavings can be characterized as:

$$\Delta\mathbb{S} = \overline{\mathbb{S}} \backslash \underline{\mathbb{S}}, \tag{2.21}$$

where $\Delta\mathbb{S}$ is called the inclusion test uncertainty, in which no decision can be made during the test. The properties of solutions are:

- if $\overline{\mathbb{S}} = \emptyset$ the problem (2.19) has no solution,
- if $\underline{\mathbb{S}} \neq \emptyset$, there exists at least one verified solution for (2.19).

2.4.1.1 Inclusion test

An inclusion test aims at verifying whether an interval, which is calculated with an inclusion function $[f]$, belongs to an *a priori* known set $[y]$. For any interval box $[x]$, three situations are evaluated:

- if $[f]([x]) \subseteq [y]$ then $[x] \subset \mathbb{S}$ and $[x]$ is called *feasible*, or *acceptable*,
- if $[f]([x]) \cap [y] = \emptyset$ then $[x]$ is called *unfeasible*, or *rejectable*,
- if $[f]([x]) \cap [y] \neq \emptyset$ then $[x]$ is called *uncertain*.

One of the purposes of SIVIA is to deal with the last situation, using the bisection.

2.4.1.2 SIVIA algorithm

The SIVIA algorithm determines the subpaving $\underline{\mathbb{S}}$ which contains the solutions and $\overline{\mathbb{S}}$ which contains the admissible boxes and undetermined boxes. This algorithm uses stacks: a stack $\mathcal{P}_{int}$ keeps all the intervals to be analyzed (the intermediate boxes). An initial box $[x](0) \in \mathbb{X}_0$ is supposed to contain all the solutions and it is placed in the stack $\mathcal{P}_{int}$.

During the execution of the algorithm, the first element of the stack is retrieved as a box $[x]$. This operation extracts the element on the top of the stack. Its image by the inclusion function $[f]$ is then compared to the known set $[y]$. If the box $[x]$ is undetermined and its width is superior to ε (a user predefined size), it is then bisected; the two subpavings $[x]_1$ and $[x]_2$ are put on the top of the stack $\mathcal{P}_{int}$. If the box $[x]$ is acceptable, $[x]$ is added to the stacks $\underline{\mathbb{S}}$ and $\overline{\mathbb{S}}$, or it is undetermined but it can no longer be divided, $[x]$ is added to the stack $\overline{\mathbb{S}}$.

Algorithm 1 Algorithm SIVIA($[f]$,$[y]$,$[x]$,ε, $\underline{\mathbb{S}}$, $\overline{\mathbb{S}}$)

Input: $[f]$,$[x](0)$,$[y]$,ε;
Output: $\underline{\mathbb{S}}$, $\overline{\mathbb{S}}$;

```
initialization: P_int := [x](0); S_in = [ ], S_out = [ ];
[x]:=getTop(P_int);
if [f]([x]) ⊂ [y] then
    S_in := S_in ∪ [x]; S_out := S_out ∪ [x];
else if [f]([x]) ∩ [y] ≠ ∅ and w([x]) < ε then
    S_out := S_out ∪ [x];
else if [f]([x]) ∩ [y] ≠ ∅ and w([x]) ≥ ε then
    bisectBox([x]) → {[x]_1, [x]_2 | [x]_1 ∪ [x]_2 = [x]};
    P_int := P_int ∪ [x]_1, P_int := P_int ∪ [x]_2;
end if
if P_int ≠ ∅ then
    SIVIA([f],[y],P_int,ε, S_in, S_out);
end if
```

The function $getTop$ retrieves a box from the stack, and $bisectBox$ divides a box into two sub-boxes. The box stack $\Delta\mathbb{S} = \overline{\mathbb{S}}\backslash\underline{\mathbb{S}}$, which represents the uncertainty of the solution set, contains the undetermined boxes, the dimension of which is smaller than the predefined threshold ε.

It is clear that SIVIA is a recursive algorithm; its complexity is exponential, depending on the size of the variable vector. The number of bisections is estimated as inferior to:

$$\left(\frac{w([x](0))}{\varepsilon} + 1\right)^n. \tag{2.22}$$

$[x](0)$ is the initial search box as mentioned above, n is the dimension of vector $[x]$. This number can be reduced using contraction or preconditioning methods, which are discussed in section 2.4.3.

Remark 2.4.1 *The strategy of bisection is an important issue, which can influence the efficiency of an algorithm. An overview of different strategies is given in [136]. The choice of strategy is based on the algorithm requirements, considering a tradeoff between efficiency, convergence, implementation complexity and speed.*

2.4.2 Direct image of a subpaving

Computing the direct image of a subpaving $\mathbb{X}$ by a function f from $\mathbb{R}^n$ to $\mathbb{R}^m$ is more complicated than computing the reciprocal image because interval analysis does not di-

rectly provide an inclusion test for the point test.
In the following, we assume that f is a continuous function and $[f]$ is a convergent inclusion function of f.
An algorithm presented in [50], called ImageSP, generates a regular subpaving $\overline{\mathbb{Y}}$ that contains the image $\mathbb{Y}$ of the regular subpaving $\mathbb{X}$ by f :

$$\mathbb{Y} = \{y \in \mathbb{R}^m \mid y \in f(\mathbb{X})\}. \tag{2.23}$$

This algorithm ImageSP allows to compute a regular subpaving $\overline{\mathbb{Y}}$ which is guaranteed to contain the set $\mathbb{Y}$.

The set $\mathbb{Y}$ is included in the box $[f]([\mathbb{X}])$, that means in the image by the inclusion $[f]$ of the smallest box containing $\mathbb{X}$:

$$\begin{array}{rcl} \mathbb{Y} & = & f(\mathbb{X}) \subset \overline{\mathbb{Y}}, \\ \overline{\mathbb{Y}} & \subset & [f]([\mathbb{X}]). \end{array} \tag{2.24}$$

The algorithm ImageSP is divided into three steps : mincing, evaluation and regularization. These steps are described below:

1. Mincing consists in generating a non-minimal regular subpaving $\mathbb{X}_\varepsilon$ from successive bisections of $\mathbb{X}$ which contains only boxes whose length is less than a required accuracy ε, with $\varepsilon > 0$ sufficiently small.

2. Evaluation computes the image by the function $[f]$ of the boxes $[x]$ in $\mathbb{X}_\varepsilon$. The resulting boxes are stored into a list $\mathcal{U}$.

3. Regularization computes a regular subpaving $\overline{\mathbb{Y}}$ that contains the union $\mathbb{U}$ of all boxes of $\mathcal{U}$. This step can be viewed as the call of SIVIA to invert $\mathbb{U}$ by the identity function. In fact if $f(\mathbb{X}) \subset \mathbb{U}$, then $f(\mathbb{X}) \subset \mathrm{Id}^{-1}(\mathbb{U})$. Thus this problem can be posed as a set-inversion problem.

The SIVIA algorithm used in ImageSP is a version based on an inclusion test [50].

2.4.3 Constraint satisfaction

To solve a problem described as an interval equation system, we can use constraint propagation [48]. In fact, the inclusion relations and equations can be interpreted as constraints and the *resolution* of such a system can then be taken into a Constraint Satisfaction Problem (CSP). Let us recall the basic definitions:

Algorithm 2 Algorithm ImageSP (f,$\mathbb{X}$,ε)

Input: $[f]$,$\mathbb{X}$,ε;
Output: $\overline{\mathbb{Y}}$;
1: $\mathbb{X}_\varepsilon :=$ mince$(\mathbb{X}, \varepsilon)$;
2: $\mathcal{U} := \emptyset$, $\mathcal{U}$ is a list and $\mathbb{U}$ is the set of boxes in $\mathcal{U}$;
3: for each $[x] \in \mathbb{X}_\varepsilon$, add $[f]([x])$ to the list $\mathcal{U}$;
4: SIVIA $\left(([y] \subset \mathbb{U}), [f](\mathbb{X}), \varepsilon, \underline{\mathbb{Y}}, \overline{\mathbb{Y}}\right)$.

Definition 2.4.1 *A Constraint Network (CN) $H = (\mathcal{X}, \mathcal{D}, \mathcal{C})$ is defined by:*
- a set of variables $\mathcal{X} = \{x_1, ..., x_n\}$,
- a set of value domains $\mathcal{D} = \{D_1, ..., D_n\}$ where D_i is the domain associated to the variable x_i,
- a set of constraints $\mathcal{C} = \{C_1, ..., C_m\}$, linking the variables $\mathcal{X}$.

The resolution of a CN is a CSP.
For example, an interval linear system of the form $(0 \in [A][X] - [B])$ can be represented as a CN: $[CN(A \in [A],\ B \in [B],\ X \in [X],\ AX = B)]$ where the interval matrices $[A]$, $[X]$ and $[B]$ are respectively in $\mathbb{IR}^{m \times n}$, $\mathbb{IR}^{n \times 1}$ and $\mathbb{IR}^{m \times 1}$.

We can rewrite the CN row by row:

$$H = \left(\begin{array}{l} \mathcal{X} = \{[x_1], ..., [x_n]\}, \\ \mathcal{D} = \{\mathbb{IR}, ..., \mathbb{IR}\}, \\ \mathcal{C} = \left\{ \mathcal{C}_i : 0 \in \sum_{k=1}^{n} [a_{i,k}][x_k] - [b_i] \right\}, \\ i = 1, ..., m. \end{array} \right). \tag{2.25}$$

The solution S of the CSP : $H = (\mathcal{X}, \mathcal{D}, \mathcal{C})$ is the set of all the values affected to the corresponding variables at the same time.

2.4.3.1 Contraction and consistency of a CSP

The resolution of a CSP starts from an infinite domain or a bounded domain. The reduction of the domain is known as a local consistency problem, which can take the form of *node consistency, arc consistency, or path consistency* [16, 69]. The operation is called *constraint propagation* or *contraction*, which is based on the equivalent relation below:

Definition 2.4.2 *Two CSP $\mathcal{H}_1$ and $\mathcal{H}_2$ are equivalent if and only if they have the same set of solutions.*

Remark 2.4.2 *For the same set of variables $\mathcal{X}$ and the same set of constraints $\mathcal{C}$, different sets of variable domains $\mathcal{D}_i$ define different CSP $\mathcal{H}_i$.*

Definition 2.4.3 *A contractor $\mathcal{R}$ for a CSP $\mathcal{H}_1 = (\mathcal{X}, \mathcal{D}_1, \mathcal{C})$ is an operator that can shrink the domain $\mathcal{D}_1$ into a domain $\mathcal{D}_2$ without losing any solution, such that:*

$$\mathcal{D}_2 \subset \mathcal{D}_1.$$

The new CSP $\mathcal{H}_2$ is equivalent to $\mathcal{H}_1$.

A CSP is solvable when it is equivalent to a CSP in which the infinite quantity domain is replaced by a larger value in computation. The contractor aims to reduce the initial domain into an as small as possible domain. The principle is to reject the parts of the domain which are not consistent with the constraints.

Definition 2.4.4 *A CSP : $\mathcal{H} = (\mathcal{X}, \mathcal{D}, \mathcal{C})$ is globally consistent if and only if:*

$$(\forall x_i \in D_i,\ \exists (x_1, ..., x_i, ..., x_n) \in \mathcal{D} \mid \forall C(x_1, ..., x_i, ..., x_n) \in \mathcal{C}, C(x_1, ..., x_i, ..., x_n) \text{ is verified},)$$

in which $C(x_1, ..., x_i, ..., x_n)$ is a single constraint with a set of variables.

Global consistency can be interpreted as the correspondance between the defined domain and the variation of the constraints for all the variables. In such a case, a globally consistent CSP gives a minimal exterior estimation of the equivalent system equation of the solution.

There is a large choice of contractors. Each has its own advantages and shortcomings, system characteristics and available information. We use these criteria to classify different contractors: constraint linearity, constraints, and size of $[x]$, which is $w([x])$. The first criterion to consider is the linearity of the constraints, which defines two categories, linear CSPs and nonlinear CSPs. More information on CSPs can be found in [15] or in [136].

2.4.3.2 Convergence of contractors

The contraction is an operation that reduces the search space to a no longer compressible domain. Its size depends on the initial uncertainty of the system. The result is yielded by an iterative process:

$$\mathcal{D}_{k+1} = \mathcal{R}(\mathcal{D}_k).$$

The algorithm stops when:

$$\mathcal{D}_{k+1} = \mathcal{R}(\mathcal{D}_k) = \mathcal{D}_k.$$

The solution $\mathcal{S}$ of CSP $\mathcal{H} = (\mathcal{X}, \mathcal{D}, \mathcal{C})$ can be provided by the suitable contractor for this CSP which verifies the properties:

- contractible: $[x] \subset \mathcal{D} \Rightarrow \mathcal{R}([x]) \in \mathcal{D}$,
- monotone: $[x] \subset \mathcal{D}, [x]' \subset \mathcal{D}; [x] \subset [x]' \Rightarrow \mathcal{R}([x]) \subset \mathcal{R}([x]')$,
- idempotent: $[x] = \mathcal{S} \Rightarrow \mathcal{R}([\mathcal{S}]) = [\mathcal{S}]$.

Monotonicity is a property of the inclusion function. If the series $\mathcal{D}_{k+1} = \mathcal{D}_k \cap \mathcal{R}(\mathcal{D}_k)$ is an inclusion function, it should be monotonic which yields to a minimal function. Among all the contractors, the fix point contractors are those that are idempotent.

For a convergent CSP , we have, from a certain k:

$$\mathcal{D}_s = \mathcal{D}_{k+1} = \mathcal{R}(\mathcal{D}_k) = \mathcal{D}_k,$$

where $\mathcal{D}_s$ represents the solution of the CSP.

In practice, the convergence is validated when the difference of the size of two domains from two successive iterations is less than a predefined size.

2.5 Guaranteed state and parameter estimation

This section concerns the integration of Equations (2.1) and set inversion computation. Thus, the objective of this section is firstly to obtain the state vector x at the sample times $\{t_1, t_2, ..., t_N\}$ corresponding to the measurement times of the outputs. Secondly, follows the SIVIA procedure to get the validated sets of feasible parameters.

2.5.1 Validated integration using Taylor expansions

Rigorous solution for dynamical nonlinear systems can be solved efficiently by considering methods based on Taylor expansions [86], [112], [9] or [92]. These methods consist in two steps: the first one verifies the existence and uniqueness of the solution using the fixed point theorem and the Picard-Lindelöf operator. At a time t_{j+1}, an a priori box $[\tilde{x}_j]$ containing all solutions corresponding to all possible trajectories between t_j and t_{j+1} is computed. In the second step, the solution at t_{j+1} is computed using a Taylor expansion, where the remainder term is $[\tilde{x}_j]$.

To obtain the set $[\tilde{x}_j]$, a classical technique consists in inflating this set until it verifies the inclusion

$[x_j] + [0, h_j] f([\tilde{x}_j]) \subseteq [\tilde{x}_j]$ (see [75], [92] for details) where h_j denotes the integration step and $[x_j]$ the first solution. In the proposed work, the package VNODE-LP ([90], [92]) has been used. In this package, the previous validated integration method is implemented.

2.5.2 Parameter Estimation

In a bounded error context, measures and modeling errors are supposed to be unknown but to stay within known and acceptable bounds. Errors between measured and predicted outputs may rely on many factors, among them: limited sensors accuracy, interferences, noise, structured uncertainties, etc. Some are quantifiable, some are not. We consider here the quantifiable error ν given by (2.2), which is added to the model output y. To estimate model parameters (2.1), we have to get the set $\mathbb{P}$ of all parameters p enclosed in an a priori search set $[\mathcal{U}_\mathcal{P}]$ such that the error between real data and model outputs belongs to $\mathbb{E}$.

The characterization of the set $\mathbb{P}$ may be defined as a set inversion problem (2.19):

$$\mathbb{P} = v^{-1}(\mathbb{E}) \cap [\mathcal{U}_\mathcal{P}]. \tag{2.26}$$

A guaranteed enclosure of $\mathbb{P}$ may be computed using the SIVIA algorithm presented in the first chapter.

2.6 Conclusion

Through this chapter, the main tools on the bounded-error models, interval analysis (and more specially interval matrices), guaranteed state and parameter estimation used in following chapers are presented. In the bounded-error context, the set of all parameters consistent with the model structure, the measurements and the bounds on the perturbations can be defined as the set estimate for the parameters. And, such as in the stochastic framework, before performing a parameter estimation procedure (or before performing a diagnosis procedure), it is necessary to analyse identifiability of the model (diagnosability of the model). The following chapter concerns original definitions of set-membership identifiability and set-membership diagnosability described by Equations given in Section 2.2. The links between these definitions are exhibited and two tests allowing to analyse them are presented.

Chapter 3

Identifiability and diagnosability for uncertain dynamical models

3.1 Introduction

In this chapter, two properties for nonlinear dynamical uncertain models are considered: identifiability and diagnosability.
Identifiability is a concept that decides to what extent it is possible to *uniquely* infer the parameter values of a mathematical model, assuming that it has the same structure as the system, from input-output measurements. In other words, if a model is identifiable, it is theoretically possible to infer the true value of the parameters from rich enough experimental data representing the system's input-output behavior. Mathematically, this is equivalent to say that there exists an unambiguous mapping between the model parameters and the output trajectories. Identifiability is hence a pre-condition for safely running a parameter estimation procedure and for obtaining trustable results.

In spite of abundant literature about set-membership identification and parameter estimation [101], the identifiability problem has only rarely been discussed in the case of uncertain models.
Following some scarce works [13] which provide the intuition of identifiability applied to bounded-error uncertain models, we propose in this work two complementary definitions, named set-membership identifiability and μ-set-membership-identifiability, that we introduced in [46, 47]. The first one is purely conceptual whereas the second one subsumes classical identifiability while nicely bringing the notion of granularity at which identifiability is considered. These two properties are carefully motivated and related to properties found in the literature, in particular interval identifiability, ε-global identifiability and partial injectivity.

On the other hand, diagnosability [123] is the property that guarantees that the sensored values delivered by the available instrumentation can be processed into an appropriate set of symptoms discriminating different faulty situations. Diagnosability can be checked at design phase so that one knows beforehand which faults the diagnoser will be able to discriminate with the specified instrumentation during operation. From another perspective, this property provides the means to identify the set of additional sensors that are required to achieve a given degree of diagnosability.

In this work, we suppose that a fault is an unpermitted deviation of at least one characteristic property or parameter of the system from the acceptable standard condition. Hence faults correspond to parameter variations and the problem of diagnosability has been shown to be closely related to the problem of being able to infer univocally the value of the parameters from the measurements. However, in most situations, it is not important to distinguish faults by their precise values; one would like to distinguish classes of faults. For example, assessing whether a hole in a pipe is of 11mm or 12mm diameter is of no interest. Nevertheless, the order of magnitude is important and one would like to distinguish a hole of 10mm of diameter from a hole of 50mm. In addition, nominal conditions are generally known with uncertainty i.e. the parameter values are given with some tolerances. We show that this problem can be solved by approaching diagnosability in a set-membership framework, hence proposing the concept of *set-membership-diagnosability*. This concept is closely linked to the properties of *set-membership-identifiability* and μ-*set-membership-identifiablity*. These three properties are deeply analysed and the links between them are established.

Set-membership-diagnosability is ultimately interpreted through a partition of the parameter space defined thanks to set-membership-identifiability and μ-set-membership-identifiablity.

Another part of this chapter provides operational methods to check the properties studied in the set-membership framework. Two methods for checking set-membership and μ-set-membership-identifiability are presented. They take inspiration from well established methods for checking classical identifiability, namely the Taylor Series approach of [95] for the first one, and the differential algebra approach [31, 76, 74, 94] for the second one. The second method, based on differential algebra, is shown to be easily extendable to nonlinear uncertain systems with parameters varying according to polynomial laws.
A method for determining the partitioning of the parameter space in terms of set-membership identifiable sets is also proposed to assess set-membership-diagnosability. Set-membership and μ-set-membership identifiability are shown to be essential to characterize a partition of the parameter space into output trajectory distinguishable regions. Thanks to this partition, we can analyze the mathematical model and derive its properties with respect to the uncertainties that are represented.

3.2 Concept of set-membership identifiability (SM-identifiability)

3.2.1 Problem formulation and motivations

The problem considered firstly in this chapter is identifiability of bounded uncertain parameter models (controlled or uncontrolled) presented in the first chapter (Equation 2.1).

We note $Y_{\Gamma_1}(t_i, P)$ the set value of the outputs of the model (Equation 2.1) arising from P at time t_i. Notice that P may be reduced to a single point.

Set-membership parameter estimation assumes uncertain output data given by sets $\{z(t_1), ..., z(t_N)\}$. These may be issued from several runs of the real system or by adding a bounded error term to measured outputs. The set-membership parameter estimation problem is formulated as finding the set of parameter vectors $\mathcal{P} = \{p^* \in \mathbb{R}^p\}$ such that the arising trajectories hit all the output data sets, i.e.:

$$\forall p^* \in \mathcal{P}, y(t_i, p^*) \in z(t_i), i = 1, \ldots, N.$$

$\mathcal{P}$ is called the feasible parameter set.

An interesting feature of set-membership parameter estimation is that it can be indifferently applied to classically identifiable and non-identifiable dynamical systems.

Example 3.2.1 *Consider for instance the following nonlinear continuous system in which p is an unknown parameter:*

$$\begin{cases} \dot{x}(t, p) = x(t, p) + t\cos(p), \\ x(0, p) = x_0. \end{cases} \tag{3.1}$$

The solution of (3.1) is $x(t, p) = x_0 e^t + (-1 - t + e^t)\cos(p)$. An admissible set for p is given by $\mathcal{U}_\mathcal{P} = [0, 2\pi]$ and it is clear that this system is not globally identifiable. It is enough to notice, for example, that the pair $(p_1 = \pi/4, p_2 = 7\pi/4)$ results in the same trajectory, as shown on Figure (3.1).

In a set-membership framework, i.e. considering set values for p, the feasible parameter set would be made of the union of two disjoint connected sets $[p_1] \subseteq [\pi/2, 3\pi/2]$ and $[p_2] \subseteq]3\pi/2, 2\pi]$. On the other hand, if the feasible parameter set is equal to $P^* = [\pi/2, 3\pi/2]$, it can be expected to be reduced to one single connected set because the trajectories arising from P^* are not shared by other regions of the parameter space. Despite non identifiability, we can consider that P^* is *set-membership-identifiable*. Nevertheless, this is not true for all the subsets of P^*, which means that *set-membership-identifiability* is lost in the parameter subspace defined by P^*. We say that P^* is not *μ-set-membership-identifiable*.

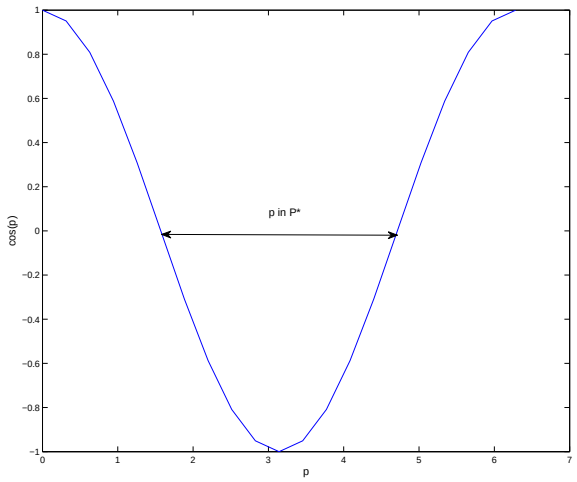

Figure 3.1: Representation of a non-identifiability model

When considering the set-membership identification of the system Γ_1 given by (2.1), we would like to know beforehand whether the feasible parameter set $\mathcal{P}$ can be expected to be reduced to one single connected set or not and in which regions of the parameter space. Like for classical parameter estimation [58], this property indicates that the problem is mathematically well-posed.

Definition 3.2.1 *A set-membership parameter estimation problem is said to be* sound *if the feasible parameter set $\mathcal{P} \subseteq \mathcal{U}_\mathcal{P}$ is reduced to one single connected set. In this case, $\mathcal{P}$ is also said to be sound.*

In practice, the feasible parameter set $\mathcal{P}$ remains implicit and the solution returned by set-member-
ship parameter estimation algorithms is a set that encloses all parameter values consistent with the measurements and the assumed uncertainty. This solution is said to be *guaranteed*. On the other hand, the enclosure may be unfortunately quite conservative due to set operations. In addition, a set-membership parameter estimation problem is always formulated with a given stopping criterion that specifies the smallest size of the sets to be considered, i.e. the *set precision*, which is at best equal to the numerical precision. The size of a connected bounded set is given by its *diameter* as defined below.

Definition 3.2.2 *Let us consider a connected bounded set Π of $\mathbb{R}^p$ and d a classical metric on $\mathbb{R}^p$. Let us define $\delta(\Pi)$ as the* diameter *of Π. $\delta(\Pi)$ is given by the least upper bound of $\{d(\pi_1,\ \pi_2),\ \pi_1, \pi_2 \in \Pi\}$. If Π is not bounded, we define $\delta(\Pi) = +\infty$ ([12]).*

The following section concerns the definitions of *set-membership identifiability*.

3.2.2 Set-membership identifiability

This section proposes a formulation of the set-membership (SM)-identifiability problem for the class of systems formalized by (Equation 2.1). The framework for SM-identifiability proposed in [47] is recalled. It provides a generalization of classical identifiability for which specializations to the set-membership context can be derived. The links with classical identifiability are exhibited and related definitions existing in the litterature are analysed.
In the following, we note $Y_{\Gamma_1}(P,u)$ (respectively $Y_{\Gamma_1}(P)$) the set of output trajectories, solution of Γ_1 with P and the input u (resp. when $u=0$). It is also called the output behavior of Γ_1 arising from P.

3.2.2.1 Definitions

The proposed definitions are given in the case of controlled systems but they can be stated similarly in the case of uncontrolled systems. In these definitions, P^* is a connected set of $\mathbb{R}^p$.

Definition 3.2.3 *For the model Γ_1 given by (2.1), $P^* \neq \emptyset$, $P^* \subseteq \mathcal{U}_\mathcal{P}$, is* globally SM-identifiable *if there exists an input u such that $Y_{\Gamma_1}(P^*,u) \neq \emptyset$ and $Y_{\Gamma_1}(P^*,u) \cap Y_{\Gamma_1}(\tilde{P},u) \neq \emptyset,\ \tilde{P} \subseteq \mathcal{U}_\mathcal{P} \Longrightarrow P^* \cap \tilde{P} \neq \emptyset$.*

Definition (3.2.3) expresses that a connected set P^* is globally SM-identifiable if the output behavior of Γ_1 arising from P^*, i.e. the output behavior of Γ_1 for any $p \in P^*$, is distinguishable from the output behavior of Γ_1 arising from its complementary set $\bar{P}^*$, i.e. $Y_{\Gamma_1}(P^*,u)$ and $Y_{\Gamma_1}(\bar{P}^*,u)$ do not share any output trajectory.

On the metric space (Π,d), let μ be a continuous map from Π to Π. μ is a *contraction* if there is a nonnegative number $\lambda < 1$ such that for all $\pi_1,\ \pi_2$ in Π, $d(\mu(\pi_1),\mu(\pi_2)) < \lambda d(\pi_1,\pi_2)$ [89].

The definition of μ-SM-identifiability is as follows.

Definition 3.2.4 *The nonempty bounded connected set $P^* \subseteq \mathcal{U}_\mathcal{P}$ is globally μ-SM-identifiable if, for all contraction μ from P^* to P^*, $\mu(P^*)$ is globally SM-identifiable.*

Under the conditions of Definition 3.2.3 (resp. 3.2.4), we equivalently say that the model Γ_1 given by (2.1) is globally SM-identifiable (resp. μ-SM-identifiable) with respect to P^*.

Definition 3.2.4 differs from Definition 3.2.3 in that the set P^* may be reduced as small as desired by the contraction μ while still retaining the SM-identifiability property. This is true by the Banach fixed-point theorem, which implies that the diameter of $\mu(P^*)$ tends to zero [89]. Hence μ-SM-identifiability meets classical identifiability and, interestingly, it means that classical identifiability holds for any $p \in P^*$. If the diameter $\delta(\mu(P^*))$ of $\mu(P^*)$ cannot be lower than ε without loosing SM-identifiability, we refer to *ε-SM-identifiability* [47].

Definition 3.2.5 *Consider a SM-identifiable nonempty bounded connected set $P^* \subseteq \mathcal{U}_\mathcal{P}$, then P^* is globally ε-SM-identifiable if there exists a contraction μ from P^* to P^* such that $\mu(P^*)$ is not SM-identifiable and $\mu(P^*) < \varepsilon$.*

To summarize, the definition of μ-SM-identifiability subsumes classical identifiability, while leading to the concept of ε-SM-identifiability, which is specific to the set-membership framework [47].

To take into account for possible singularities in $\mathcal{U}_\mathcal{P}$, μ-SM-identifiability can be generically extended to *structural μ-SM-identifiability*, which means that the model set Γ_1 is μ-SM-identifiable with respect to $P^* \subset \mathcal{U}_\mathcal{P}$ except for a subset of points of zero measure in $\mathcal{U}_\mathcal{P}$. Let us notice that defining the structural counterpart of SM-identifiability, as given by Definition 3.2.3, is not relevant because in this definition, P^* cannot be of zero measure. The same is true for ε-SM-identifiability as explained in [13].

Like for classical identifiability, local counterparts of SM-identifiability, ε-SM-identifiability, and μ-SM-identifiability can be defined when these properties do not hold in the whole parameter space $\mathcal{U}_P$ but only in an open neighborhood W of P^* such that the properties hold for Γ_1 with $\mathcal{U}_\mathcal{P}$ restricted to W. In the following, SM-identifiability, ε-SM-identifiability, and μ-SM-identifiability are understood as global when not indicated otherwise.

The above concepts are illustrated with the model described by Equation (3.1) in which p is now considered as an uncertain parameter for which the admissible set is $\mathcal{U}_\mathcal{P} = [0, 2\pi]$. The formal solution is $x(t, p) = x_0 e^t + (-1 - t + e^t)\cos(p)$. If we consider $P_1^* = [\pi/2, 3\pi/2]$, the model is globally SM-identifiable with respect to P_1^*. Global SM-identifiability is easy to verify from the plot of the function $\cos$ on $[0, 2\pi]$. Indeed, there is no trajectory arising from $[\pi/2, 3\pi/2]$ that is identical to a trajectory arising from its complementary set in $\mathcal{U}_\mathcal{P}$. However, P_1^* is not μ-SM-identifiable. Indeed, it is enough to find a contraction μ such that $\mu(P_1^*) \subseteq [\pi/2, \pi]$, which is obviously possible.

3.2.2.2 Links with classical identifiability

In this subsection, Γ_1^{p,x_0} denotes a specific model of the family of models represented by (2.1), with $p \in P$ and $x_0 \in \mathbb{X}_0$. Thus, for this model, $Y_{\Gamma_1}(p, u)$ is reduced to a unique

trajectory and will be denoted $y(.,p,u)$. x_0 is assumed to be no equilibrium point of the system.
The following definitions of identifiability are considered.

Definition 3.2.6 *The parameter p_i is globally identifiable if there exists $u(t) \in \mathbb{R}^r$ such that for all $(\hat{p}, p^*) \in \mathcal{U}_p$, $\hat{p} \neq p^*$:*

$$(\forall t \in [0,T],\ y(t,\hat{p},u) = y(t,p^*,u)) \Rightarrow (\hat{p}_i = p_i^*),$$

and the parameter vector p is globally identifiable in $\mathcal{U}_p$ if all its components p_i are globally identifiable in $\mathcal{U}_p$.
The model Γ_1^{p,x_0} is said to be globally identifiable if all parameters p_i are globally identifiable.

The previous definitions have been generically extended to local and structural identifiability.

The following proposition gives the link between Definitions 3.2.4 and 3.2.6.

Proposition 3.2.1 *If for all $x_0 \in \mathbb{X}_0$, Γ_1^{p,x_0} is (structurally) globally identifiable, then Γ_1 is (structurally) globally μ-SM-identifiable and in particular ε-SM-identifiable.*
Reciprocally, if P^* is (structurally) globally μ-SM-identifiable for Γ_1 then for all $x_0 \in \mathbb{X}_0$, Γ_1^{p,x_0} is (structurally) globally identifiable on P^* [1].

Remark 3.2.1 *Global SM-identifiability does not imply global identifiability with respect to P^*. Indeed, according to example 3.2.1, the model is globally SM-identifiable for P_1^* but not globally identifiable (in the classical sense) at p^* with respect to P_1^*.*
Ultimately, μ-SM-identifiability subsumes classical identifiability and SM-identifiability as defined in Definition 3.2.3 as it provides the means to control the set P^*. This is possible thanks to the contraction $\mu(.)$.

3.2.2.3 Links with interval identifiability

The notion of interval identifiability has been introduced in [32] for compartmental models and has been generalized in [127]. These works concern the identifiability analysis of unidentifiable linear models of the form ([131]):

$$\begin{cases} \dot{x}(t,p) = Kx(t,p) + Bu(t), \\ y(t,p) = Cx(t,p), \\ x(0,p) = 0, \end{cases} \tag{3.2}$$

[1] Γ_1^{p,x_0} is not necessary globally identifiable on $\mathcal{U}_\mathcal{P}$ since two parameters in the complement of P^* can lead to the same trajectory.

where the hypothesis are same as (2.1). $K = [k_{ij}]$, $B = [b_{ij}]$ and $C = [c_{ij}]$ are constant and $p \in \mathbb{R}^p$ is the unknown parameter vector.

The entries of K (fractional transfer rates when x_i's are masses) satisfy the following compartmental constraint relations for $i, j = 1, ..., n$:

$$k_{ij} \geq 0,\ i \neq j,$$
$$-k_{0i} = \sum_{j=1}^{n} k_{ji} \leq 0.$$

The model parameter vector p is defined as all the unknowns k_{0i} and k_{ij}, $i \neq j$ and all unkowns b_{ij} and c_{ij}. The k_{ij} components of p are nonnegative, b_{ij} and c_{ij} are also usually nonnegative. Thus the a priori parameter domain $\mathbb{R}^v_+$ is defined by: $\mathbb{R}^p_+ = \{p :\ p_i \geq 0,\ i = 1, 2, ..., p\}$.
To consider the identifiability properties of p at any particular (nominal) parameter value $p^* \in \mathbb{R}^p_+$, the dependance of the output y on p and the input u, denoted $y(t, p, u)$ is emphasized.
If the model is unidentifiable, then for almost any $p^* \in \mathbb{R}^p_+$ there exists an uncountable subset $\Omega(p^*) \subset \mathbb{R}^p_+$ such that every $\bar{p} \in \Omega(p^*)$ generates the same input-output behaviour, that is $y(t, \bar{p}, u) = y(t, p^*, u)$. The parameter interval strategy is based on the idea that in most compartmental models, the set $\Omega(p^*)$ is bounded for almost every $p^* \in \mathbb{R}^v_+$ where:

$$\Omega(p^*) = \{\bar{p} \in \mathbb{R}^v_+,\ y(t, \bar{p}, u) = y(t, p^*, u)\ \forall t\ \forall u\}. \tag{3.3}$$

Moreover, the inequalities implied for all components of p localize unidentifiable parameters within finite intervals. The following definitions were proposed in [127] to take into account the above concept[2].

Definition 3.2.7 *The model described by (3.2) is interval-identifiable at $p^* \in \mathbb{R}^p_+$ if it is unidentifiable at p^* and the set $\Omega(p^*)$ defined by (3.3) is bounded.*

Definition 3.2.8 *The model described by (3.2) is (structurally) interval-identifiable if it is interval-identifiable for (almost) all $p^* \in \mathbb{R}^v_+$.*

A bounded set $\Omega(p^*)$ yields lower and upper bounds $\bar{p}_i^{min}$ and $\bar{p}_i^{max}$ on each $\bar{p}_i$.

Local and global interval identifiability can be differentiated in the same way as local and global identifiability. Two methods to analyze (local) interval-identifiability can be found in [127] or [32]. They are based on a transfer function approach or on a similarity transformation approach.

[2]Without changing the definitions, their names have been adapted to be consistent with the other definitions presented in this work.

3.2.2.4 Links with ε-global identifiability

Most of the time, one gets structural identifiability which can be inconvenient for the experimenter since there may exist atypical regions in $\mathcal{U}_p$ for which identifiability's conclusions are false. The authors in [13] have proposed to introduce the notion of global identifiability in $P \subset \mathcal{U}_P$ (g.i.i.P) which does not allow any more the existence of such regions. The definition is the following:

Definition 3.2.9 *Given $(u, x_0) \in \mathbb{R}^r \times X_0$, the parameter p_i is globally identifiable in P (g.i.i.P) if:*

$$\forall (p^*, \hat{p}) \in P^2,\ y(., \hat{p}, u) \equiv y(., p^*, u) \Rightarrow \hat{p}_i = p_i^*,$$

and the parameter vector p is g.i.i.P if all its components are g.i.i.P.

Another way to formulate this condition is:

$$y(., \hat{p}, u) \equiv y(., p^*, u),\ \| p^* - \hat{p} \|_\infty > 0 \tag{3.4}$$

has no solution for $(p^*, \hat{p}) \in P \times P$.
Indeed, this problem comes back to a constraint satisfaction problem described in chapter 2. It can be solved by an *Interval constraint propagation* (ICP) which guarantees outer approximations of the solutions of CSP's. This definition is close to the μ-SM-identifiability definition.

In practice, condition (3.4) is substituted by

$$y(., \hat{p}, u) \equiv y(., p^*, u),\ \| p^* - \hat{p} \|_\infty > \varepsilon \tag{3.5}$$

and we talk of ε-g.i.i.P which is close to the ε-SMI.
The difference between the definitions proposed in [13] and our definitions is of structural order. First of all, in our definitions, the trajectories arising from P^* and its complement are compared so that all the admissible parameters domain is viewed. It allows one to know if the feasible parameters set has to be reduced to initiate an algorithm for estimating the parameters. On the contrary, using the definitions proposed in [13], we verify that a domain P^* does not contain atypical regions in order to use ICP with no ambiguity. In that case, it is important to be insured that P^* contains the desired parameters value.

Example 3.2.2 *Consider the following model ([13]) $\eta(p) = p(p-1)(p+1)$ with $p \in [-2, 2]$. If $P^* = [-a, a]$, $a = 2/\sqrt{3}$ then the model is g.i.i.P^* but not μ-SMI with respect to P^* [3]. Obviously, if $\mathcal{U}_p$ is restricted to P^*, P^* is μ-SMI.*

[3] In plotting the function η, it is clear that η is injective on P^* but some p^* in P^* and $\hat{p}$ in the complement of P^* will give the same value of η.

Furthermore, our definitions are naturally adapted to set-membership-identification. Indeed, if the μ-SM-identifiability for example is verified, we know that in decomposing P^* into two boxes, the trajectories arising from these two sub-boxes will be distinct and a criteria on the trajectories will allow one to reject one of the sub-box.

3.2.2.5 Links with partial injectivity

The definition of partial injectivity of a function has been introduced in [63]. This notion perfectly characterizes μ-SM-identifiability. A second definition named restricted-partial injectivity is proposed in this work in order to characterize global SM-identifiability.

Definition 3.2.10 *Consider a function $f : \mathcal{A} \to \mathcal{B}$ and any set $\mathcal{A}_1 \subseteq \mathcal{A}$. The function f is said to be a partial injection of $\mathcal{A}_1$ over $\mathcal{A}$, noted $(\mathcal{A}_1, \mathcal{A})$-injective, if $\forall a_1 \in \mathcal{A}_1$, $\forall a \in \mathcal{A}$,*

$$a_1 \neq a \Rightarrow f(a_1) \neq f(a).$$

f is said to be $\mathcal{A}$-injective if it is $(\mathcal{A}, \mathcal{A})$-injective.

In [63], an algorithm based on interval analysis for testing the injectivity of a given differentiable function is presented and a solver called ITVIA (Injectivity Test Via Interval Analysis) implemented in C++ is mentioned[4]. From a given function, the solver partitions a given box into two domains: a domain on which the function is partially injective and an indeterminate domain on which the function may be injective or not. When the latter is empty, the function is injective over the initial box. In [63], the authors give an example for testing structural identifiability of a model.

In order to characterize global SM-identifiability, the notion of restricted-partial injectivity is introduced. The algorithm proposed in [63] can be easily adapted for testing this new definition.

Definition 3.2.11 *Consider a function $f : \mathcal{A} \to \mathcal{B}$ and any set $\mathcal{A}_1 \subseteq \mathcal{A}$. The function f is said to be a restricted-partial injection of $\mathcal{A}_1$ over $\mathcal{A}$ or a $(\mathcal{A}_1, \mathcal{A})$-restricted-injection if $\forall a_1 \in \mathcal{A}_1$, $\forall a \in \mathcal{A}_1^c$,*

$$a_1 \neq a \Rightarrow f(a_1) \neq f(a),$$

where $\mathcal{A}_1^c$ is the complement of $\mathcal{A}_1$ in $\mathcal{A}$.

In the following proposition, (restricted-)partial injectivity is given in terms of trajectories and this formulation makes the direct link with the definition of identifiability possible.
Consider the set of outputs S_u arising from $\mathcal{U}_\mathcal{P}$ for a given input u.

[4]Let us notice that the solver ITVIA has been implemented only for particular functions $f : \mathbb{R} \to \mathbb{R}^2$ and $f : \mathbb{R}^2 \to \mathbb{R}^2$.

Property 3.2.1 *Given the model Γ_1, P^* is SM-identifiable (resp. μ-SM-identifiable) for an input u if and only if the function $\phi : \mathcal{U}_\mathcal{P} \rightarrow S_u : p \rightarrow y(.,p)$ is a restricted-partial injection of P^* over $\mathcal{U}_P$ (resp. partial injection of P^* over $\mathcal{U}_P$), i.e. if for all $p^* \in P^*$ and $\bar{p} \in \bar{P}^*$, $p^* \neq \bar{p} \Rightarrow y(.,p^*,u) \not\equiv y(.,\bar{p},u)$ (resp. for all $p^* \in P^*$ and $\bar{p} \in \mathcal{U}_\mathcal{P}$, $p^* \neq \bar{p} \Rightarrow y(.,p^*,u) \not\equiv y(.,\bar{p},u)$).*

Proof – Sufficiency Suppose that $y(.,p^*,u) \equiv y(.,\bar{p},u)$ for $p^* \in P^*$, $\bar{p} \in \bar{P}^*$. It leads to $Y_{\Gamma_1}(P^*,u) \cap Y_{\Gamma_1}(\bar{P},u) \neq \emptyset$ with $P^* \cap \bar{P}^* = \emptyset$ and P^* is not globally SM-identifiable. Proving that SM-identifiability of P^* implies the partial injection of ϕ comes back to define a contraction μ such that $\mu(P^*) \cap \bar{P} = \emptyset$ where $\bar{P}$ is in the complement of $\mu(P^*)$. *Necessity* Suppose that $Y_{\Gamma_1}(P^*,u) \cap Y_{\Gamma_1}(\bar{P}^*,u) \neq \emptyset$. There exist $p^* \in P^*$ and $\bar{p} \in \bar{P}^*$ such that $y(.,p^*,u) \equiv y(.,\bar{p},u)$. If ϕ is a restricted partial injection of P^* over $\mathcal{U}_p$, one gets $p^* = \bar{p}$, that is $P^* \cap \bar{P} \neq \emptyset$. Thus, P^* is μ-SMI. □

3.3 Set-membership diagnosability (SM-diagnosability)

3.3.1 Problem formulation and motivations

Diagnosability is the property that guarantees that the sensored values delivered by the available instrumentation can be processed into an appropriate set of symptoms discriminating different faulty situations. Importantly, diagnosability can be checked at design phase so that one knows beforehand which faults the diagnoser will be able to discriminate with the specified instrumentation during operation. From another perspective, this property provides the means to identify the set of -additional- sensors that are required to achieve a given degree of diagnosability.

A fault is an unpermitted deviation of at least one characteristic property or parameter of the system from the acceptable standard condition. Faults hence correspond to parameter variations and the problem of diagnosability has been shown to be closely related to the problem of being able to infer univocally the value of the parameters from the measurements. In this work, links between identifiability and diagnosability are established through the new concept of *functional diagnosability*.

However, as said in introduction, in most situations, it is not important to distinguish faults by their precise values but one would like to distinguish classes of faults.
We introduce the concept of *SM-diagnosability*.

3.3.1.1 Introduction

Two definitions of SM-diagnosability are provided: strong or weak SM-diagnosability. We consider the diagnosability analysis of set-membership (controlled or uncontrolled) models of the form (2.1) in which faults and disturbances have been explicitely introduced:

$$\Gamma_2 \begin{cases} \dot{x}(t,\theta) = g(x(t,\theta), u(t), v(t), f, \varepsilon, p), \\ y(t,p) = h(x(t,p), u(t), v(t), f, \varepsilon, p), \\ x(t_0,p) = x_0 \in \mathbb{X}_0, \\ p \in P \subset \mathcal{U}_{\mathcal{P}}, \\ t_0 \leq t \leq T, \end{cases} \tag{3.6}$$

where the hypothesis are same as (2.1).
The function g is real and analytic on M, where M is an open set of $\mathbb{R}^n$ such that $x(t,p) \in M$ for every $t \in [t_0,\ T]$ and $p \in P$. The vector of faults f belongs to a connected set of faults F wich belongs to $\mathcal{F}_{\mathcal{SYS}}$, where $\mathcal{F}_{\mathcal{SYS}}$ is an exhaustive set of known faults, $f \in \mathbb{R}^e$. $v(t)$ is some unknown input vector and ε is some stochastic vector ($v = 0$ means no perturbation, $f = 0$ means no fault and $\varepsilon = 0$ means no noise). p denotes the parameters vector.

$Y(P,F,u)$ (resp. $Y(P,F)$) denotes the set of outputs, solution of Γ_2 with the input u (resp. when $u = 0$), the vector of P and the vector of faults F. In this work, a fault f_i is defined as a variation of one parameter.

In the following definitions, F_1 and F_2 are two connected sets describing two fault situations in $\mathcal{F}_{\mathcal{SYS}}$. These situations correspond to the two following cases:

> -the occurence of the fault F_1 or F_2 introduces perturbations on the system that are assumed to be bounded,
>
> -the magnitude of the fault is assumed to vary within a bounded set. For example think about a clogged pipe section for which the clog increases with time (because a dirt accumulation).

F_1 and F_2 are called "bounded faults".

In this work, *set-membership diagnosability* is shown through the notion of *functional signature* which is established firstly in classical context. The *functional signature* can be linked to differential algebra concepts and more specially variable eliminations.

From elimination theory, some differential polynomials or analytical redundancy relations (ARR) linking system inputs, outputs and their derivatives can be obtained. In the last decade, algorithms for obtaining such ARRs have been developed and implemented in softwares as Maple [11]. They are based on differential algebra [60] and consist in

eliminating unobservable state variables in order to obtain relations linking outputs, inputs and parameters. The use of ARRs permit to detect [47], isolate and estimate the severity of a fault which, in this work, is an unpermitted deviation of parameter of the system from the standard deviations.

Several definitions of diagnosability have been formed around the use of ARRs. The classical diagnosability definition consists in comparing fault signatures [23]. The fault signature is a function which associates to a fault the set containing indicators obtained from measured variables. Typically, the fault signature of f_j is the m-vector formed of zeros and ones: when the fault f_j acts on the residual ρ_i formed from an ARR, the number 1 is put in the i^{th} component of the f_j signature otherwise it is 0. The authors in [26] consider that a system is diagnosable if each fault component can be written as a solution of a polynomial equation in f_j and finitely many time derivatives of inputs and outputs. This definition is close to the one of identifiability proposed by [74]. However, the definition of diagnosability proposed in [26] is based on the obtention of particular differential polynomials which may require lots of manipulations of the model equations. In case of complex models, it is often impossible to obtain such relations even in using dedicated symbolic softwares. Furthermore, the order of derivatives is so high that the obtained relations can not be exploited for fault detection.
Thus, in our work, we propose to use the works proposed in [29] to study identifiability and consequently diagnosability. In [29], according to a particular elimination order, the authors propose to study identifiability of models' parameters from differential polynomials containing one or fewer parameters. The advantages of these polynomials are that they are easier to obtain and they contain derivatives of lower orders.
We propose the definition of *functional diagnosability*; this definition is based on ARRs. This definition allows to know if the generated trajectories can be distinguished and at the same time, if single faults can be detected.

In the following subsections, the expression and obtention through variable elimination of ARRs are presented in a stochastic framework.

3.3.1.2 Diagnosability and detectability from ARRs in the stochastic framework

In [119], the authors propose to use ARRs for fault detection and isolation in algebraic dynamic systems. An ARR links the system inputs and outputs and their derivatives. The following notations are used. If ϑ is a vector, $\bar{\vartheta}^{(k)}$ is the vector whose components are ϑ and its time derivatives up to order $k > 0$, $\bar{\vartheta}$ stands for ϑ and its time derivatives up to some (unspecified) order. Consider the set of ARRs: $w(\bar{y}, \bar{u}, \bar{v}, f, \bar{\varepsilon}, p) = 0$. It can be

decomposed as:

$$w(\bar{y}, \bar{u}, \bar{v}, f, \bar{\varepsilon}, p) = w_d(\bar{y}, \bar{u}, \bar{v}, f, p) - w_s(\bar{y}, \bar{u}, \bar{v}, f, \bar{\varepsilon}, p) = 0,$$

where $w_d(\bar{y}, \bar{u}, \bar{v}, f, p) = w_0(\bar{y}, \bar{u}, p) - w_1(\bar{y}, \bar{u}, f, p) - w_2(\bar{y}, \bar{u}, \bar{v}, f, p)$ is the deterministic part (a polynome of degree zero in the components of $\bar{\varepsilon}$): $w_0(\bar{y}, \bar{u}, p)$ the perturbation and fault-free part, $w_1(\bar{y}, \bar{u}, f, p)$ is the part without unknown input vector, $w_2(\bar{y}, \bar{u}, \bar{v}, f, p)$ is the part of the polynomial depending on the unknown input vector. $w_s(\bar{y}, \bar{u}, \bar{v}, f, \bar{\varepsilon}, p)$ is the stochastic part (a polynomial of degree at least one in some components of $\bar{\varepsilon}$).
To simplify the problem, the authors supposed that there are no unknown inputs, that is $v = 0$ which implies $w_2(\bar{y}, \bar{u}, 0, f, p) = 0$. Afterwards, v is no longer considerated in the ARRs and w can be rewritten:

$$w(\bar{y}, \bar{u}, f, \bar{\varepsilon}, p) = w_0(\bar{y}, \bar{u}, p) - w_1(\bar{y}, \bar{u}, f, p) - w_s(\bar{y}, \bar{u}, f, \bar{\varepsilon}, p) = 0. \tag{3.7}$$

Thus, the following relation is always true:

$$w_0(\bar{y}, \bar{u}, p) = w_1(\bar{y}, \bar{u}, f, p) + w_s(\bar{y}, \bar{u}, f, \bar{\varepsilon}, p).$$

The residual defined by $\rho = w_0(\bar{y}, \bar{u}, p)$ which involves only known variables is used for detecting faults. In absence of noise and faults, ρ is identically zero for any triple $(\bar{y}, \bar{u}, p)$ which satisfies (2.1) since $w_1(\bar{y}, \bar{u}, 0, p) = w_s(\bar{y}, \bar{u}, 0, 0, p) = 0$.
In most cases, there is no simple characterization of the residual's stochastic behavior, in particular for established fault detection procedures. That is why, the authors in [119] propose to detect fault from the deterministic part of the residual. A fault is also detectable if $w_1(\bar{y}, \bar{u}, f, p) \neq 0$.

Afterwards, if several ARRs are obtained, they will be denoted $w_i(\bar{y}, \bar{u}, f, \varepsilon, p)$ and their corresponding deterministic part, $w_{0,i}(\bar{y}, \bar{u}, p) - w_{1,i}(\bar{y}, \bar{u}, f, p)$.

In the following section, a method for obtaining ARRs from existing softwares is presented. The advantage of this method is to give ARRs of a particular form from which a functionally diagnosability method has been deduced.

3.3.1.3 Obtaining ARRS through variable elimination in the stochastic framework

A way to obtain ARRs is to use the Rosenfeld-Groebner algorithm implemented in Maple [11]. The original version of this method does not consider initial conditions and some interesting results have been obtained on the number of ARRs and their form ([31], [76] and [74], [29]). The following results are inspired from [29] in which faults are not considered. Their results are adapted to the fault case.
The system Γ_2 can be rewritten as a differential polynomial system completed with $\dot{p}_i = 0$,

$i = 1, \ldots, p$, $\dot{f}_j = 0$, $j = 1, \ldots, e$ thus the following system composed of polynomial equations and inequalities is obtained:

$$\begin{cases} p(\bar{x}, \bar{u}, f, p) = 0, \\ q(\bar{x}, \bar{y}, f, p) = 0, \\ r(\bar{x}, \bar{y}, f, p) \neq 0, \\ \dot{p}_i = 0,\ i = 1, \ldots, p,\ \dot{f}_j = 0,\ j = 1, \ldots, e \end{cases} \tag{3.8}$$

Let $\mathcal{I}$ the radical of the differential ideal generated by (3.8): $\mathcal{I}$ is endowed with the following ranking which eliminates the state variables:

$$[p, f] \prec [y, u] \prec [x]. \tag{3.9}$$

It admits a characteristic presentation $\mathcal{C}$ (i.e. a canonical representant of the ideal) which has the following form [11]:

$$\begin{aligned} &\Big\{\dot{p}_1, \ldots \dot{p}_p, \dot{f}_1, \ldots \dot{f}_e, w_1(\bar{y}, \bar{u}, f, p), \ldots, w_m(\bar{y}, \bar{u}, f, p), \\ &Q_1(\bar{y}, \bar{u}, f, p, x), \ldots, Q_n(\bar{y}, \bar{u}, f, p, x)\} \end{aligned} \tag{3.10}$$

where the leader of the polynomial w_i is y_i for $i = 1, \ldots, m$.
$\mathcal{C}(f, p)$, the particular characteristic presentation $\mathcal{C}$ evaluated in $(f,\ p)$ is proved to contain the differential polynomials $w_1(\bar{y}, \bar{u}, f, p), \ldots, w_m(\bar{y}, \bar{u}, f, p)$ which can be expressed as:

$$w_i(\bar{y}, \bar{u}, f, p) = m_{0,i}(\bar{y}, \bar{u}) + \textstyle\sum_{k=1}^{n_i} \gamma_k^i(p) m_{k,i}(\bar{y}, \bar{u}) - \sum_{k=1}^{s_i} \tilde{\gamma}_k^i(f, p) \tilde{m}_{k,i}(\bar{y}, \bar{u}) \tag{3.11}$$

where $(\gamma_k^i(p))_{1 \leq k \leq n_i}$ (resp. $\tilde{\gamma}_k^i(f, p)$) are rational in p (resp. f, p), $\gamma_u^i \not\equiv \gamma_v^i$ $(u \neq v)$ and $\tilde{\gamma}_u^i \not\equiv \tilde{\gamma}_v^i$ $(u \neq v)$, $(m_{k,i}(\bar{y}, \bar{u}))_{1 \leq k \leq n_i}$ (resp. $(\tilde{m}_{k,i}(\bar{y}, \bar{u}))_{1 \leq k \leq s_i}$) are differential polynomials with respect to y and u and $m_{0,i}(\bar{y}, \bar{u}) \not\equiv 0$.
According to the previous notations, $w_i = w_{0,i} - w_{1,i}$ with $\rho_i = w_{0,i} = m_{0,i}(\bar{y}, \bar{u}) + \displaystyle\sum_{k=1}^{n_i} \gamma_k^i(p) m_{k,i}(\bar{y}, \bar{u})$ and $w_{1,i} = \displaystyle\sum_{k=1}^{s_i} \tilde{\gamma}_k^i(f, p) \tilde{m}_{k,i}(\bar{y}, \bar{u})$ where the index i corresponds to the i^{th} polynomial.

In the following section, the functional diagnosability definition is proposed.
We can notice that in the classical sense of diagnosability, if two faults act on the same residuals, their classical signatures, noted Sig in the following, are the same. Thus theoretically it is not possible to distinguish them. With the proposed definition, the residuals can have different behaviors depending on the fault that acts. The proposed work has been published in [130].

3.3.1.4 Functional diagnosability in the stochastic framework

The following definition of functional fault signature is proposed.

Definition 3.3.1 *The functional fault signature is a function Sig_{funct} which associates to a fault f_j the vector $(w_{1,i}(\bar{y}, \bar{u}, f_j, p))_{i=1,\dots,m}$.*

We note $Sig^{(i)}_{funct}(f_j) = w_{1,i}(\bar{y}, \bar{u}, f_j, p)$, the ith component of $Sig_{funct}(f_j)$.

Example 3.3.1 *Consider the following Bernoulli equation in which, to simplify the expression, we omit p in $y(t,p)$ where $p = (\beta_1, \beta_2)^T$. This omission is made in the whole chapter 3:*

$$\dot{y}(t) = \beta_1 y(t) + \beta_2 y(t)^2, \text{ for } t \in [0,5],\ y(0) = 1. \tag{3.12}$$

The solution is $y(t) = \frac{\beta_1 e^{\beta_1 t}}{\beta_1 + \beta_2 - \beta_2 e^{\beta_1 t}}$.
We have directly $w_0(\bar{y}, p) = \dot{y}(t) - \beta_1 y(t) - \beta_2 y(t)^2$.
Suppose that some positive single faults f_1 and f_2 impact respectively on the two parameters β_1 and β_2, hence $w_1(\bar{y}, f, p) = -f_1 y(t) - f_2 y(t)$ and $f = (f_1, f_2)$. One can deduce that $Sig(f_1) = Sig(f_2) = 1$ and $Sig_{funct}(f_1) = f_1 y(., f_1)$, $Sig_{funct}(f_2) = f_2 y(., f_2)^2$ where $y(., f_i)$ denotes the output depending only on the fault f_i for $i = 1, 2$. As it will be seen in the following section, the behavior of residuals can be distinguished.

$Sig_{funct}(f_j)$ is also a vector of functions, each component of which constitutes a trajectory. The following definitions propose to link the functional signature and the notions of discriminality and diagnosability. The first one is true for all inputs, whereas the second one is verified only for one input.

Definition 3.3.2 *Two faults f_j and f_l are input-strongly functionally discriminable if $Sig_{funct}(f_j) \neq Sig_{funct}(f_l)$ in the sense that for all input u, there exists at least one index i^*, a finite time $t_1 > t_0$ such that for all $t \in [t_0, t_1]$, $Sig^{(i^*)}_{funct}(f_j) \neq Sig^{(i^*)}_{funct}(f_l)$.*
When all the faults are input-strongly functionally discriminable, the model is said input-strongly functionally diagnosable.

Definition 3.3.3 *Two faults f_j and f_l are input-weakly functionally discriminable if $Sig_{funct}(f_j) \neq Sig_{funct}(f_l)$ in the sense that there exits an input u, there exists at least one index i^*, a finite time $t_1 > t_0$ such that for all $t \in [t_0, t_1]$, $Sig^{(i^*)}_{funct}(f_j) \neq Sig^{(i^*)}_{funct}(f_l)$.*
When all the faults are input-weakly functionally discriminable, the model is said input-weakly functionally diagnosable.

When the model is uncontrolled, we have the following definition:

Definition 3.3.4 *Two faults f_j and f_l are functionally discriminable if $Sig_{funct}(f_j) \neq Sig_{funct}(f_l)$ in the sense that there exists at least one index i^*, a finite time $t_1 > t_0$ such that for all $t \in [t_0, t_1]$, $Sig^{(i^*)}_{funct}(f_j) \neq Sig^{(i^*)}_{funct}(f_l)$.*
When all the faults are functionally discriminable, the model is said functionally diagnosable.

Remark– Signatures of faults can be collected in a tabular whose i^{th} line and j^{th} column component contains the i^{th} residual with the fault f_j, that is $w_{1,i}(\bar{y}, \bar{u}, f_j, p)$. For example, consider the following model:

Example 3.3.2 *We consider the following model:*

$$\begin{cases} \dot{x}_1(t) = (p_1 + f_1)(p_2 + f_2)x_1(t)^2 + x_1(t)x_2(t), \\ \dot{x}_2(t) = (p_2 + f_2)(p_3 + f_3)x_2(t)^2 + x_2(t)x_3(t), \\ \dot{x}_3(t) = (p_1 + f_1)(p_3 + f_3)x_3(t)^2 + x_1(t)x_3(t), \\ y_1(t) = x_1(t),\ y_2(t) = x_2(t),\ y_3(t) = x_3(t). \end{cases} \tag{3.13}$$

It is easy to verify that:

$$\begin{array}{l} w_{0,1}(\bar{y}, \bar{u}, p) = \dot{y}_1 - y_1 y_2 - p_1 p_2 y_1^2, \\ w_{0,2}(\bar{y}, \bar{u}, p) = \dot{y}_2 - y_2 y_3 - p_2 p_3 y_2^2, \\ w_{0,3}(\bar{y}, \bar{u}, p) = \dot{y}_3 - y_1 y_3 - p_1 p_3 y_2^2. \end{array} \tag{3.14}$$

and

$$\begin{array}{l} w_{1,1}(\bar{y}, \bar{u}, f, p) = (p_1 f_2 + p_2 f_1 + f_1 f_2) y_1^2, \\ w_{1,2}(\bar{y}, \bar{u}, f, p) = (p_2 f_3 + p_3 f_2 + f_2 f_3) y_2^2, \\ w_{1,3}(\bar{y}, \bar{u}, f, p) = (p_1 f_3 + p_3 f_1 + f_1 f_3) y_3^2. \end{array} \tag{3.15}$$

The following functional signatures are also $Sig_{funct}(f_1) = (p_2 f_1 y_1^2, 0, p_3 f_1 y_3^2)^T$, $Sig_{funct}(f_2) = (p_1 f_2 y_1^2, p_3 f_2 y_2^2, 0)^T$, $Sig_{funct}(f_3) = (0, p_2 f_3 y_2^2, p_1 f_3 y_3^2)^T$.
Diagnosability can be seen according to the following table:

$Sig_{funct}(f)\,/\,f$	f_1	f_2	f_3
$Sig^{(1)}_{funct}(f)$	$p_2 f_1 y_1^2$	$p_1 f_2 y_1^2$	0
$Sig^{(2)}_{funct}(f)$	0	$p_3 f_2 y_2^2$	$p_2 f_3 y_2^2$
$Sig^{(3)}_{funct}(f)$	$p_3 f_1 y_3^2$	0	$p_1 f_3 y_3^2$

Clearly, for $j, l = 1, 2, 3$, $j \neq l$, $Sig_{funct}(f_j) \neq Sig_{funct}(f_l)$ and the model is functionally diagnosable.

Afterwards, the considered ARRs are those obtained at section 3.3.1.3. Thus, the functional signature will is:

$$Sig_{func}(f_i) = \left(\sum_{k=1}^{s_i} \tilde{\gamma}^i_k(f, p) \tilde{m}_{k,i}(\bar{y}, \bar{u}) \right)_{i=1,\ldots,m}.$$

3.3.2 Extension to the set-membership framework

In this subsection, we consider the model Γ_2 with $\varepsilon = 0$.

Definition 3.3.5 *The set-membership functional signature is a function Sig_{SM} which associates to the connected set F_j the interval vector $(w_{1,i}(Y(P,u),u,F_j,P))_{i=1,\ldots,m}$. $Sig^{(i)}_{SM}(F_j)$ designates the ith component of $Sig_{SM}(F_j)$ and corresponds to an interval functional vector.*

Definition 3.3.6 *Two bounded faults F_1 and F_2 are weakly SM-discriminable if $Sig_{SM}(F_1)$ and $Sig_{SM}(F_2)$ are distinct in the sense that there exists at least one index i^* and $[t_1,\ t_2]$ such that $\forall t \in [t_1,\ t_2]$, $(Sig^{(i^*)}_{SM}(F_1) \not\subseteq Sig^{(i^*)}_{SM}(F_2)$ or $Sig^{(i^*)}_{SM}(F_2) \not\subseteq Sig^{(i^*)}_{SM}(F_1))$ and $Sig^{(i*)}_{SM}(F_1) \cap Sig^{(i*)}_{SM}(F_2) \neq \emptyset$.*

Definition 3.3.7 *Two bounded faults F_1 and F_2 are strongly SM-discriminable if there exists $i^* \in \{1,...,m\}$ and $[t_1,\ t_2]$ such that $\forall t \in [t_1,\ t_2]$, $Sig^{(i^*)}_{SM}(F_1) \cap Sig^{(i^*)}_{SM}(F_2) = \emptyset$.*

Definition 3.3.8 *The model Γ_2 given by (3.6) is weakly SM-diagnosable for $\mathcal{F}_{\mathcal{SYS}}$ if for any two bounded faults, these two faults are weakly SM-discriminable.*

Definition 3.3.9 *The model Γ_2 given by (3.6) is strongly SM-diagnosable for $\mathcal{F}_{\mathcal{SYS}}$ if for all*
$F_1,\ F_2 \subset \mathcal{F}_{\mathcal{SYS}}$, these two faults are strongly SM-discriminable. [5]

3.3.3 Links between SM-diagnosability and SM-identifiability

F corresponds to a vector of connected sets-valued components. When single faults are considered, only one of the components of F is not equal to zero. Without loss of generality, only uncontrolled systems are considered.

Property 3.3.1 *In the case of single faults, if the model Γ_2 is strongly SM-diagnosable then it is globally SM-identifiable "according to the faults". Under the hypothesis that $\Delta w_{1,i}(\bar{y},\bar{u})$ is not identically equal to zero, the reciprocal is true.*

Proof – Sufficiency by contrapositive. Suppose, there exists $\bar{F} \in \mathcal{F}_{\mathcal{SYS}}$ such that $Y(P,F^*) \cap Y(P,\bar{F}) \neq \emptyset$ and $F^* \cap \bar{F} = \emptyset$. Thus, there exist $f^* \in F^*$, $\bar{f} \in \bar{F}$, $p \in P$ such that $y^* = y(p,f^*) = y(p,\bar{f})$. Considering again the ARR (3.11), one gets for all $i = 1,\ldots,m$, $w_i(\bar{y},f^*,p) = w_i(\bar{y},\bar{f},p)$ which implies $w_{1,i}(\bar{y}^*,f^*) = w_{1,i}(\bar{y}^*,\bar{f})$. Finally,

[5] If the input u is not equal to zero then the previous definitions are available in input-weak and input-strong.

$Sig^{(i)}_{SM}(F^*) \cap Sig^{(i)}_{SM}(\bar{F}) \neq \emptyset$ and the model is not SM-diagnosable.
Necessity by contrapositive. Suppose that the model is not strongly SM-diagnosable, that is there exist two distinct simple bounded faults F^* and $\bar{F}$ and at least one index i such that $Sig^{(i)}_{SM}(F^*) \cap Sig_{SM}(\bar{F}) \neq \emptyset$. Consequently, there exist $f^* \in F^*$, $\bar{f} \in \bar{F}$, $f^* \neq \bar{f}$ such that $w_{1,i}(\bar{y}^*, f^*, p) = w_{1,i}(\bar{y}, \bar{f}, p)$, in particular $\sum_{k=1}^{n_i} (\tilde{\gamma}^i_k(f^*, p)\tilde{m}_{k,i}(\bar{y}^*) - \tilde{\gamma}^i_k(\bar{f}, p)\tilde{m}_{k,i}(\bar{y})) = 0$.
If y^* and $\bar{y}$ are identically equal, the hypothesis, $det(\tilde{m}_{k,i}(\bar{y}),\ k = 1, \ldots, n_i) \neq 0$ implies that $\gamma^i_k(f^*, p) = \tilde{\gamma}^i_k(\bar{f}, p)$, in particular the function ϕ defined in Proposition 1.2.1 verifies $\phi(f^*) = \phi(\bar{f})$ with $f^* \neq \bar{f}$ and the model is not SM-identifiable. □

3.4 Methods to analyze SM-identifiability

In the literature, different approaches have been proposed to study global identifiability of nonlinear systems: for example, the revisited Taylor Series approach of [52], those based on the local state isomorphism theorem [132], [18], [17], [28] or those based on differential algebra [74], [4], [118]. In this work, two methods are proposed: the first one is based on the power series expansion of the solution and the second one on differential algebra. For these two methods, the notion of (weak-)partial injectivity using interval analysis is needed.

3.4.1 Power Series Expansion Method (PSE Method)

The PSE method is inspired of [95], which studied identifiability according to the Taylor series expansion of the solution. In this approach, the outputs are expanded in a Taylor series around $t = 0$ and the successive terms of the expansion are expressed as functions of the model unknowns. Then, an equivalence is given between identifiability of the initial system and the existence of a unique solution of an algebraic system that is specified. In our approach, for having global SM-identifiability of P^*, the solutions of the algebraic system must be in P^*. Otherwise, there would exist common trajectories arising from P^* and its complementary set. For having μ-SM-identifiability, an injectivity assumption on P^* is needed.

Consider the set of model outputs $Y^m_{\Gamma_1}$ and $a_k(.) \in Y^m_{\Gamma_1}$: the k^{th} derivative of $a_0(.)$ which is a particular output. Then, consider the following assumptions which are refered as H in the following:

- S is the set of feasible states,

- $u(.)$ and $x(0)$ are such that $x(t) \in S$ for all $t \in [0, T]$,
- for all possible trajectories $x(.)$, the function $f(x(.), u(.), p)$ admits a Taylor series expansion on $[0, T]$ or the function $f(x, u(.), p)$ is Lipschitz continuous on $[0, T]$ for all states $x \in S$.

P^* is supposed to be a given connected set and $a_0(.) \in Y_{\Gamma_1}(P^*, u) \subset Y^m_{\Gamma_1}$.
The following theorem gives a necessary condition for having global (μ-)SM-identifiability. It allows one to insure that no trajectory arising from the complement of P^* is the same as one among those arising from P^*. It can be used for proving non (μ/ε) SM-identifiability.

Theorem 3.4.1 *Under the assumptions H, if for an input u^*, $P^* \neq \emptyset$ is globally SM-identifiable (resp. μ-SM-identifiable), the system:*

$$\frac{d^k}{dt^k}[g(x(0, p), p)] = a_k(0),\ k = 0, 1, \ldots, +\infty, \tag{3.16}$$

where g is the observation function of system Γ_1, admits at least one solution in the connected set P^* (resp. a unique solution).

Proof – By assumption, g is analytic and (3.16) admits solutions in P^*. If P^* is μ-SM-identifiable, there is a one-to-one correspondence between a trajectory and a parameter vector and hence the unicity of the solution.□

The following theorem gives a sufficient condition for proving that P^* is globally SM-identifiable.

Theorem 3.4.2 *If there exists u^* such that $Y_{\Gamma_1}(P^*, u^*) \neq \emptyset$ and all the solutions of (3.16) are in $P^* \neq \emptyset$ then P^* is globally SM-identifiable.*

Proof – Suppose that $Y_{\Gamma_1}(P^*, u^*) \cap Y_{\Gamma_1}(\bar{P}, u^*) \neq \emptyset$ for $\bar{P} \subset \mathcal{U}_{\mathcal{P}}$. There exists a trajectory $y^* \in Y_{\Gamma_1}(P^*, u^*) \cap Y_{\Gamma_1}(\bar{P}, u^*)$. In particular, there exist $p^* \in P^*$, $\bar{p} \in \bar{P}$ solutions of (3.16) for which the right member $a_k(.)$ corresponds to $y^{*(k)}(.)$. Hence, $\bar{p} \in P^*$ and $P^* \cap \bar{P} \neq \emptyset$.□

An additional condition is required for P^* to be globally μ-SM-identifiable. Indeed, since the global SM-identifiability must be verified for any $\mu(P^*)$ where $\mu : P^* \to P^*$ is a contraction, the parameter $\bar{p}$ may not be included in $\mu(P^*)$. A supplementary injectivity hypothesis allows one to obtain μ-SM-identifiability as it is seen in the following theorem.

Theorem 3.4.3 *Suppose there exists u^* such that $Y_{\Gamma_1}(P^*, u^*) \neq \emptyset$ and the solutions of (3.16) for a finite number d of equations are in the connected set $P^* \neq \emptyset$. If the function*

$\phi : p \in \mathcal{U}_p \mapsto (g(x(0,p),p), \ldots, \frac{d^{d-1}}{dt^{d-1}}[g(x(0,p),p)]) \in (\mathbb{R}^m)^d$ *is* $(P^*, \mathcal{U}_\mathcal{P})$*-injective, then* P^* *is* μ*-SM-identifiable.*

Remark 3.4.1 *The exponent* $d-1$ *is the number of times that* $y(t,p) = g(x(t,p),p)$ *must be derived so that the resulting system taken at* $t = 0$ *admits solutions.*

Proof – The injectivity hypothesis ensures that the trajectories evaluated with parameters in P^* are all distinct.□

For obtaining the system (3.16), complex mathematical developments are generally required. However, some classes of systems have nice properties and are easily solved, for example linear systems ([95]).

Example 3.4.1 *Consider the following uncertain system taken from [126]:*

$$\begin{cases} \dot{x}_1(t) = -(k_{21} + k_{31})x_1(t) + u(t), \ x_1(0) = x_{10}, \\ \dot{x}_2(t) = k_{21}x_1(t) - x_2(t), \ x_2(0) = 0, \\ \dot{x}_3(t) = k_{31}x_1(t) - c_{13}x_3(t), \ x_3(0) = x_{30}, \\ y(t) = x_2(t) + c_{13}x_3(t), \end{cases} \tag{3.17}$$

where the unknown parameters are k_{21}, c_{13}, $\mathcal{U}_p = \mathbb{R}^2$. *Assume that* $x_{i0} \in [\underline{x_{i0}}, \overline{x_{i0}}]$, $i = 1, 3$ *and* $a_0(.) \in Y^m_{\Gamma_1}$. *Assume also that* $0 \notin [\underline{x_{30}}, \overline{x_{30}}]$.

In this example, the set of parameters P^* *containing* (k_{21}, c_{13}) *is searched so that* P^* *is globally* μ*-SM-identifiable. For doing this, the PSE Method relies on studying the solutions of the following system:*

$$\begin{cases} c_{13}x_{30} = a_0(0), \\ (k_{21} + c_{13}k_{31})x_{10} - c_{13}^2 x_{30} = a_1(0), \end{cases} \tag{3.18}$$

According to Theorem 3.4.3, it is sufficient to find the solutions of (3.18). From the first equation, one gets $c_{13} = a_0(0)/x_{30}$. *Then, if* $0 \in [\underline{x_{10}}, \overline{x_{10}}]$, *the model is not globally SM-identifiable since the particular case* $x_{10} = 0$ *induces the following equations* $a_k(0) = (-1)^k c_{13}^{k+1} x_{30}$ *for all* $k \geq 0$. *Otherwise, if* $0 \notin [\underline{x_{10}}, \overline{x_{10}}]$, *the second equation gives:*

$$k_{21} = \frac{a_1(0) - c_{13}k_{31}x_{10} + c_{13}^2 x_{30}}{x_{10}}. \tag{3.19}$$

Denote by γ *the right member of (3.19). Solutions of (3.18) are in* $P^* = [\underline{\gamma}, \overline{\gamma}] \times [\underline{a_0}(0), \overline{a}_0(0)]/[\underline{x_{30}}, \overline{x_{30}}]$ *and according to Theorem 3.4.2, the system (3.17) is globally SM-identifiable for* P^*.
Furthermore, the function $\phi : (k_{21}, c_{13}) \mapsto (c_{13}x_{30}, (k_{21} + c_{13}k_{31})x_{10} - c_{13}^2 x_{30})$ *is* $(P^*, \mathbb{R}^2)$*-injective. Thus, the system (3.17) is* μ*-set membership identifiable with respect to* P^*.

3.4.2 Differential Algebra Method (DA method)

The differential algebra method [60] consists in eliminating unmeasurable state variables in order to obtain relations linking outputs, inputs and parameters. For this, an appropriate elimination order has to be chosen. In this work, the elimination order is $\{p\} < \{y, u\} < \{x\}$. The latter is chosen so that formal calculus, made by Maple for example, can be successful in most of the cases. Besides, the particular form of the obtained relations leads to an easy criteria for verifying the notions of identifiability. Indeed, the identifiability study is reduced to verify the (partial) injectivity, or not, of a function and fewer tests based on the tools of interval analysis and interval constraint propagation are available in the literature. According to the previous elimination order, the Rosenfeld-Groebner algorithm implemented in the package DifferentialAlgebra of Maple can be used for obtaining the desired relations. This algorithm gives an union of subsets each of them corresponding to a solution of the system. One of them called the characteristic presentation corresponds to the general case, the others to particular solutions. The characteristic presentation contains differential polynomials linking outputs, inputs and parameters which can be expressed as (see [30] for more details)

$$R_i(\bar{y}, \bar{u}, p) = m_0^i(\bar{y}, \bar{u}) + \sum_{k=1}^{n_i} \theta_k^i(p) m_k^i(\bar{y}, \bar{u}),\ i = 1, \ldots, m, \tag{3.20}$$

where $(\theta_k^i(p))_{1 \leq k \leq n_i}$ are rational in p, $\theta_u^i \neq \theta_v^i$ $(u \neq v)$, $(m_k^i(\bar{y}, \bar{u}))_{0 \leq k \leq n_i}$ are differential polynomials with respect to y, u and $m_0^i(\bar{y}, \bar{u}) \neq 0$.
$\{\theta_k^i(p)\}_{1 \leq k \leq n_i}$ is called the exhaustive summary of R_i.

The size of the system is the number of outputs. For the time being, we suppose that $i = 1$, that is there is one output and $n_1 = n$, $R_1 = R$, $m_k^1(\bar{y}, \bar{u}) = m_k(\bar{y}, \bar{u})$.

Consider t_0^+ the right limit of t_0 [6] and l the higher order derivative of y in (3.20). Hereafter, $\Delta R(y, u)$ will design the functional determinant formed from the $\{m_k(\bar{y}, \bar{u})\}_{1 \leq k \leq n}$. The following theorem permits to obtain necessary and sufficient conditions for having global SM-identifiability or μ-SM-identifiability.

Theorem 3.4.4 *Assume that the functional determinant $\Delta R(y, u)$ is not identically equal to zero. Consider P^* a connected subset of $\mathcal{U}_\mathcal{P}$.*
If the function $\phi : p = (p_1, \ldots, p_p) \mapsto (\theta_1(p), \ldots, \theta_n(p), y(t_0^+, p), \ldots, y^{(l-1)}(t_0^+, p))$ is $(P^*, \mathcal{U}_\mathcal{P})$-restricted injective (resp. $(P^*, \mathcal{U}_\mathcal{P})$-injective) then P^* is globally SM-identifiable (resp. μ-SM-identifiable). Furthermore, if P^* has a diameter equal to ε and ϕ is $(P^*, \mathcal{U}_\mathcal{P})$-restricted injective but not $(P^*, \mathcal{U}_\mathcal{P})$ injective then P^* is ε-SM-identifiable.

[6] t_0^+ is considered to ensure the existence of derivatives.

In the two cases, if the coefficient of $y^{(l)}$ in (3.20) is not equal to 0 at t_0, then the reciprocal is valid [7].

Proof – Sufficiency Let P^* verify the hypothesis of the theorem. Suppose there exists an input u^* such that $Y_{\Gamma_1}(P^*, u^*) \neq \emptyset$ and $y^* \in Y_{\Gamma_1}(P^*, u^*) \cap Y_{\Gamma_1}(\tilde{P}, u^*)$. Thus, there exists $p^* \in P^*,\ \tilde{p} \in \tilde{P}$ such that $y^*(.) = y(., p^*) = y(., \tilde{p})$ and $R(y^*, u^*, p^*) = R(y^*, u^*, \tilde{p})$. Denote $Q(y^*, u^*) = R(y^*, u^*, p^*) - R(y^*, u^*, \tilde{p})$.
Since $det(Q)(y^*, u^*) = det(m_k(y^*, u^*),\ k = 0, \ldots, n) = \triangle(R)(y^*, u^*)$ is not equal to zero, $\theta_k(p^*) = \theta_k(\tilde{p})$ for $k = 1, \ldots, n$. Besides, we have $y(., p^*) = y(., \tilde{p})$ in particular $y^{(k)}(t_0, p^*) = y^{(k)}(t_0, \tilde{p})$ for $0 \leq k \leq l-1$. Since the function ϕ is a weak-injection of P^* over $\mathcal{U}_\mathcal{P}$, one gets $\tilde{p} \in P^*$ and $P^* \cap \tilde{P} \neq \emptyset$.
For any contraction $\mu : P^* \to P^*$ such that $p^* \in \mu(P^*)$, ϕ is $(\mu(P^*), \mathcal{U}_\mathcal{P})$-injective and $p^* = \tilde{p}$ is always verified which implies that $P^* \cap \tilde{P} \neq \emptyset$.
Necessity Let's prove the contrapositive. Suppose there exists $\tilde{P} \neq \emptyset$, such that $P^* \cap \tilde{P} = \emptyset$ and $\phi(p^*) = \phi(\tilde{p})$ for a certain $p^* \in P^*$ and a $\tilde{p} \in \tilde{P}$. Since the coefficient of $y^{(l)}$ in (3.20) is not equal to 0 at t_0 and the differential polynomials $(m_k(y, u))_{k=1,\ldots,n}$ have a degree 1 in $y^{(l)}$ (see [30] for more details), any time derivative $y^{(r)}(t_0^+, p^*)$, $r \geq l$ can be rewritten in function of $y^{(l-1)}(t_0^+, p^*),\ \ldots,\ y(t_0^+, p^*), \theta_1(p^*), \ldots, \theta_n(p^*)$. According to the hypothesis on ϕ, the $(l-1)$ first coefficients of $y(t, p^*)$ in the Taylor expansion are the same as those of $y(t, \tilde{p})$, thus $y^* := y(t, p^*) = y(t, \tilde{p})$ and $y^* \in Y_{\Gamma_1}(P^*, u) \cap Y_{\Gamma_1}(\tilde{P}, u)$. Thus, the model is not globally-SM-identifiable for P^*. □

Remark 3.4.2 *In the case of m outputs, the procedure is the following. For each of the m differential polynomials $R_i(\bar{y}, \bar{u}, p)$, the functional determinant is evaluated. If it is not identically equal to zero, the associated exhaustive summary is added to the image of the function ϕ whose (partial) injectivity has to be studied.*

The two methods consist in reducing the study of (μ-)SM-identifiability of the initial model set to the study of algebraic systems and to use interval analysis tools. Indeed, the main advantage of interval analysis is that it can guarantee that numerical solutions provided as sets, are guaranteed to contain all actual solutions. The PSE method is easy to implement but can lead to complex systems essentially in the case of nonlinear systems. And, even if it can be used for the construction of P^*, better estimate can be obtained using indirect methods and the whole measurement trajectory. The DA method is probably more difficult to master but in the case of nonlinear models, it enables to obtain more easily the identifiability's results. Moreover, some recent developments in SM estimation as the solver ITVIA enable the user to determine quickly the area on which the model is μ-SM-identifiable.

[7] When initial conditions are not considered, the function ϕ becomes $\phi : p = (p_1, \ldots, p_p) \mapsto (\theta_1(p), \ldots, \theta_n(p))$ and the reciprocal of the theorem is not yet valid.

3.4.3 Testing SM-identifiability

The steps for proving SM-identifiability are summed up below.

1. Find the differential polynomials R_i using, for example, the package DifferentialAlgebra of Maple.
2. Evaluate the functional determinants and construct the function ϕ.
3. Verify the (restricted)-partial injectivity.
   - If the function ϕ is injective on $\mathcal{U}_\mathcal{P}$, P^* is μ-SM-identifiable. This test can be done using an interval Newton solver to enclose all the zeros in an union of interval vectors. If ϕ is not injective or the resolution is too hard, the following numerical procedure can be used.
   - Use ICP algorithms (Interval constraint propagation implemented in realpaver for example) to verify the $(P^*,\mathcal{U}_\mathcal{P})$-injectivity. For example, to verify global SM-identifiability of P^*, the following numerical test can be used:
     find $p \in \mathcal{U}_\mathcal{P}$ such that
     $$\forall p^* \in P^*,\ \phi(p) - \phi(p^*) = 0.$$
     If there is no solution outside P^*, P^* is globally SM-identifiability.

Example 3.4.2 *Consider the model:*

$$\begin{cases} \dot{x}_1(t) = p_1 x_1(t)^2 + \sin(p_2) x_1(t) x_2(t),\ x_1(0) = 1 \\ \dot{x}_2(t) = p_3 x_1(t)^2 + x_1(t) x_2(t),\ x_2(0) = b \\ y(t) = x_1(t). \end{cases} \tag{3.21}$$

where $(p_1, p_2, p_3) \in \mathcal{U}_\mathcal{P} = \mathbb{R} \times [0, 2\pi[\times \mathbb{R}^+$ *are the unknown parameters. Let* $p_4 = \sin(p_2)$. *In using the Rosenfeld-Groebner algorithm in Maple with the elimination order* $\{p_1, p_3, p_4\} < \{y\} < \{x_1, x_2\}$, *there are three cases: the impossible one* $y = 0$ *since* $y(0) = 1$, *the particular case* $p_4 = 0$ *(thus* $p_2 = 0$ *or* π*) and the general characteristic presentation* $\mathcal{C} = \{R(\bar{y})\}$ *with* $R(\bar{y}) = \dot{y}^2 - y\ddot{y} + \dot{y}y^2 + p_1(\dot{y}y^2 - y^4) + p_4 p_3 y^4$. *The functional determinant* $2y^5\dot{y}^2 - y^6\ddot{y}$ *of* $R(y) = \det(\dot{y}y^2 - y^4, y^4)$ *is not identically equal to 0.*
Thus, we have to study the following function
$\phi : (p_1, p_2, p_3) \to (p_1, \sin(p_2)p_3, p_1 + \sin(p_2)b)$. *The first two components correspond to the exhaustive summary of* R *and the third one to the first derivative of* y *taken at the initial time* [8].

[8] It is sufficient to compute only the first derivative since the higher order derivative of R is equal to 2.

The model set is globally SM-identifiable for $P_1^* = \mathbb{R}\times]0,\pi[\times\mathbb{R}^+$ *and* $P_2^* = \mathbb{R}\times]\pi,2\pi[\times\mathbb{R}^+$. *Indeed, it is sufficient to remark that:* $\forall p_2^* \in]0,\pi[, \forall \bar{p}_2 \in]\pi,2\pi[, \sin(p_2^*) > 0$ *and* $\sin(\bar{p}_2) < 0$. *However, the model set is clearly not* μ*-SM-identifiable with respect to* P_1^* *and* P_2^* *since the function* sin *is not injective on these two subsets.*

Example 3.4.3 *Consider the model:*

$$\begin{cases} \dot{x}_1(t) = (p_1 + 2(1-p_2)\cos(p_1))x_1(t)^2 + (1-p_2)x_2(t), \\ \dot{x}_2(t) = \sin(p_1)x_1(t), \\ y(t) = x_1(t). \end{cases} \tag{3.22}$$

where $(p_1,p_2) \in P^* = [-1,4]\times[0,1/10]$.
We want to know if P^* *is globally (*μ*-)SM-identifiable. By setting* $c_1 = \sin(p_1)$*, with the elimination order* $\{c_1,p_2\} < \{y\} < \{x_1,x_2\}$*, the Rosenfeld-Groebner algorithm gives the following differential polynomial:*

$$R(\bar{y}) = \ddot{y} - 2(p_1 + 2(1-p_2)\cos(p_1))\dot{y}y - (1-p_2)\sin(p_1)y. \tag{3.23}$$

In that case, the functional determinant is reduced to $\triangle R(\bar{y}) = \det(\dot{y}y, y) = -y^2\ddot{y}$ *and is not identically equal to 0.*
In order to consider the initial condition, the function $\phi : (p_1,p_2) \to ((p_1 + 2(1-p_2)\cos(p_1)), (1-p_2)\sin(p_1))$ *has to be studied. Using the solver ITVIA (see [63]), Figure 3.2 is obtained. The box* P^* *has been partitioned in two domains: a domain on which the function is partially injective and an indeterminate domain. Thus,* ϕ *is not injective over* P^* *and* P^* *is not* μ*-SM-identifiable.*

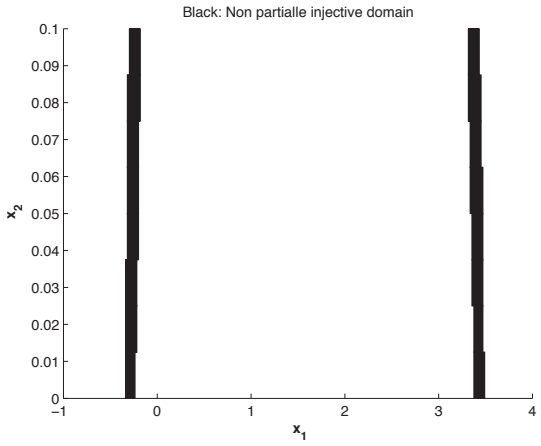

Figure 3.2: Partition of the box P^* for the function ϕ.

3.5 Partitionning the parameter space into SM-identifiable sets and not SM-identifiable sets

The proposed work has been achieved within the framework of the MAGIC-SPS project and has been published in [109].

The aim of this section is to determine numerically the set-membership identifiable connected sets that correspond to different output behaviors for the considered system. For doing this, a method based on differential algebra is proposed. This method consists in linking μ-set-membership-identifiability and set-membership-identifiability definitions to the partial injectivity and restricted-partial injectivity of a real rational function. An algorithm based on interval analysis is presented for determinig the μ-SM-identifiable sets.

In order to determine numerically the SM-identifiable sets, we have implemented an algorithm composed of three steps based on ImageSP algorithm [50]. Indeed, the method consists in calculating the image of the real rational function obtained by the theoretical part. Using ImageSP, the obtained boxes, supposed to correspond to SM-identifiable sets, are composed of non desired parts, which are parts of non SM-identifiable sets. That is why, we propose other algorithms to find a regular internal subpaving.

3.6 Determination of the (μ)-SM-identifiable sets

The proposed algorithms find the connected sets in the range of a continuous differentiable function such that their image is distinct to the one obtained with their complement. Afterwards, they are named SM-identifiable sets to be put in correspondence with the SM-identifiable sets defined from the model Γ_1. They take back the algorithm ITVIA ([63] [64]) which partitions the domain of a differentiable function into two domains: an *undetermined domain* not proved partially injective and a *partial injective domain*. The latter corresponds to a list of μ-SM-identifiable sets. To complete the partition, we have to find the SM-identifiable sets in the undetermined domain.

Denote $f : \mathbb{R}^n \rightarrow \mathbb{R}^m$ ($f \in \mathcal{C}^1$) a differentiable vector function defined over a given n-dimensional box $[x] \in \mathbb{IR}^n$, where $\mathbb{IR}$ is the set of all intervals. Regarding to [15], a subpaving of $[x]$ is a set of non-overlapping boxes included in $[x]$. A subpaving can be considered either as a collection (list) of boxes $\mathbb{K} = \left\{[x]^{(1)}, [x]^{(2)}, ...\right\}$ or as a union $\mathbb{K} = [x]^{(1)} \bigcup [x]^{(2)} \bigcup ....$ Hence, a subpaving can either be viewed as a discrete subset of $\mathbb{IR}^n$ or as a convex subset of $\mathbb{IR}^n$. Subpavings permit to approximate convex sets with arbitrary precision. A regular subpaving is a subpaving generated by successive bisections and it can be easily represented by a binary tree.

After obtaining a paving of μ-SM-identifiable sets by the algorithm ITVIA, we determine its complement and, to complete the work, we proceed as in *Image evaluation* [50]. Firstly, we consider a subpaving with boxes of width smaller than ε (*mince step*). Secondly, we find SM-identifiable sets as a list of non-overlapped boxes (*evaluate step*). Finally, we transform this list to a regular subpaving (*regularize step*).
We begin by the case of $m = 1$ and then we generalize our algorithm to the multidimensional case.

3.6.1 The case of unidimensional functions

Let $\mathcal{P}$ a list of non overlapped boxes included in $[x]$, we introduce the following notations. Q corresponds to the length of the list $\mathcal{P}$. $\max_{[f],\{\mathcal{P}\}}$ (resp. $\min_{[f],\{\mathcal{P}\}}$) denotes the sequence of the maximal values (resp. the minimal values) of $[f]$ on each box of $\mathcal{P}$ and the two following, $\mathcal{M}ax_{[f],\{\mathcal{P}\}}{}^{+}$ and $\mathcal{M}in_{[f],\{\mathcal{P}\}}{}^{+}$ (resp. $\mathcal{M}ax_{[f],\{\mathcal{P}\}}{}^{-}$ and $\mathcal{M}in_{[f],\{\mathcal{P}\}}{}^{-}$), the maximal and minimal values of the sequence $\max_{[f],\{\mathcal{P}\}}$ (resp. $\min_{[f],\{\mathcal{P}\}}$). Then, $i_{\mathcal{M}ax}$ and $i_{\mathcal{M}in}$ are the minimal corresponding indexes. Finally, ε is the maximal diameter of the boxes considered in the list $\mathcal{P}$. Mathematically, these definitions can be rewritten in the form:

- length($\mathcal{P}$) $= Q$,

- $\max_{[f],\{\mathcal{P}\}} = \{\max([f](\mathcal{P}_i)),\ 1 \leq i \leq Q\} \in \mathbb{R}^Q$,
- $\min_{[f],\{\mathcal{P}\}} = \{\min([f](\mathcal{P}_i)),\ 1 \leq i \leq Q\} \in \mathbb{R}^Q$,
- $\mathcal{M}ax_{[f],\{\mathcal{P}\}}{}^{+} = \max(\max_{[f],\{\mathcal{P}\}}) \in \mathbb{R}$,
- $\mathcal{M}ax_{[f],\{\mathcal{P}\}}{}^{-} = \max(\min_{[f],\{\mathcal{P}\}}) \in \mathbb{R}$,
- $\mathcal{M}in_{[f],\{\mathcal{P}\}}{}^{-} = \min(\min_{[f],\{\mathcal{P}\}}) \in \mathbb{R}$,
- $\mathcal{M}in_{[f],\{\mathcal{P}\}}{}^{+} = \min(\max_{[f],\{\mathcal{P}\}}) \in \mathbb{R}$,
- $\varepsilon = \max((w(\{\mathcal{P}\})_{i=1,\ldots,Q}))$.

Example 3.6.1 *To illustrate these notations, consider the following function f defined by:*

$$f(x) = \sin(10(x-0.1)^2)/x, \text{ where } [x] \in [0.1,\ 2]. \tag{3.24}$$

It is represented in Figure 3.3. $\mathcal{P}$ consists of equal boxes of width $\varepsilon = 0.05$ in $[0.1,\ 2]$.

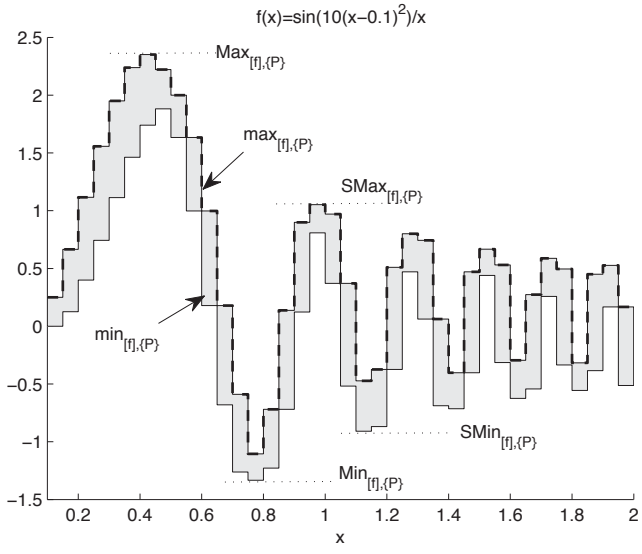

Figure 3.3: Illustration of the notations (to simplify, the subscript $\{[f], \mathcal{P}\}$ is omitted).

3.6.1.1 Second maximum and second minimum

The aim of the two following sections is to isolate the domain around the maximum (resp. minimum) of f which constitutes a SM-identifiable set as the interval $[0.2; 0.6]$ in Figure 3.3. For doing this, the second maximum of f (resp. minimum) has to be determined first, in particular the lower and the upper values of the box containing this second maximum (resp. minimum). The lower value will be denoted $\mathcal{SM}ax_{[f],\{\mathcal{P}\}}{}^{-}$ and the upper value, $\mathcal{SM}ax_{[f],\{\mathcal{P}\}}{}^{+}$ (see Figure 3.3).
While $\mathcal{M}ax_{[f],\{\mathcal{P}\}}{}^{+}$ and $\mathcal{M}ax_{[f],\{\mathcal{P}\}}{}^{-}$ can be directly evaluated from $\max([f](\mathcal{P}))$, Algorithm 3 is used for evaluating $\mathcal{SM}ax_{[f],\{\mathcal{P}\}}{}^{+}$ or $\mathcal{SM}ax_{[f],\{\mathcal{P}\}}{}^{-}$. There, $\mathcal{SM}ax_{[f],\{\mathcal{P}\}}{}^{+}$ and $\mathcal{SM}ax_{[f],\{\mathcal{P}\}}{}^{-}$ are computed in replacing $M \in \mathbb{R}^N$ by $max([f](\mathcal{P}))$ and $min([f](\mathcal{P}))$, respectively. For example, consider that $M = max([f](\mathcal{P}))$.
In this algorithm, we find $\mathcal{M}ax_{[f],\{\mathcal{P}\}}{}^{+}$, that is the maximum value of the list $max([f](\mathcal{P}))$ and we initialize a list named $\{\mathcal{L}\}$ by the corresponding box of $\mathcal{M}ax_{[f],\{\mathcal{P}\}}{}^{+}$ in $\mathcal{P}$. Then, we find the next maximum value of $max([f](\mathcal{P}))$. If its corresponding box $[x]_{temp}$ in $\mathcal{P}$ is connected to one of the component of $\{\mathcal{L}\}$, that is, it intersects one of the box of $\{\mathcal{L}\}$ (see [50] for the definition of connected box), we add it to $\{\mathcal{L}\}$ and we continue. If there exists a box $[x]_{temp}$ not connected with one of the box of $\{\mathcal{L}\}$, one gets the box containing the second maximum of the function f. The second maximum is named disconnected afterwards; an example is shown in Figure 3.3. If all the boxes $[x]_{temp}$ are connected with one of the box of $\{\mathcal{L}\}$ then the second maximum is found at the boundary, i.e. at $\mathcal{P}_1$ or $\mathcal{P}_N$.
The same work can be done for finding $\mathcal{SM}in_{[f],\{\mathcal{P}\}}{}^{+}$ and $\mathcal{M}in_{[f],\{\mathcal{P}\}}{}^{-}$.

3.6.1.2 Relation between partitioning and second maximum or minimum

For the final step, we construct the SM-identifiable set defined around the maximum or minimum value of f. Indeed, when we search the second maximum or minimum, we obtain the list of boxes $\{\mathcal{L}\}$ which are the image of the function f and are not connected with its complement. However, we are not insured to obtain a connected set. For being convinced, see for example the second figure of Figure 3.4. Owing to the third box, we do not obtained a connected set. First, let us define the list of boxes $\{\mathcal{L}\}^{+}_{[f],\mathcal{P},a}$ (resp. $\{\mathcal{L}\}^{-}_{[f],\mathcal{P},a}$) such that their image by the inclusion function has their minimum larger (resp. maximum smaller) than a.

Definition 3.6.1 *The list of boxes $\{\mathcal{L}\}^{+}_{[f],\mathcal{P},a}$ is defined by:*

$$\{\mathcal{L}\}^{+}_{[f],\mathcal{P},a} = \{\mathcal{P}_i,\ \min([f](\mathcal{P}_i)) \geq a\} \tag{3.25}$$

Algorithm 3 $\mathcal{SM}ax$ =SecondMax($\mathcal{P},\ M$)

Input: $\mathcal{P},\ M$;
Output: $\mathcal{SM}ax$;

initialization: $\{\mathcal{L}\} = \emptyset$;
$\mathcal{M}ax = \max(M)$;
$i_{\mathcal{M}ax} = \min_i (M(i) = \mathcal{M}ax)$;
$\{\mathcal{L}\} = \{\mathcal{P}_{i_{\mathcal{M}ax}}\}$;
$M(i_{\mathcal{M}ax}) = -\infty$;
for $i = 1$:length($\mathcal{P}$) $- 1$ **do**
  $\mathcal{M}ax_{temp} = \max(M)$;
  $i_{temp} = \min_i (M(i) = \mathcal{M}ax_{temp})$;
  $[x]_{temp} = \mathcal{P}_{i_{temp}}$;
  if $[x]_{temp}$ connected to $\{\mathcal{L}\}$ **then**
    $\{\mathcal{L}\} = \{\mathcal{L}, [x]_{temp}\}$;
    $M(i_{temp}) = -\infty$;
  else if $\mathcal{SM}ax = \mathcal{M}ax_{temp}$ **then**
    it is disconnected, return
  end if
end for
$\mathcal{SM}ax = \mathcal{M}ax_{temp}$;

Definition 3.6.2 *The list of boxes* $\{\mathcal{L}\}^{-}_{[f],\mathcal{P},a}$ *is defined by:*

$$\{\mathcal{L}\}^{-}_{[f],\mathcal{P},a} = \{\mathcal{P}_i,\ \max([f](\mathcal{P}_i)) \leq a\}\,. \tag{3.26}$$

The notion of connected lists formed of intervals is introduced before giving a sufficient condition for having a connected SM-identifiable set in $[x]$.

Definition 3.6.3 *A list* $\{\mathcal{L}\}$ *formed of intervals is said connected if the union of its components is an interval of* $\mathbb{IR}$.

Proposition 3.6.1
In (3.25), for $a = \mathcal{SM}ax_{[f],\{\mathcal{P}\}}{}^{+}$, *if the list* $\{\mathcal{L}\}$ *is a connected set, then it is a SM-identifiable set. We denote it by* $\{\mathcal{L}\}^{+}_{SMI,[f],\mathcal{P}}$.

Proof – The list $\{\mathcal{L}\}$ corresponds, by construction, to the list of boxes not having a common intersection with its complement. Concretely, the image $\{\mathcal{L}\}$ of f is distinct with its complementary image. Since $\{\mathcal{L}\}$ is supposed to be connected, it constitutes a SM-identifiable set.
Similarly, we get the following proposition.

Proposition 3.6.2
In (3.26), for $a = \mathcal{SM}in_{[f],\{\mathcal{P}\}}{}^{-}$, *if the list* $\{\mathcal{L}\}$ *is a connected set, then it is a SM-identifiable set. We denote it by* $\{\mathcal{L}\}^{-}_{SMI,[f],\mathcal{P}}$.

Figure 3.4 illustrates the importance of the connected property verification.

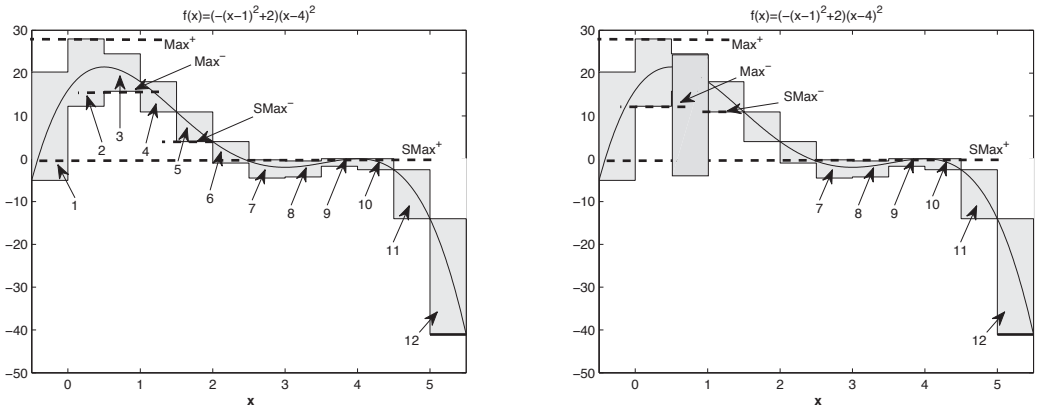

Figure 3.4: Connected and non connected sets.

In the first Figure, we get $a = \mathcal{SM}ax_{[f],\{\mathcal{P}\}}{}^{+} = \max([f](\mathcal{P}_7))$, $\{\mathcal{L}\}^{+}_{[f],\mathcal{P},a} = \{\mathcal{P}_2, \mathcal{P}_3, \mathcal{P}_4, \mathcal{P}_5\}$ and it can be easily seen that $\{\mathcal{L}\}^{+}_{[f],\mathcal{P},a}$ is the list $\{\mathcal{L}\}^{+}_{SMI,[f],\mathcal{P}}$ since it is connected.
However, in the second Figure, $\{\mathcal{L}\}^{+}_{[f],\mathcal{P},a} = \{\mathcal{P}_2, \mathcal{P}_4, \mathcal{P}_5\}$ is no more connected and can not be a SM- identifiable set.

Algorithm 4 is used to find the connected sets verifying Proposition 3.6.1. In this algorithm, two lists $\{\mathcal{L}_1\}$ and $\{\mathcal{L}_2\}$ verify $\{\mathcal{L}_1\} = \{\mathcal{L}_2\}$, if they are composed of the same elements even in different order. Moreover, the notation $[x_a]$ designates the component $\{\mathcal{P}\}_i$ of the list $\{\mathcal{P}\}$ for which $\min([f](\{\mathcal{P}\}_i)) = a$.

Algorithm 4 $\{\mathcal{L}\}^{+}_{SMI,[f],\mathcal{P}} = \text{ConnectedSet}^{+}(\mathcal{P}, \max_{[f],\{\mathcal{P}\}}, \min_{[f],\{\mathcal{P}\}})$

Input: $\mathcal{P}$, $\max_{[f],\{\mathcal{P}\}}$, $\min_{[f],\{\mathcal{P}\}}$;
Output: $\{\mathcal{L}\}^{+}_{SMI,[f],\mathcal{P}}$;
1: Initialization: $a = \mathcal{SM}ax_{[f],\{\mathcal{P}\}}{}^{+}$, $\{\mathcal{L}_1\} = \emptyset$, $\{\mathcal{L}_2\} = \{\mathcal{L}\}^{+}_{[f],\mathcal{P},a}$;
2: **while** $\{\mathcal{L}_2\} \neq \{\mathcal{L}_1\}$ **do**
3: $\{\mathcal{L}_1\} = \{\mathcal{L}_2\}$;
4: $a = \mathcal{SM}ax^{-}_{[f],\{\mathcal{L}_1\}}$;
5: $\{\mathcal{L}_2\} = \{\mathcal{L}\}^{+}_{[f],\{\mathcal{L}_1\},a}$;
6: **if** a is a disconnected maximum **then**
7: $\{\mathcal{L}_2\} = \{\mathcal{L}_2\} - [\mathbf{x}_a]$;
8: **end if**
9: **end while**
10: $\{\mathcal{L}\}^{+}_{SMI,[f],\mathcal{P}} = \{\mathcal{L}_2\}$;

Another algorithm can be deduced from Algorithm 3 in substituting $+$ and $\max$ by $-$ and $\min$.

3.6.1.3 Algorithms

The following algorithms 5 and 6 are the final algorithms to determine the SM-identifiable sets in the definition domain of a function. They take again the previous algorithms. $\{\mathcal{U}\}_{SMI,[f],\mathcal{P}}$ corresponds to the set of the two lists $\{\mathcal{L}\}^{+}_{SMI,[f],\mathcal{P}}$ and $\{\mathcal{L}\}^{-}_{SMI,[f],\mathcal{P}}$.

As it can be seen, these algorithms are different only in the order of treating the partitions $\{\mathcal{U}^{+}\}$ and $\{\mathcal{U}^{-}\}$.

Algorithm 5 $\{\mathcal{U}\}_{SMI,[f],\mathcal{P}}$ =SMISet1($[f],\ \mathcal{P}$)

Input: $[f],\ \mathcal{P}$;
Output: $\{\mathcal{U}\}_{SMI,[f],\mathcal{P}}$;
1: Initialization: $\{\mathcal{U}^+\} = \emptyset$, $\{\mathcal{U}^-\} = \emptyset$, $\{\mathcal{L}_1\} = \mathcal{P}$;
2: $\{\mathcal{U}^+\} = \{\mathcal{L}\}^+_{SMI,[f],\{\mathcal{L}_1\}}$;
3: $\{\mathcal{L}_2\} = \{\mathcal{L}_1\} - \{\mathcal{U}^+\}$;
4: $\{\mathcal{U}^-\} = \{\mathcal{L}\}^-_{SMI,[f],\{\mathcal{L}_2\}}$;
5: $\{\mathcal{U}\}_{SMI,[f],\mathcal{P}} = \{\{\mathcal{U}^+\},\ \{\mathcal{U}^-\}\}$;

Algorithm 6 $\{\mathcal{U}\}_{SMI,[f],\mathcal{P}}$ =SMISet2($[f],\ \mathcal{P}$)

Input: $[f],\ \mathcal{P}$;
Output: $\{\mathcal{U}\}_{SMI,[f],\mathcal{P}}$;
1: Initialization: $\{\mathcal{U}^+\} = \emptyset$, $\{\mathcal{U}^-\} = \emptyset$, $\{\mathcal{L}_2\} = \mathcal{P}$;
2: $\{\mathcal{U}^-\} = \{\mathcal{L}\}^-_{SMI,[f],\{\mathcal{L}_2\}}$;
3: $\{\mathcal{L}_1\} = \{\mathcal{L}_2\} - \{\mathcal{U}^-\}$;
4: $\{\mathcal{U}^+\} = \{\mathcal{L}\}^+_{SMI,[f],\{\mathcal{L}_1\}}$;
5: $\{\mathcal{U}\}_{SMI,[f],\mathcal{P}} = \{\{\mathcal{U}^+\},\ \{\mathcal{U}^-\}\}$;

3.6.2 The case of multidimensional functions

In this section, we consider the case of $m > 1$. We suppose that an interval function vector $[f] = [\,[f_1],\ ...,\ [f_m]\,]$ and a subpaving $\mathcal{P}$ of $[x]$ are available.
Based on previous algorithms, Algorithm 7 has been implemented.

Algorithm 7 $\{\mathcal{U}\}_{SMI,[f],\mathcal{P}}$ =SMISetN1($[f],\ \mathcal{P}$)

Input: $[f],\ \mathcal{P}$;
Output: $\{\mathcal{U}\}_{SMI,[f],\mathcal{P}}$;
1: Initialization: $\{\mathcal{U}^+\} = \emptyset$, $\{\mathcal{U}^-\} = \emptyset$, $\{\mathcal{L}_1\} = \mathcal{P}$;
2: **for** i=1:m **do**
3: $\quad \{\mathcal{U}^+\}_i = \{\mathcal{L}\}^+_{SMI,[f_i],\{\mathcal{L}_1\}}$;
4: $\quad \{\mathcal{L}_2\} = \{\mathcal{L}_1\} - \{\mathcal{U}^+\}_i$;
5: $\quad \{\mathcal{U}^-\}_i = \{\mathcal{L}\}^-_{SMI,[f_i],\{\mathcal{L}_2\}}$;
6: $\quad \{\mathcal{L}_1\} = \{\mathcal{L}_2\} - \{\mathcal{U}^-\}_i$;
7: **end for**
8: $\{\mathcal{U}\}_{SMI,[f],\mathcal{P}} = \{\{\mathcal{U}^+\},\ \{\mathcal{U}^-\}\}$;

However, as in the case of $m = 1$, other algorithms can be considered, for example the following algorithm:

Algorithm 8 $\{\mathcal{U}\}_{SMI,[f],\mathcal{P}}$ =SMISetN2($[f],\ \mathcal{P}$)

Input: $[f],\ \mathcal{P}$;
Output: $\{\mathcal{U}\}_{SMI,[f],\mathcal{P}}$;
1: Initialization: $\{\mathcal{U}^+\} = \emptyset$, $\{\mathcal{U}^-\} = \emptyset$, $\{\mathcal{L}_2\} = \mathcal{P}$;
2: **for** i=1:m **do**
3: $\quad \{\mathcal{U}^-\}_i = \{\mathcal{L}\}^-_{SMI,[f_i],\{\mathcal{L}_2\}}$;
4: $\quad \{\mathcal{L}_1\} = \{\mathcal{L}_2\} - \{\mathcal{U}^-\}_i$;
5: $\quad \{\mathcal{U}^+\}_i = \{\mathcal{L}\}^+_{SMI,[f_i],\{\mathcal{L}_1\}}$;
6: $\quad \{\mathcal{L}_2\} = \{\mathcal{L}_1\} - \{\mathcal{U}^+\}_i$;
7: **end for**
8: $\{\mathcal{U}\}_{SMI,[f],\mathcal{P}} = \{\{\mathcal{U}^+\},\ \{\mathcal{U}^-\}\}$;

Changing the order of the interval functions, $[f_i]$, $i = 1, ..., m$ and also the order of computing partitions $\{\mathcal{U}^-\}_i$ and $\{\mathcal{U}^+\}_i$; altogether, there are $(2m)!$ algorithms like Algorithms 5 and 6.

3.6.3 Regularization

In [50], in order to evaluate the image of a function at a domain set, three main sequential steps, *mince*, *evaluate* and *regularize* are introduced. In the previous sections, the two first steps, the mince and the evaluate ones have been explained. In this section, the last step, i.e. the regularization is realized.

Figure 3.5 illustrates an example for the regularization step where the algorithm presented in [50] is used.

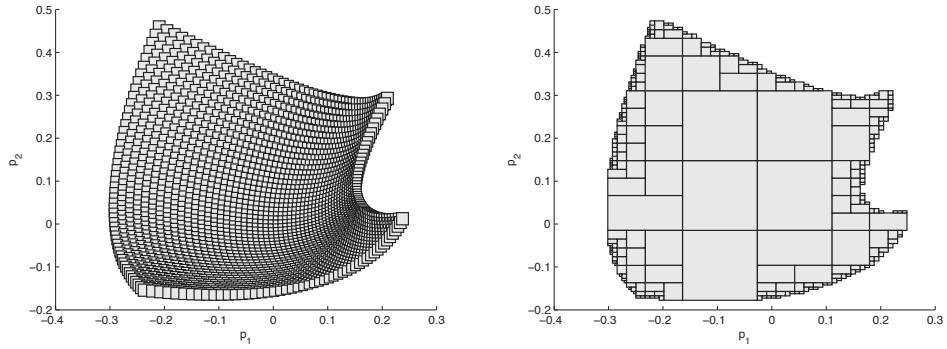

Figure 3.5: (a): list of overlapped boxes , (b): external regular subpaving

This algorithm can be also applied to a list composed of overlapped or non overlapped boxes. However, as it can be seen in Figure 3.5, the initial list, here consisting of overlapped boxes in Figure 3.5 (a), is inside the regular subpaving of the Figure 3.5 (b), or, in other words, the subpaving is an external regular subpaving. If we apply this algorithm to a list of SM-identifiable sets, some parts of the initial domain which are not SM-identifiable are included in the obtained regular subpaving.
To cope with this problem, the following algorithm is proposed to find a regular subpaving inside a list. However, the list must only consist of non overlapping boxes which is fortunately the case of a list of SM-identifiable sets found by the method presented in the last sections.

In Algorithm 9, the function volume of the interval box $[\mathbf{x}] \in \mathbb{IR}^n$ is defined as volume$([\mathbf{x}]) = (\mathbf{x}_{12} - \mathbf{x}_{11})(\mathbf{x}_{22} - \mathbf{x}_{21})...(\mathbf{x}_{n2} - \mathbf{x}_{n1})$.

Algorithm 9 $\mathcal{P}_R$ =InternalRegularization($\mathcal{P},\ \varepsilon$)

Input: $\mathcal{P}, \varepsilon$;
Output: $\mathcal{P}_R$;

Initialization: $\mathcal{P}_R = \emptyset$, $\{\mathcal{L}\} = \emptyset$, STOP=0;
$[a] = \bigcup_i \mathcal{P}_i$;
$\{\mathcal{L}\} = \{[a]\}$;
while STOP$\neq 1$ **do**
  $[\mathbf{x}] = \{\mathcal{L}\}_1$;
  v_x=volume($[\mathbf{x}]$);
  $v_t = \sum_i volume(\mathcal{P}_i \bigcap [\mathbf{x}])$;
  if $v_t \neq 0$ **then**
    if $|v_t - v_x|\ v_t < 0.01 v_x$ **then**
      $\mathcal{P}_R = \{\mathcal{P}_R, [\mathbf{x}]\}$;
    else if $w([\mathbf{x}]) > \varepsilon$ **then**
      $[\mathbf{x}_1, \mathbf{x}_2] = bisect([\mathbf{x}])$;
      $\{\mathcal{L}\} = \{\mathcal{L}, [\mathbf{x}_1], [\mathbf{x}_2]\}$;
    end if
  end if
  if length($\{\mathcal{L}\}$) > 1 **then**
    $\{\mathcal{L}\} = \{\mathcal{L}\}_{2:end}$;
  else if then
    $STOP = 1$;
  end if
end while

Figure 3.6 shows the difference between internal and external regular subpavings found for a list. As it can be seen, the list consists of non overlapped boxes (Figure 8 (a)), the internal regular subpaving is inside the list (Figure 8 (b)), and the external regular subpaving is outside the list (Figure 8 (c)).

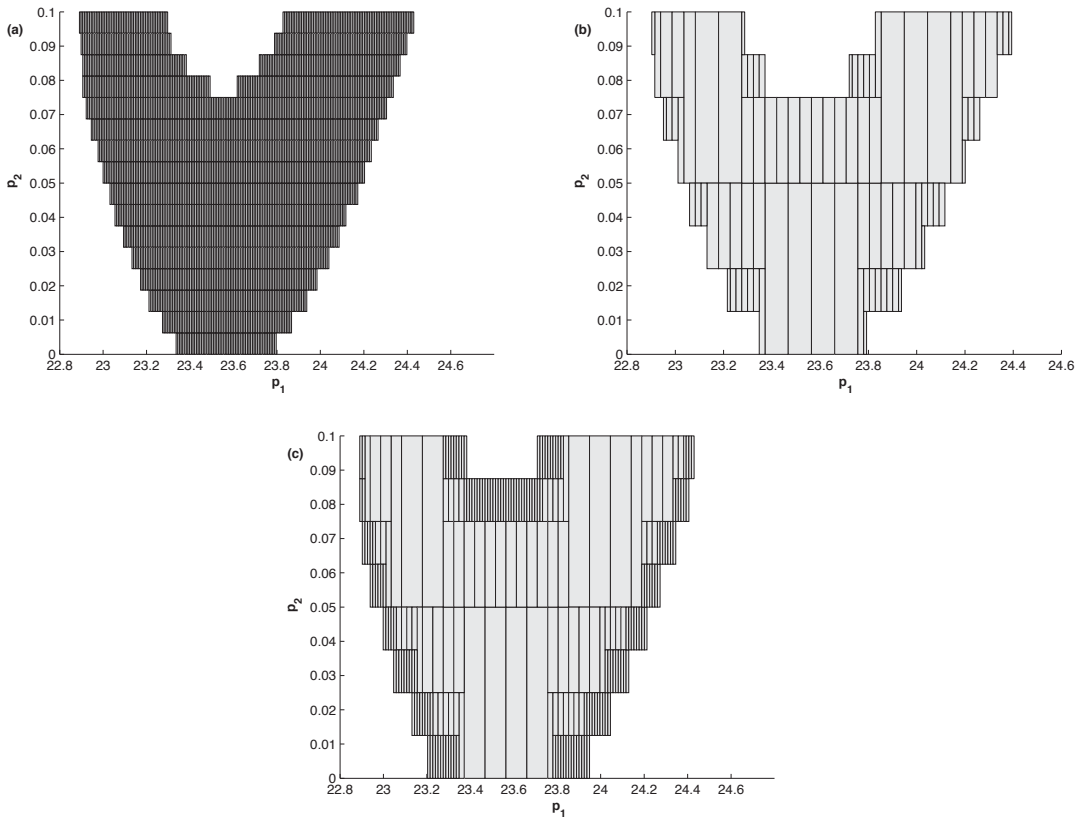

Figure 3.6: (a) non overlapped boxes; internal (b) and (c) external regular subpavings

3.7 Examples

Example 3.7.1 *Consider the Bernoulli equation* $\dot{y}(t) = -p_1^2 y(t) + p_2^2 y(t)^2$ *and let us applied the steps proposed previously.*

1. *We have directly*

$$w(\bar{y}, p) = \dot{y}(t) + p_1^2 y(t) - p_2^2 y(t)^2. \tag{3.27}$$

2. *Its functional determinant is equal to $\dot{y}y^2$ which is not identically equal to zero. In that case, the function ϕ is defined by $\phi : \mathbb{R}^2 \to \mathbb{R}^2$,*
$\phi(p) = \begin{bmatrix} p_1^2 \\ -p_2^2 \end{bmatrix}$

3. *Algorithm 5 is used with a regular paving such that its resolution is $\varepsilon = 0.05$. The results are illustrated in Figure 3.7 after regularization. Light gray, dark gray and black color boxes correspond to SM-identifiable sets but which are not μ SM-identifiable. The red color boxes represent the μ-SM-identifiable sets.*
With Algorithm 6, we do not obtain such SM-identifiable sets.

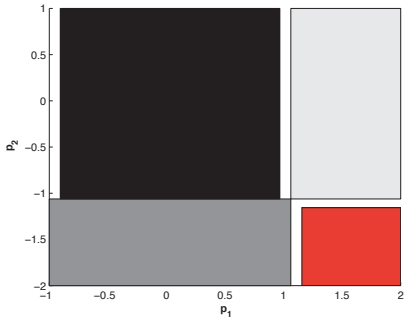

Figure 3.7: Red: μ-SM-identifiable sets, Grays and Black: SM-identifiable sets.

Example 3.7.2 *Consider the following example:*

$$\begin{cases} \dot{x}_1(t) = x_1(t) + x_2(t) + u(t), \quad x_1(0) = p_1(1 + \sin(p_1) - p_2\sin(p_1)) + p_2\cos(p_1), \\ \dot{x}_2(t) = -x_1^2(t) - ((1-p_2)p_1\cos(p_1) - p_2\sin(p_1) - 2p_2)x_1x_2, \quad x_2(0) = 0, \\ y = x_1. \end{cases} \tag{3.28}$$

1. *By setting $c_1 = \cos(p_1)$ and $c_2 = \sin(p_1)$, the Rosenfeld-Groebner algorithm, implemented in the package DifferentialAlgebra of Maple gives the following differential polynomial:*

$$w(\bar{y}, \bar{u}, p) = -\dot{u} - \dot{y} + \ddot{y} + y^2 + ((1-p_2)p_1\cos(p_1) - p_2\sin(p_1) - 2p_2)(\dot{y}y - uy - y^2). \tag{3.29}$$

2. *Clearly the associated functional determinant is not identically equal to zero. Suppose also that $u(0) = 0$, then the following function $\phi : \mathbb{R}^2 \to \mathbb{R}^2$ can be considered:*
$\phi(p) = \begin{bmatrix} (1-p_2)p_1\cos(p_1) - p_2\sin(p_1) - 2p_2 \\ p_1(1 + \sin(p_1) - p_2\sin(p_1)) + p_2\cos(p_1) \end{bmatrix}$.

3. *Choosing* $\varepsilon = 0.01$ *and Algorithm 5, the results illustrated in Figure 3.8 are obtained.*

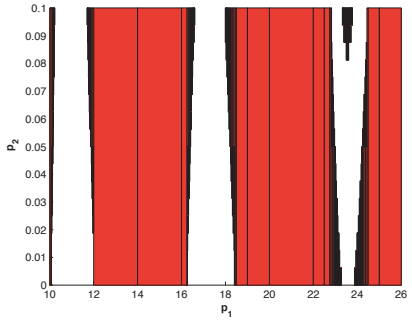

Figure 3.8: Red: μ-SM-identifiable sets, Black: SM-identifiable sets.

3.8 Conclusion

In this chapter, the definitions of (μ-) SM-identifiability and SM-diagnosability are introduced and the links between these three properties established.

Two methods are proposed to test set-membership identifiability. These two methods consist in reducing the study of (μ-)SM-identifiability of the initial model set into the study of algebraic systems and to use interval analysis tools. Interval analysis guarantees that numerical solutions provide sets guaranteed to contain all solutions. The PSE method is easy to implement but can lead to complex systems essentially in the case of nonlinear systems. And, even if it can be used for the construction of P^*, better estimate can be obtained using indirect methods and the whole measurement trajectory. The DA method is probably more difficult to master but in the case of nonlinear models, it can permit to obtain more easily the identifiability results. Moreover, some recent developments in SM estimation as the solver ITVIA allow the user to determine quickly the area on which the model is μ-SM-identifiable.

To finish this chapter, we proposed a guaranteed method for determining, in the parameter space of a model, the SM-identifiable sets, each of them corresponding to different output behaviors from their complement. For doing this, differential algebra tools have been used to obtain differential polynomials. From them, a real function depending only on the parameters has been constructed. We show that the domains on which this function is partially injective correspond to μ-SM-identifiable sets, otherwise if the function verifies only restricted-partial injectivity, the corresponding domain determines SM-identifiable sets. An algorithm based on interval analysis tools has been

proposed to determine the SM-identifiable sets in the function's range.

In the bounded-error framework, the set of all parameters consistent with the model structure, the measurements and the bounds on the perturbations can be defined as the set estimate for the parameters. The following chapter concerns optimal input design to improve this parameter estimation.

Chapter 4

Optimal input design for parameter estimation of dynamical uncertain models

4.1 Introduction

As said in the general introduction, experiment design is important to identify more precisely mathematical models of complex systems.

The conventional approach for experiment design assumes stochastic models for uncertain parameters and measurement errors. Several criteria for experiment design have been proposed involving a scalar function of the Fisher information matrix. When the model is nonlinear with respect to the parameters to be estimated, the local methods lead often to bad results in terms of estimation. Moreover, some sources of uncertainty are not well-suited to the stochastic approach and are better modeled as bounded uncertainties. Thus, in the presented work, the context of bounded-error estimation is considered where the experiment design consists in designing experiments which minimize the estimate parameter domain. The obtained optimal experiment is optimal for the a priori box of parameters.

Thus, to minimize the volume of the estimate parameter set, I and co-workers (L. Denis-Vidal and Z. Cherfi) exhibit an explicit expression linking this set of parameters with the Gram matrix of sensitivities which is presented in this chapter. This work follows a study on the optimization of the initial conditions in the same context but with a different approach [73]. To obtain an explicit expression of the set of parameters to be estimated, the authors in [56] used a centered inclusion function for the model output involving the sensitivity functions. Starting from this idea, we explicitly build some criteria to find

an optimal experiment in the bounded-error context. In our work, we consider only the optimal input design. The proposed methodology requires a parametrization of the input with a finite number of parameters.

This chapter is organized as follows. In Section 4.2, the problem statement is presented. Section 4.3 concerns the acquisition of the proposed criteria for optimal input. An aerospace application is given in Section 4.4.

4.2 Problem formulation

In this chapter, we consider nonlinear dynamical systems described by the form presented in Section 2.2, chapter 2:

$$\begin{cases} \dot{x}(t,p) = f(x(t,p),u(t),p), \\ y(t,p) = g(x(t,p),p), \end{cases} \tag{4.1}$$

where the hypotheses are relatively similar to those given in the second chapter. $p \in \mathbb{P}_0$ is an a priori initial domain for the parameters to be estimated included in $\mathcal{U}_{\mathcal{P}}$.
$u(t)$ represents the input. We suppose that $u(t)$ belongs to a class of admissible inputs $\mathcal{U}$. The time t is assumed to belong to $[t_0, T]$ and to simplify, we get $t_0 = 0$.

Interval arithmetic is used to compute guaranteed bounds for the considered problem at the sample times $\{t_1, t_2, ..., t_N\}$.
$y(t_k, p)$ is a vector with components $y_i^k(p) = y_i(t_k, p)$ for $i = 1, ..., m$, $k = 1, \ldots, N$ and we note $y^k(p) = y(t_k, p)$.

Let $z(t_k)$ be the measurements vector at sample time t_k and $z^k = z(t_k)$. Suppose that there exists a "true" value of parameters p^* such that we have $z^k = y^k(p^*) + v(t_k)$ for k from 1 to N.

Finally $[y^k(p)] = [z^k - \overline{v}(t_k), z^k - \underline{v}(t_k)]$.

In a bounded-error estimation context, one is interested in estimating the set $\mathbb{P} \subset [\mathbb{P}_0]$ of all parameters p consistent with the model structure and the bounds on the measurement noise.

In order to obtain the most accurate estimates, we choose to minimize a cost function, for example the volume, of the set $\mathbb{P}$ (or of an enclosure of $\mathbb{P}$). It may generally depend on the values of the input, the initial time, the sample times, among others. In this work, only the input is considered.

Our aim is to design an input that minimizes the cost function. More formally, one has to find an input u^* such that:

$$u^* = arg \min_{u \in \mathcal{U}} \Phi(\mathbb{P}). \tag{4.2}$$

Obtaining $\mathbb{P}$ is difficult in practice. Nevertheless there are efficient algorithms to obtain an outer-approximation $[p]$ of $\mathbb{P}$. The Problem (4.2) is thus relaxed as follows:

$$u^* = arg \min_{u \in \mathcal{U}} \Phi([p]),$$

This point is explained in the following section.

4.3 Criteria for optimal input

In this section, we exhibit criteria involving the input u to be used to minimize the volume of $[p]$ for an appropriate choice for u. In [56], the authors have used a centered inclusion function at $m \in \mathbb{R}^p$ for the model output. The use of sensitivity functions leads to reduce more quickly the size of outer approximations of the sets of interest. Thus we start from this idea which leads to obtain an explicit expression of $[p] - m$.
Considering $[p]$ such that $\mathbb{P} \subset [p] \subset [\mathbb{P}_0]$, $m \in [p]$ and a mean value form for $y^k([p])$, $[p]$ has to satisfy:

$$y^k(m) + \sum_{j=1}^{p} ([p_j] - m_j) \left[\frac{\partial y^k}{\partial p_j}\right] ([p]) \subseteq [z^k]. \tag{4.3}$$

Then:

$$\sum_{j=1}^{p} ([p_j] - m_j) \left[\frac{\partial y^k}{\partial p_j}\right] ([p]) \subseteq [z^k] - y^k(m). \tag{4.4}$$

Let us denote $[S_i^k]$ the row vector whose entries are:
$[S_{ij}^k] = \left[\frac{\partial y_i^k}{\partial p_j}\right] ([p])$, $[S_i^k] \in \mathbb{IR}^{1\times p}$, $i = 1, ..., m$.

The interval matrix $[S^k] \in \mathbb{IR}^{m\times p}$ is built with the m rows $[S_i^k]$.
In the following, the interval matrix $[S^k]^T[S^k]$ is assumed to be positive definite and to simplify the notation, we take $([S^k]^T[S^k])^{-1}[S^k]^T[S^k] = [I^k]$.
One has to find u such that $\| [p] - m \|$ is as small as possible.

Thus (4.4) becomes:

$$[S^k]([p] - m) \subseteq [v^k], \tag{4.5}$$

where $[v^k] = [z^k] - y^k(m)$.

From (4.5), we obtain: $[S^k]^T[S^k]([p] - m) \subseteq [S^k]^T[v^k]$, then using $([S^k]^T[S^k])^{-1}$ the following inclusion is obtained:

$$[I^k]([p]-m) \subseteq ([S^k]^T[S^k])^{-1}[S^k]^T[v^k]. \tag{4.6}$$

The following proposition gives two upper bounds for $[I^k]([p]-m)$.

Proposition 4.3.1 *For all $k \in \{1,...,N\}$, the two following inequalities hold:*

$$\| [I^k]([p]-m) \|^2 \leq \| ([S^k]^T[S^k])^{-1}[S^k]^T \|_F^2 \| \tilde{v}^k \|_2^2, \text{ and}$$

$$\| [I^k]([p]-m) \|^2 \leq | \operatorname{tr}([I^k]([S^k]^T[S^k])^{-1}) | \| \tilde{v}^k \|_2^2$$

with $\tilde{v}^k = | [v^k] |$.

Proof:
Let $[A] = ([S^k]^T[S^k])^{-1}[S^k]^T$ and $[a_{ij}]$ be the entries of $[A]$:

$$[I^k]([p]-m) \subseteq [A][v^k], \tag{4.7}$$

and:

$$\| [I^k]([p]-m) \|^2 \leq \| [A][v^k] \|^2 \leq \left(\max_i \sum_{j=1}^{p} | [a_{ij}] | | [v_j^k] | \right)^2. \tag{4.8}$$

Since $\left(\sum_{j=1}^{p} | [a_{ij}] | | [v_j^k] |\right)^2 \leq \sum_{j=1}^{p} | [a_{ij}] |^2 \sum_{j=1}^{p} | [v_j^k] |^2$,
one obtains:

$$\begin{aligned} \max_i \left(\sum_{j=1}^{p} | [a_{ij}] | | [v_j^k] | \right)^2 &\leq \max_i \sum_{j=1}^{p} | [a_{ij}] |^2 \| \tilde{v}^k \|^2 \\ &\leq \| [A] \|_F^2 \| \tilde{v}^k \|^2 . \end{aligned} \tag{4.9}$$

Then $\| [A] \|_F^2 = | \operatorname{tr}([I^k]([S^k]^T[S^k])^{-1}) |$ because $\operatorname{tr}([A][A]^T) = \operatorname{tr}([A]^T[A])$ and:

$$\begin{aligned} [A][A]^T &= ([S^k]^T[S^k])^{-1}[S^k]^T[S^k]([S^k]^T[S^k])^{-1} \\ &= [I^k]([S^k]^T[S^k])^{-1} \end{aligned}$$

This leads to Proposition (4.3.1).□

An upper bound of $| \operatorname{tr}([I^k]([S^k]^T[S^k])^{-1}) |$ depending on $| \operatorname{tr}(([S^k]^T[S^k])^{-1}) |$ is given in Proposition 4.3.2.

Proposition 4.3.2 *For all $k \in \{1,...,N\}$:*

$$| \operatorname{tr}([I^k]([S^k]^T[S^k])^{-1}) | \leq \lambda_{max}(| [I_\epsilon] |) | \operatorname{tr}(([S^k]^T[S^k])^{-1}) |$$

where $\lambda_{max}(| [I_\epsilon] |) = 1 + n_p\epsilon$ is the maximum eigenvalue of $| [I_\epsilon] |$.

Proof:
For each $k \in 1, ..., N$ there exists ϵ_k such that $[I^k] \subset [I_{\epsilon_k}]$
$[I^k]([S^k]^T[S^k])^{-1} \subseteq [I_{\epsilon_k}]([S^k]^T[S^k])^{-1}$,
Let $\epsilon = \max_{k\in\{1,...,N\}} \epsilon_k$ then $[I_{\epsilon_k}] \subset [I_\epsilon]$.
Let $[C] = ([S^k]^T[S^k])^{-1}$, the following inequalities are obtained:

$$\begin{aligned} \mid \mathrm{tr}([I^k]\,[C]) \mid \quad &\leq \mid \mathrm{tr}([I_\epsilon]\,[C]) \mid, \\ &\leq \mathrm{tr}(\mid [I_\epsilon] \mid \mid [C] \mid), \\ &\leq \lambda_{max}(\mid [I_\epsilon] \mid)\mathrm{tr}(\mid [\mathrm{C}] \mid), \end{aligned}$$

because the matrices $\mid [I_\epsilon] \mid$ and $\mid [C] \mid$ are symmetric [83]. □

Then $\parallel [I^k]([p] - m) \parallel$ depends on $\mid \mathrm{tr}(([S^k]^T[S^k])^{-1}) \mid$. Propositions 4.3.1 and 4.3.2 lead, for all $k \in \{1, ..., N\}$, to:

$$\parallel [I^k]([p] - m) \parallel^2 \leq \lambda_{max}(\mid [I_\epsilon] \mid) \mid \mathrm{tr}(([S^k]^T[S^k])^{-1}) \mid \parallel \tilde{v}^k \parallel_2^2$$

which gives a criterion J_1 for optimal input design. It may be defined as follows:

$$J_1(u) = \sum_k \mid \mathrm{tr}(([S^k]^T[S^k])^{-1}) \mid.$$

This criterion is similar to the A-optimality in the stochastic framework. Then this leads to the following definitions.

Definition 4.3.1 *The criterion J_1 is called the set-membership-A-optimality criterion.*

This criterion consists in considering the largest absolue value of $\mathrm{tr}\left(([S^k]^T[S^k])^{-1}\right)$.

Definition 4.3.2 *An input u^* is said to be set-membership-A-optimal when:*

$$u^* = \min_{u\in\mathcal{U}} J_1(u).$$

In order to avoid the inverse matrix computation $([S^k]^T[S^k])^{-1}$, the following criterion is proposed:

$$J_2(u) = \sum_k \mathrm{mig}\left(\mathrm{tr}\left([S^k]^T[S^k]\right)\right). \tag{4.10}$$

This criterion consists in considering the smallest absolue value of $\mathrm{tr}\left([\mathrm{S^k}]^{\mathrm{T}}[\mathrm{S^k}]\right)$.

Definition 4.3.3 *The criterion J_2 is called the set-membership-T-optimality criterion.*

Definition 4.3.4 *An input u^* is said to be set-membership-T-optimal when:*

$$u^* = \max_{u \in \mathcal{U}} J_2(u).$$

This criterion is similar to the criterion based on the trace of the Fisher matrix in the stochastic case.
In this case it is necessary to verify the invertibility of the matrix $[S^k]^T[S^k]$ that is $0 \notin \det([S^k]^T[S^k])$.

The following section is devoted to the obtention of optimal input for a case study described below.

4.4 Application to a model from aerospace

4.4.1 Model equations

Consider the model describing the longitudinal motion of a glider developped in [24]. The projection of the general equations of motion onto the aerodynamic reference frame of the aircraft and the linearization of aerodynamic coefficients give the pfollowing system:

$$\left\{\begin{array}{rl}
\dot{V} = & -g\sin(\theta-\alpha) - \dfrac{1}{2m}\rho S V^2 (C_x^0 + C_{x\alpha}(\alpha-\alpha_0) + C_{x\delta_m}(\delta_m - \delta_{m_0})), \\
\dot{\alpha} = & \dfrac{2}{2mV + \rho S l V C_{z\dot{\alpha}}}\Big\{ mVq + mg\cos(\theta-\alpha) - \dfrac{1}{2}\rho S V^2 (C_z^0 + C_{z\alpha}(\alpha-\alpha_0) \\
& + C_{zq}\dfrac{ql}{V} + C_{z\delta_m}(\delta_m - \delta_{m_0}))\Big\}, \\
\dot{q} = & \dfrac{1}{2B}\rho S l V^2 \Big\{ C_m^0 + C_{m\alpha}(\alpha-\alpha_0) + C_{mq}\dfrac{ql}{V} + C_{m\dot{\alpha}}\dfrac{2l}{2mV^2 + \rho S l V^2 C_{z\dot{\alpha}}}\Big[mVq \\
& + mg\cos(\theta-\alpha) - \dfrac{1}{2}\rho S V^2 (C_z^0 + C_{z\alpha}(\alpha-\alpha_0) + C_{zq}\dfrac{ql}{V} \\
& + C_{z\delta_m}(\delta_m - \delta_{m_0}))\Big] + C_{m\delta_m}(\delta_m - \delta_{m_0})\Big\}, \\
\dot{\theta} = & q.
\end{array}\right. \tag{4.11}$$

In these equations, the state vector x is given by $(V, \alpha, q, \theta)^\top$, the whole state is observed (i.e., $y = x$), the input u is δ_m given in degree (δ_{m_0} represents the initial condition). The variable $V\,(m/s)$ denotes the speed of the aircraft, $\alpha\,(deg)$ the angle of attack, α_0 the trim value of α, $\theta\,(deg)$ the pitch angle, $q\,(deg/s)$ the pitch rate. The other constants

represent δ_{m_0} the elevator deflection angle, ρ the air density, g the acceleration of gravity, l a reference length and S the area of a reference surface. B represents a moment of inertia. The parameters to be estimated are $p = (C_{z\dot{\alpha}}, C_{zq}, C_{m\dot{\alpha}}, C_{mq})$, which are assumed to be uncertain. The other coefficients correspond to the dynamic stability derivatives and are supposed to be known.
The initial conditions are supposed to belong to:

$$[\mathbb{X}_0] = \begin{bmatrix} 28.48, & 28.52 \\ 6.27, & 6.73 \\ -0.23, & 0.23 \\ 2.20, & 2.66 \end{bmatrix}. \tag{4.12}$$

The parameters are supposed to be included in:

$$[\mathbb{P}_0] = \begin{bmatrix} 1.71, & 1.89 \\ 4.75, & 5.25 \\ -5.25, & -4.75 \\ -23.1, & -20.9 \end{bmatrix}. \tag{4.13}$$

The output error (2.2) is supposed to be bounded by:

$$[v] = \begin{bmatrix} -0.05, & 0.05 \\ -0.25, & 0.25 \\ -0.25, & 0.25 \\ -0.25, & 0.25 \end{bmatrix}. \tag{4.14}$$

The measurements have been simulated using the parameters equal to $p^* = (1.8, 5, -5, -22)^T$. The test duration is fixed at one second. The stop criterion for the SIVIA algorithm is $\epsilon = (0.01, 0.05, 0.05, 0.1)$ that means that the stop threshold for the first parameter is 0.01, the second and third are 0.05 and the last one is 0.1.

4.4.2 Optimal input

4.4.2.1 Procedure description

In this application, the admissible input has been limited to full amplitude square waves. In fact, analytic works for similar problems demonstrate that inputs similar to square waves were superior to sinusoidal inputs for parameter estimation [20]. In this work, the test time is divided into discrete steps called stages.

The inputs tested by our procedure are given by:

$$u(t) = u_0 + \sum_{i=1}^{r} (a_i \varepsilon_i - a_{i-1}\varepsilon_{i-1}) H(t - \tau_{i-1}),\ \varepsilon_0 = 0\,, \tag{4.15}$$

where u_0 is an input trim value, H is the Heaviside function. The variable r represents the total number of stages. The variables τ_i are the switching times with τ_0 the initial test time. Indeed, the variables a_i are chosen to be equal to the square wave full positive amplitude [88]. The given variables τ_i satisfy $\tau_0 < \tau_1 < ... < \tau_r$ and ε_i is equal to 0, 1 or -1 (for $i = 1, ..., r$).

Thus, we obtain the optimal number of square waves (with fixed time and fixed amplitude) to be realized; the corresponding signal is noted u^*. In order to obtain an optimal input, criterium (4.10) is used. Sensitivities $\dfrac{\partial y(t_i, p)}{\partial p}$ are solutions of the following equations:

$$\frac{d}{dt}\left(\frac{\partial x}{\partial p_j}\right) = \sum_{k=1}^{n}\left[\frac{\partial f}{\partial x_k}\frac{\partial x_k}{\partial p_j}\right] + \frac{\partial f}{\partial p_j} \tag{4.16}$$

$$\frac{\partial y}{\partial p_j} = \sum_{k=1}^{n}\left[\frac{\partial g}{\partial x_k}\frac{\partial x_k}{\partial p_j}\right] + \frac{\partial g}{\partial p_j},\ j = 1, ..., p. \tag{4.17}$$

The Algorithm for obtaining the optimal input is described in following subsection.

4.4.2.2 Optimal input: Algorithm

In this algorithm, the variables r and t_r describe the number of stages and the number of sample times by stages respectively. The functions $eval - ODE$ and $eval - sensitivity$ allow to compute respectively the guaranteed solutions of ordinary differential equations and to compute the sensitivities respectively. The function $eval - cout$ allows to evaluate the value of the criterion.

Algorithm 10 Search for optimal input (u^*)

Input: f, $[x](0)$, r ;
Output: u^*;
initialization: $\mathbb{L} := [x](0)$;
for i=1:r **do**
$u(i) = \text{input} - \text{signal(i)}$;
$[x](i) := Pop(\mathbb{L})$;
for j=1:t_r-1 **do**
$[x](j) = eval - ODE([x](j-1), u(i))$;
$\mathbb{L} := \mathbb{L} \cup [x](j)$;
sensibility:=$\text{eval} - \text{sensibility}([\text{x}](\text{j}), \text{u(i)})$;
cout-intermediaire:=$\text{eval} - \text{criterion}(\text{sensibility})$;
cout:=cout $\cup$ (cout-intermediaire, u(i));
$j := j + 1$;
end for
$i := i + 1$;
parcours-cout(cout);
return(u^*)
end for

Numerical results are given in following subsection.

4.4.2.3 Numerical results

The criterion J_2 has been maximized for different total numbers of stages r. The values are given in Tables 4.1 and 4.2. The variable T represents the computing time (in seconds). The fourth column of thse Tablee represents the optimal value of $u(t)$ on each stage, for the value of r given in the first column. The time length of each stage is linked to the number of stages, the test time being fixed at one second. For example, if the test time is divided in four stages, each stage duration is fixed at 0.25 seconds. The total number of sample times is $N = 120$ in Table 4.1 and $N = 10$ in Table 4.2.

Number of stages	$J_2(u^*)$	T	$u^*(t)$
2	3266	223	[-4.2 -4.2]
3	3522	646	[-4.2 -1 -4.2]
4	3440	1935	[-4.2 -4.2 -1 -4.2]
5	3542	6031	[-4.2 -4.2 -1 -4.2 -4.2]
6	3509	16416	[-4.2 -4.2 -1 -1 -4.2 -4.2]

Table 4.1: Values of the optimal input u^* / $J_2(u^*) = \max_{u \in \mathcal{U}} J_2(u)$ and $N = 120$.

For $N = 120$, the optimal value for the input is obtained with 5 stages.
In Table 2, we use $N = 10$:

Number of stages	$J_2(u^*)$	T	$u^*(t)$
2	249	49	[-4.2 -4.2]
3	264	151	[-4.2 -1 -4.2]
4	252	442	[-4.2 -4.2 -1 -4.2]
5	272	1340	[-4.2 -4.2 -1 -4.2 -4.2]
6	263	4036	[-4.2 -4.2 -1 -1 -4.2 -4.2]

Table 4.2: Values of the optimal input u^* / $J_2(u^*) = \max_{u \in \mathcal{U}} J_2(u)$ and $N = 10$.

Through this second Table, we show that the optimal input is obtained with five stages and this optimal input is the same as the one with 120 sample times. The computing time is divided by approximatively 4.5 using $N = 10$.

As previously explained, the state and parameter estimation process is combined with a set inversion mechanism, which consists of many branch and bound operations slowing down the whole procedure. Using less measurements for the state and parameter estimation procedure, it is possible to reduce significantly the computation time. Therefore, in the next section, we use $N = 10$ points to estimate the parameters of interest.

4.4.3 Parameter estimation

To highlight the efficiency of the proposed optimal input design, we compare the estimation results obtained using three different inputs: the first one is a constant input and the second one is an optimized input proposed in [44] which is optimal for the same case study with Gaussian noise and parameters in an a priori known box; the last one is the optimal input obtained above (with five stages):

$$u^*(t) = \delta_{m_0} + a \sum_{i=1}^{5} (\epsilon_i - \epsilon_{i-1}) H(t - \tau_{i-1}), \tag{4.18}$$

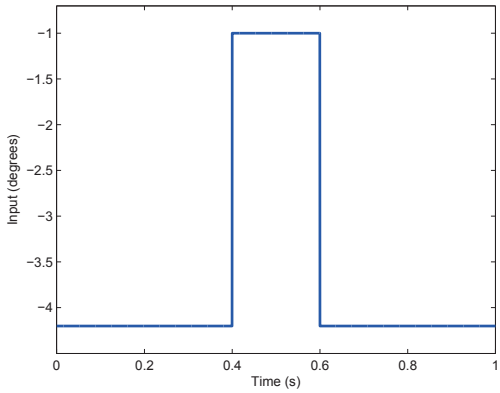

Figure 4.1: Optimal input obtained via the set-membership-T-optimality criterion

with $a = 1.6\ degree$ and $\tau_0 = 0\ s$, $\tau_1 = 0.2\ s$, $\tau_2 = 0.4\ s$, $\tau_3 = 0.6\ s$, $\tau_4 = 0.8\ s$.

The order of the Taylor expansion is chosen automatically by VNODE-LP. As said previously, we use $N = 10$ measurement times.
The parameter estimation results are compared only for admissible parameters, which are given in Figures 4.2 and 4.3. The red boxes represent the acceptable sets for parameters. The black border cube represents the box $[\mathbb{P}_0]$.

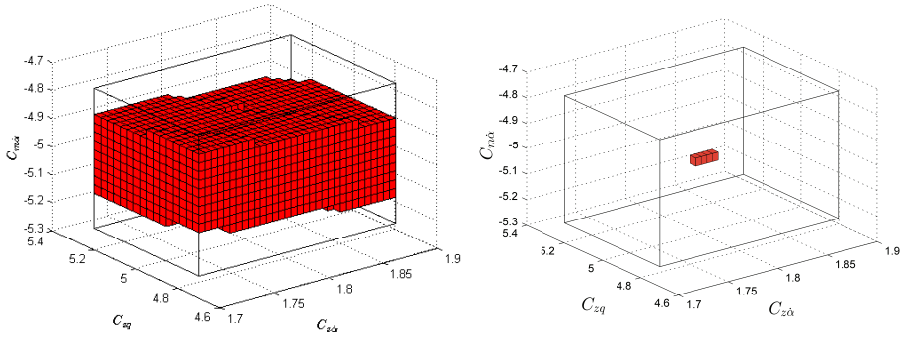

Figure 4.2: Admissible $C_{z\dot{\alpha}}$, C_{zq}, $C_{m\dot{\alpha}}$ with constant (left) and optimal (right) inputs

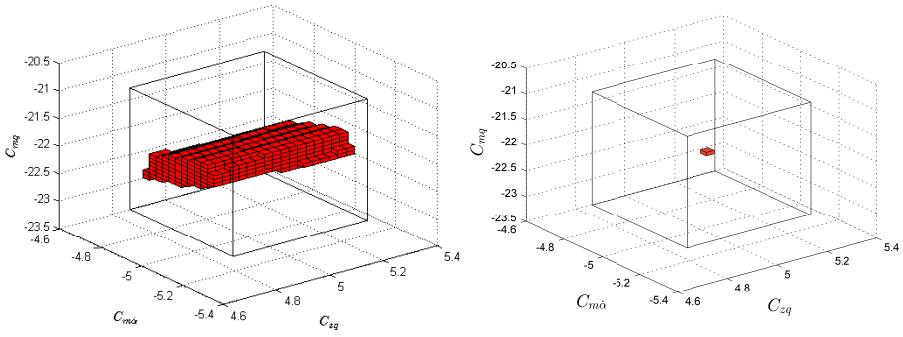

Figure 4.3: Admissible C_{zq}, $C_{m\dot{\alpha}}$, C_{mq} with constant (left) and optimal (right) inputs

In the following Table, the eliminated part in $[\mathbb{P}_0]$ for each estimated parameter is given (in percentage). It is given by:

$$\%p_i = w([\mathbb{P}_{0_i}]) - w([p_{accepted_i}]), \tag{4.19}$$

with i from 1 to 4 and $[p_{\text{accepted}_\text{i}}]$ means the solution interval for the i^{th} parameter of interest enhanced for a constant input, the input in [44] and the optimal input.

Parameter	with constant input	with optimized input (Gaussian noise)	with optimal input
$C_{z\dot{\alpha}}$	0	0	81.50
C_{zq}	0	75.00	93.75
$C_{m\dot{\alpha}}$	25.00	80.00	93.75
C_{mq}	62.62	65.62	96.87

Table 4.3: Eliminated percentage of initial intervals

Through this table, we see that the estimations of parameters $C_{z\dot{\alpha}}$ and C_{zq} are well improved with an optimal input.

4.5 Conclusion

In this chapter, two set-membership optimal input criteria have been proposed to improve parameter estimation for a class of nonlinear dynamical models requiring a parametrization of the input with a finite number of parameters: the set-membership-T-(and A)-optimality criteria. The set-membership-T-optimality criterion has been successfully used to improve parameter estimation of a case study taken from the aeronautical domain. Moreover, with the set-membership-T-optimal input, the computational time for

parameter estimation process is reduced compared to the computational time obtained with a non-optimal input.

After the presentation of my works in the set-membership framework, the following chapter concerns the filtering of linear dynamical systems in the case of mixed uncertainties.

Chapter 5

Accounting for mixed uncertainties in dynamical models: the iIKF

In this chapter, I consider the filtering problem in the case of *mixed uncertainties* meaning that I consider some bounded uncertainties on parameters whereas perturbations/noise are modeled through appropriate probability distributions. This chapter details the contribution in the filtering of such models when L. Travé-Massuyès and I were supervisors of the thesis of J. Xiong (defended in 2013).

5.1 Interval Kalman filtering: problem formulation

5.1.1 Introduction

In [19], the classical Kalman filter [54] has been extended to interval linear models. Two filterings are proposed: the first one is called Interval Kalman filtering (IKF) which is a direct extension of the classical Kalman filtering to intervals. The filtering result produced by the IKF is generally conservative and expanding rapidly. The second proposed filtering is a sub-optimal version in which the authors consider the upper bound of the interval matrix to be inverted. We note this algorithm sIKF (sub-optimal interval Kalman filtering). Starting from this work, we propose several operations that improve the filtering. In particular, the sub-optimal approach proposed in [19] does not provide guaranteed results because it avoids interval matrix inversion. Our main contribution consists in proposing a method to solve the interval matrix inversion problem without loss of solutions while controlling the inherent pessimism of interval calculus.

In particular the gain of the filter is obtained by a calculus based on the set inversion algorithm SIVIA combined with constraint propagation techniques.

We consider linear dynamical systems described by a set of state differences and observation equations (Kalman model [54]):

$$\begin{cases} x_{k+1} = Ax_k + Bu_k + w_k, \\ y_k = Cx_k + Du_k + v_k, k \in \mathbb{N}, \end{cases} \tag{5.1}$$

where $x_k \in \mathbb{R}^n$, $y_k \in \mathbb{R}^m$ and $u_k \in \mathbb{R}^p$ denote state, observation and input vectors, respectively. The matrices A, B, C and D are constant matrices such that $A \in \mathbb{R}^{n\times n}$, $B \in \mathbb{R}^{n\times p}$, $C \in \mathbb{R}^{m\times n}$ and $D \in \mathbb{R}^{m\times p}$. $\{w_k\}$ and $\{v_k\}$ are independent centered Gaussian white noise sequences, with covariance matrices Q and R definite positive by definition, respectively:

$$\begin{array}{l} E\{w_k, w_l\} = Q\delta_{kl}, E\{v_k, v_l\} = R\delta_{kl}, \\ E\{w_k, v_l\} = E\{w_k, x_0\} = E\{v_k, x_0\} = 0, \\ \forall (k, l) \in \mathbb{N}^2, \end{array}$$

where δ_{kl} represents the Kronecker symbol.

Given the system (5.1), the conventional Kalman filter provides the minimum variance estimate $\hat{x}_k$ of x_k and the associated covariance matrix P_k. The estimation problem can be written under the form:

$$(\hat{x}_k, P_k) = \mathcal{K}(A, B, C, D, x_0, P_0, u_l, y_l)_{l<k},$$

where $\mathcal{K}$ means the estimation procedure developped by R.E. Kalman which is briefly described below.

When matrices $A,\ B,\ C$, and D are only known to belong respectively to interval matrices $[A],\ [B],\ [C]$ and $[D]$, respectively, both $\hat{x}_k$ and P_k are tainted by bounded uncertainty. The interval Kalman filter aims at computing (an enclosure of) the set of all possible $(\hat{x}_k, P_k)$, i.e.:

$$\begin{array}{rl} \mathcal{X} = ([\hat{x}_k], [P_k]) = \{(\hat{x}_k, P_k) \mid \exists A \in [A], B \in [B], C \in [C], D \in [D], \\ (\hat{x}_k, P_k) = \mathcal{K}(A, B, C, D, x_0, P_0, u_l, y_l)_{l<k}\}. \end{array}$$

5.1.2 Conventional Kalman filtering

There are several ways to deduce Kalman equations [54]. We can use mathematical curve-fitting function of data points from a least-squares approximation [135] or also use probabilist methods such as the Likelihood function to maximize the conditional probability of the state estimate from measurement incomes [82]. We consider the following notations:

1) $\hat{x}_{k+1|k} \in \mathbb{R}^n$ the *a priori* state estimate vector at time $k + 1$ given state estimate at time k,

2) $\hat{x}_{k|k} \in \mathbb{R}^n$ the *a posteriori* state estimate vector at time k given observations at time k,

3) $P_{k+1|k} \in \mathbb{R}^{n\times n}$ the *a priori* error covariance matrix,

4) $P_{k|k} \in \mathbb{R}^{n\times n}$ the *a posteriori* error covariance matrix.

$P_{.|.}$ is a key indicator that defines the accuracy of the state estimate :

$$P_{l|k} \quad = \quad E\left((x_l - \hat{x}_{l|k})(x_l - \hat{x}_{l|k})^T\right), l = k \text{ or } k+1. \tag{5.2}$$

It is known that the Kalman filtering algorithm contains two steps for each iteration: a prediction step and a correction step [54]. Thus the filtering algorithm is the following in which N denotes the total number of sample times:

Algorithm 11 Algorithm Kalman Filter ($\hat{x}$,$\hat{P}_{.|.}$)

Input: A,B,C, D, ;
Output: $k = 0$;
1: $P_{0|0} = Cov\{x_0\},\ m_0 = E(x_0)$;
2: $x_0 \sim \mathrm{N}(m_0, P_{0|0})$;
3: **for** $k = 1 : N$ **do**
4: *Prediction:*
5: $\hat{x}_{k+1|k} = A\hat{x}_{k|k} + Bu_k$,;
6: $\hat{P}_{k+1|k} = A\hat{P}_{k|k}A^T + Q$;
7: *Correction:*
8: $K_{k+1} = \hat{P}_{k+1|k}C^T\left(C\hat{P}_{k+1|k}C^T + R\right)^{-1}$;
9: $\hat{P}_{k+1|k+1} = (I_n - K_{k+1}C)\hat{P}_{k+1|k}$;
10: $\hat{x}_{k+1|k+1} = \hat{x}_{k+1|k} + K_{k+1}(y_{k+1} - \hat{y}_{k+1|k})$;
11: $k = k + 1$;
12: **end for**

The algorithm proposed by [19] is based on interval conditional expectation for interval linear systems and has the same structure as the conventional Kalman filter algorithm. Its drawback is that it does not guaranty to provide an enclosure of $\mathcal{X}$. In other words, some solutions are lost and the results are not guaranteed. This occurs because singularity problems in interval matrix inversion are avoided by taking the upper bound of the interval matrix to be inverted. We note this algorithm sIKF (sub-optimal interval Kalman filtering).

5.2 Interval Kalman filtering and its improvement

In addition to considering parameter bounded uncertainties through the interval matrices $[A],\ [B]$,
$[C]$ and $[D]$, notice that $x_{0|0}, P_{0|0}, u_k, y_k$ could be boxes due to deterministic measurement errors and instrument precision. In the following, we evaluate the changes impacted by these assumptions on the different steps of the Kalman filtering algorithm.

5.2.1 IKF algorithm presentation

In the interval context, the estimation error covariance matrix is an interval matrix which can be rewritten as:

$$[\hat{P}_{l|k}] \triangleq E\left(([x_l] - [\hat{x}_{l|k}])([x_l] - [\hat{x}_{l|k}])^T\right), \tag{5.3}$$

where $l = k$ or $k+1$. $[\hat{P}_{k|k}]$ is the estimation error covariance and $[\hat{P}_{k+1|k}]$ is the prediction error covariance.

All elements on the diagonal of $P_{.|.}$ are positive as they represent the variance of each state, thus the trace of $P_{.|.}$ is positive. In the case of an interval matrix $[P_{.|.}]$, this constraint must also hold. If interval calculus pessimistically generates intervals containing non positive values, these are spurious and can be removed. Thus a first constraint is introduced :

$$[P_{.|.}]_{(i,i)} \geq 0, i = 1, 2..., n. \tag{5.4}$$

The calculus of the *a priori* state estimate vector is directly inherited from the determinate model, while real variables are replaced by boxes :

$$[\hat{x}_{k+1|k}] = [A][\hat{x}_{k|k}] + [B][u_k]. \tag{5.5}$$

At the previous time k, the estimation error is characterized by $[P_{k|k}]$. The prediction model does not include noise so the estimation error should also be updated:

$$[\hat{P}_{k+1|k}] = [A][\hat{P}_{k|k}][A]^T + Q. \tag{5.6}$$

This equation can be interpreted as providing all possible *a priori* estimation error covariances between the real state and the *a priori* state estimate at time $k + 1$. Accounting for (5.4), this leads to the following CSP :

$$\begin{cases} [\hat{P}_{k+1|k}] = [A][\hat{P}_{k|k}][A]^T + Q, \\ \mathcal{C} : [\hat{P}_{k+1|k}]_{(i,i)} \geqslant 0, i = 1, 2..., n. \end{cases} \tag{5.7}$$

From [19], the correction equation holds in the interval context:

$$[\hat{x}_{k+1|k+1}] = [\hat{x}_{k+1|k}] + [K_{k+1}]\left([y_{k+1}] - [\hat{y}_{k+1|k}]\right). \tag{5.8}$$

Intuitively, $[K_{k+1}]$ aims to bring back the estimate enclosure around the real state while still retaining all the possible values corresponding to uncertainty. Equations (5.3) and (5.8) give the estimation error covariance expression. This manipulation is only valid when $E\{v_k\} = 0$:

$$\begin{array}{rl}[\hat{P}_{k+1|k+1}] & = [\hat{P}_{k+1|k}] - [K_{k+1}][C][\hat{P}_{k+1|k}] - [\hat{P}_{k+1|k}][C^T][K_{k+1}]^T \\ & +[K_{k+1}]\left([C][\hat{P}_{k+1|k}][C^T] + R\right)[K_{k+1}]^T.\end{array} \tag{5.9}$$

We want to find the box gain $[K_{k+1}]$ minimizing $trace([\hat{P}_{k+1|k+1}])$. Indeed, state variance, given by the diagonal elements of this matrix, is the value that indicates the estimation error:

$$\begin{array}{ll}\frac{\partial trace([\hat{P}_{k+1|k+1}])}{\partial [K_{k+1}]} & = -2[\hat{P}_{k+1|k}][C]^T + 2[K_{k+1}]\left([C][\hat{P}_{k+1|k}][C]^T + R\right), \\ \frac{\partial^2 trace([\hat{P}_{k+1|k+1}])}{\partial [K_{k+1}]\partial [K_{k+1}]^T} & = 2\left([C][\hat{P}_{k+1|k}][C]^T + R\right).\end{array}$$

The second derivative is always positive in the conventional Kalman filter, which guarantees the existence of a solution to the minimization problem. In the interval context, this condition must be forced by a constraint of the same type as (5.4). From the annulation of the first order derivative, we have:

$$[K_{k+1}] = [\hat{P}_{k+1|k}][C]^T\left([C][\hat{P}_{k+1|k}][C]^T + R\right)^{-1}. \tag{5.10}$$

$$\tag{5.11}$$

Thus equations (5.9) and (5.10) give the estimation error covariance expression:

$$[\hat{P}_{k+1|k+1}] = (I_n - [K_{k+1}][C])[\hat{P}_{k+1|k}]. \tag{5.12}$$

Equations (5.5), (5.6), (5.10), (5.12) and (5.8) constitute a discrete interval Kalman filter algorithm:

5.2.2 Interval matrix inversion and overestimation control: the iIKF

A major issue is the pessimism introduced by interval arithmetic. Uncertainty is cumulated at each iteration and the interval matrix inversion involved in equation (5.10) is time consuming, sometimes divergent.

Algorithm 12 Algorithm Interval Kalman Filter ($[\hat{x}]$,$[\hat{P}_{.|.}]$)

Input: A,B,C, D, ;
Output: $k = 0$;
1: $P_{0|0} = Cov\{x_0\},\ m_0 = E(x_0)$;
2: $[x_0] \sim \mathrm{N}(m_0, P_{0|0})$;
3: **for** $k = 1 : N$ **do**
4: *Prediction:*
5: $[\hat{x}_{k+1|k}] = [A][\hat{x}_{k|k}] + [B][u_k]$;
6: $[\hat{P}_{k+1|k}] = [A][\hat{P}_{k|k}][A]^T + Q$;
7: *Correction:*
8: $[K_{k+1}] = [\hat{P}_{k+1|k}][C]^T \left([C][\hat{P}_{k+1|k}][C]^T + R\right)^{-1}$;
9: $[\hat{P}_{k+1|k+1}] = (I_n - [K_{k+1}][C])[\hat{P}_{k+1|k}]$;
10: $[\hat{x}_{k+1|k+1}] = [\hat{x}_{k+1|k}] + [K_{k+1}]\left([y_{k+1}] - [\hat{y}_{k+1|k}]\right)$;
11: $k = k + 1$;
12: **end for**

Equation (5.10) involves the inversion of the interval matrix $([C][\hat{P}_{k+1|k}][C]^T + R)$. The first problem refers to singularities, which means that the following condition should be fulfilled:

$$0 \notin det\left([C][\hat{P}_{k+1|k}][C]^T + R\right).$$

Besides, the interval matrix inverse is obtained by approximation algorithms, like in [114], and is generally over estimated.

We propose an approach using the algorithm SIVIA.
The idea is to solve the interval matrix inversion problem by a set of constraint propagation problems. Equation (5.10) is rewritten as:

$$[K_{k+1}]\left([C][\hat{P}_{k+1|k}][C]^T + R\right) = [\hat{P}_{k+1|k}][C]^T.$$

Each component in matrix $[K_{k+1}]$ is considered separately and the search space is the following cartesian product :

$$[K_{k+1}]_{1,1} \times [K_{k+1}]_{1,2} \times ... \times [K_{k+1}]_{n,m}.$$

This search space is bisected and tested under SIVIA properly adapted to matrix operation. The result is a set of small boxes that satisfy the above Equation, each box providing a "small acceptable gain". The set of boxes is then injected at the correction step to update the covariance matrix and the state estimate vector. The final result is the hull of all covariance matrices and state estimate vectors corrected by each small gain.

5.2.2.1 Constraint Propagation

Constraint propagation is very useful to reduce the width of the boxes involved in a set of constraints [15]. In this work, we use the well-known forward-backward algorithm. The principle is to decompose the constraint equation $f([x_1], ..., [x_n]) = 0$ in a sequence of elementary operations of primitive functions like $\{+, -, *, /\}$ and obtain a list of primitive constraints [70]. For example, consider the following equation:

$$[\hat{x}_{k+1|k+1}] = [\hat{x}_{k+1|k}] + [K_{k+1}]([y_{k+1}] - [C][\hat{x}_{k+1|k}]).$$

This equation can be decomposed, following the computation tree, into the following set of primitive constraints:

$$\begin{cases} [a_1] = [C][\hat{x}_{k+1|k}], \\ [a_2] = [y_{k+1}] - [a_1], \\ [a_3] = [K_{k+1}][a_2], \\ [\hat{x}_{k+1|k+1}] = [\hat{x}_{k+1|k}] + [a_3]. \end{cases}$$

In our problem, we want to contract $\{[\hat{x}_{k+1|k+1}],\ [\hat{x}_{k+1|k}],\ [K_{k+1}]\}$ without changing $\{[C], [y_{k+1}]\}$, which are considered as inputs.

5.2.2.2 Interval intersection rule

As the associative law is no longer valid in interval arithmetic, we must redefine the product of three and four interval matrices [71]. This is the principle of the interval intersection rule.

$$\prod_{i=1}^{n} [M_i] \triangleq \left[(\prod_{i=1}^{n-1} [M_i]) \cdot [M_n] \right] \cap \left[[M_1] \cdot (\prod_{i=1}^{n-1} [M_{i+1}]) \right]. \tag{5.13}$$

where $[M_1], ..., [M_n]$ are interval matrices.

5.2.2.3 Adaptative calibration

When the interval matrix to be inverted is not regular, we must find a way to cut down the uncertainty accumulated by interval arithmetic. In this case, a calibration can be implemented to reset the iteration for limiting divergence [71]. We propose the following calibration mechanism:

$$[\hat{x}_k] \triangleq \hat{x}_k + [\zeta_k],\ [P_k] = [P_0]. \tag{5.14}$$

where $\hat{x}_k$ is the conventional Kalman state estimate from the nominal system and $[\zeta_k]$ is set from the state variances.

5.3 Numerical results

In this section, we apply previously presented filters on an example proposed in [19] given by the following form:

$$\begin{cases} x_{k+1} = [A]x_k + w_k, \\ y_k = [C]x_k + v_k, k = 0, 1, 2, ... \end{cases}$$

where w_k and v_k are Gaussian noises, with zero mean and covariance matrices $[Q]$ and $[R]$ given by:

$$[Q] = \begin{bmatrix} [-8, 8] & 0 \\ 0 & [-8, 8] \end{bmatrix}, \ [R] = [0.1, 2.1].$$

Moreover, the matrices $[A]$ and $[C]$ are given by:

$$[A] = \begin{bmatrix} [0.3, 0.5] & [-0.05, 0.25] \\ -0.1 & [-0.05, 0.45] \end{bmatrix}, \ [C] = \begin{bmatrix} 0 & [0.9, 1.1] \end{bmatrix}.$$

The initial conditions are:

$$E\{x_0\} = \begin{bmatrix} 1 \\ 1 \end{bmatrix}, \ Cov\{x_0\} = \begin{bmatrix} 0.5 & 0.0 \\ 0.0 & 0.5 \end{bmatrix}.$$

In the following, we want to compare the results provided by three filters: the original interval Kalman filter (noted IKF), its sub-optimal version (sIKF), and our improved approach (iIKF). The variables N , O and D are introduced where N is the number of calibration times, O is the number of times for which the interval state estimate does not contain the real state, and D is the norm describing the distance between interval estimate bounds and the true value. D is obtained by:

$$\begin{cases} D = \dfrac{\sqrt{\sum_{k=1}^{K} d([\hat{x}_k], x_k)^T d([\hat{x}_k], x_k)}}{\sqrt{\sum_{k=1}^{K} x_k^T x_k}}, \\ d([\hat{x}_k], x_k) = \overline{|[\hat{x}_k] - x_k|} + \underline{|[\hat{x}_k] - x_k|}, \end{cases} \tag{5.15}$$

where K represents the maximal iteration number. D and O indicate the efficiency of algorithm. Besides, the algorithm SIVIA requires an user-specified precision threshold ε. This adjustable parameter is also analysed. $\epsilon = 1$ means that no gain value propagation takes place. t is the execution time. By using the toolbox Intlab of Matlab ([117]), the results are given in Table 5.1:

Filter	ε	N	O	D	t
IKF	-	20	14	575.38	0.83s
sIKF	-	0	56	0.85	0.75s
iIKF	1	0	0	3.07	0.91s
	0.2	0	0	2.60	46s
	0.05	0	0	2.56	784s

Table 5.1: Results for N, O, D and t using IKF and iIKF with different bisection factors ε.

The results in Table 5.1 are consistent with those shown in Figures 5.1 and 5.2. We can see that the original IKF has the largest D while sub-optimal IKF has the minimum D value, which is explained by the narrow bounds for the interval estimates. But since it replaces the uncertainty matrix to be inverted by its upper bound, some solutions are lost, which leads to the largest value of O: the real state is outside the estimated interval state half of the time.

D is larger when using iIkF than when using sIKF, because it retains all solutions. We notice that the real state and the optimal estimate provided by the conventional Kalman filter are both always contained in boundaries of the iIKF state estimate. The gain value propagated from SIVIA actually refines the interval estimation value, but it is more time consuming as the predefined precision increases. Compared to the original IKF, the iIKF prevents unnecessary recalibration due to the divergent interval operations; compared to sIKF, iIKF retains all the solutions consistent with the bounded error uncertainty. The iIKF hence represents a good compromise.

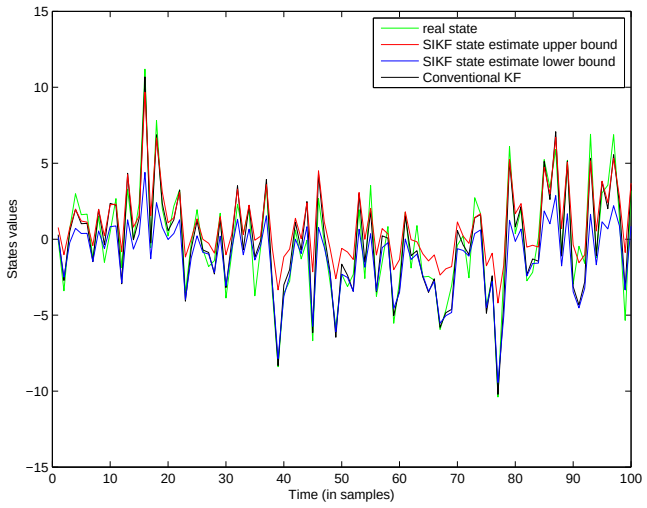

Figure 5.1: Simulation results from original sub-optimal IKF

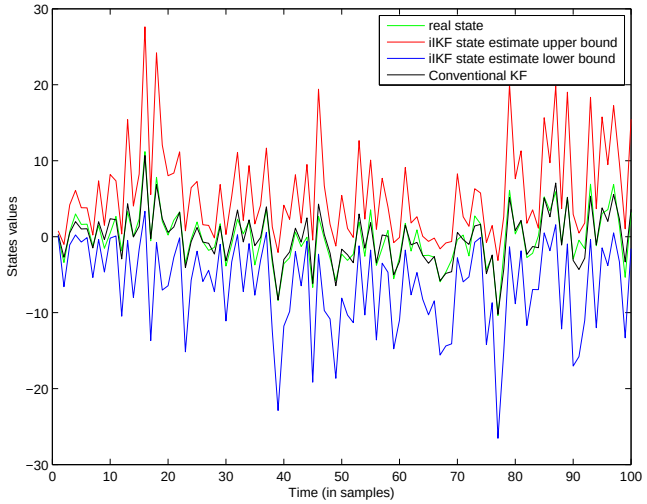

Figure 5.2: Simulation results from improved IKF with $\epsilon = 0.05$

5.4 Conclusion

The improved interval Kalman filter iIKF proposed in this chapter provides all the optimal estimates consistent with bounded-errors and achieves good control of the pessimism inherent to interval analysis. Through a set of simulations, the advantages of the iIKF with respect to previous versions are exhibited. This work shows that the integration of statistical and bounded uncertainties in the same model can be successfully achieved, which opens wide perspectives from a practical point of view. On the theoretical ground, this work calls for a unifying well-posed integrative theory.

The following chapter deals with fault detection and diagnosis by using concepts described previously in this manuscript. A fault detection algorithm based on iIKF is also developped.

Chapter 6

Application to fault detection and diagnosis

In this chapter, I am interested in fault detection and diagnosis relying on previously presented concepts such as set-membership identifiability, diagnosability, parameter and state estimation in a bounded error context.

6.1 Fault detection relying on set-membership identifiability

The results presented in this section are collaborative works with L. Travé-Massuyès and N. Verdière.
Fault detection via parameter estimation relies on the principle that possible faults in the monitored system can be associated with specific parameters and states of the mathematical model of the system given in the form of an input-output relation. This approach supposes that there exists a relationship between the model parameters p and the physical system parameters. Decision on whether a fault has occurred, is based either on the changes of model parameter values or on the changes of physical system parameters and tolerances limits.

Example 6.1.1 *Case of a macrophage mannose receptor*

The following example taken from [129] is considered. The proposed work has been published in [47]. This example allows to explore the capacity of the macrophage mannose receptor to endocytose soluble macromolecule and to quantify the different aspects of such a process. The model is the following:

$$\begin{cases} \dot{x}_1(t) = \alpha_1(x_2(t) - x_1(t)) - \dfrac{V_m x_1(t)}{1 + x_1(t)}, \\ \dot{x}_2(t) = \alpha_2(x_1(t) - x_2(t)), \\ x_1(0) \in [0.62,\ 0.63],\ x_2(0) = 0, \\ y(t) = x_1(t), \end{cases} \tag{6.1}$$

where x_1 (resp. x_2) is the enzyme concentration outside (resp. inside) the macrophage and $p = (\alpha_1, V_m, \alpha_2)$ are the unknown parameters which have to be identified. The parameter α_1 is the rate of the transfer from Compartment 1 (or the central compartment), practically plasma, to Compartment 2 (or the peripheral compartment), which represents, in the model, the part of the extravascular extracellular fluid accessible. Furthermore, α_2 is the rate of the transfer from Compartment 2 to Compartment 1. In this work, we consider a fault as an unpermitted deviation of at least one parameter of the system from the acceptable standard condition.
This model has been proved to be globally SM identifiable in chapter 3. The numerical study has been conducted in simulation in Matlab using Intlab [117]. The simulated outputs are disturbed by a truncated Gaussian noise ν such that $\nu(t) \in [-0.001,\ 0.001]$. Thus, $z(t) = \bar{y}(t) + \nu(t)$ where $\bar{y}$ is the exact output corresponding to the exact value of parameters: $\alpha_1 = 0.011,\ \alpha_2 = 0.02$ and $V_m = 0.1$. The measures are supposed to be done at discrete times $(t_j)_{j=1,\dots,N}$ on the interval $[0, 60]$ with a sample period equal to 1s. As seen in chapter 3, to test SM-identifiability, we obtain a differential polynomial in y, u and the derivatives using the Rosenfeld-Groebner algorithm in Maple.
We use this polynomial to estimate parameters and consequently detect the occurence of a fault.
The polynom $R(\bar{y}, \bar{u})$ is given by:

$$R(\bar{y}, \bar{u}) = \ddot{y}(1 + y)^2 + \gamma_1 \dot{y}(1 + y)^2 + \gamma_2 y(1 + y) + \gamma_3 \dot{y},$$

with $\gamma_1 = \alpha_1 + \alpha_2$, $\gamma_2 = \alpha_2 V_m$ and $\gamma_3 = V_m$.
If we denote $y_p^{(1)}(t_j)$ (resp. $y_p^{(2)}(t_j)$) the estimate of $\dot{y}(t_j)$ (resp. $\ddot{y}(t_j)$), the system which has to be solved is $[A][x] = [b]$ where $[A]_j = ([y_p^{(1)}(t_j)(1 + y(t_j))^2],\ [y(t_j)(1 + y(t_j))],\ [y_p^{(1)}(t_j)])$ and $[b]_j = [-y_p^{(2)}(t_j)(1 + y(t_j))^2]$.
$y_p^{(1)}(t_j)$ and $y_p^{(2)}(t_j)$ are obtained using Higher-order sliding modes (HOSM) differentiators [66, 68, 67]. The parameters of the HOSM differentiators are given by $\lambda_0 = 3$, $\lambda_1 = 0.2$ and $\lambda_2 = 0.1$.

Solving this system can be cast into the set inversion framework for which we use the SIVIA algorithm. To use SIVIA, it is necessary to give initial intervals for γ_1, γ_2 and γ_3. The problem solved here is to find $[x]$ such that $0 \in [A][x] - [b]$. We use the

forward-backward propagation to contract the initial parameter box.
Some prior knowledge of the model can provide initial boxes γ_1, γ_2 and γ_3.

Case of nominal behaviour*: using initial intervals given by $\gamma_1 = [0,\ 0.04]$, $\gamma_2 = [0,\ 0.003]$, $\gamma_3 = [0,\ 0.2]$ and the bisection precision $\varepsilon = 0.001$, we obtain in 14.18 seconds : $\alpha_1 = [0,\ 0.0401]$, $\alpha_2 = [0,\ 0.0437]$ and $V_m = [0.06875,\ 0.13203]$, Using the equations: $V_m = \gamma_3,\ \alpha_2 = \gamma_2/V_m,\ \alpha_1 = \gamma_1 - \alpha_2$. All these intervals contain the normal values, confirming normal behavior.*

Then, using $\gamma_1 = [0,\ 0.04]$, $\gamma_2 = [0,\ 0.003]$, $\gamma_3 = [0,\ 0.2]$ and the bisection precision $\varepsilon = 0.0001$, we obtain in 177.55 seconds : $\alpha_1 = [0,\ 0.0329]$, $\alpha_2 = [0.0071,\ 0.0317]$ and $V_m = [0.094824,\ 0.10527]$.
All these intervals contain the normal values.

Case of a fault on parameter α_2*: In this simulation, we assume a fault on $\alpha_2 = 2$, which means that the rate of the transfer from Compartment 2 to Compartment 1 is high. After 25.15 minutes, using $\gamma_1 = [0,\ 3]$, $\gamma_2 = [0,\ 1]$, $\gamma_3 = [0,\ 0.2]$, we obtain: $\alpha_1 = [0.0000,\ 0.5050]$, $\alpha_2 = [1.1200,\ 2.4950]$ and $V_m = [0.0242,\ 0.1790]$. The real faulty value of α_2 is contained in the estimated interval for α_2 which allows to detect and localize the fault. Moreover, there is no intersection between the estimated interval for α_2 and the one obtained in normal behaviour.*

Case of a fault on parameter α_2 **at** $t = 15$**s***: Consider now the case of an abrupt change in the value of α_2 during the test and let us assume a fault $\alpha_2 = 1$ at time $t = 15s$. This fault is detected in $t = 0.05s$ after its occurence.*
After the detection of this fault, using $\gamma_1 = [0,\ 1.05]$, $\gamma_2 = [0,\ 0.12]$, $\gamma_3 = [0,\ 0.12]$, we obtain in 22.6 seconds $\alpha_1 = [0,\ 0.0238]$, $\alpha_2 = [0.0738,\ 1.0500]$ and $V_m = [0,\ 0.1200]$. These intervals on α_1 and V_m contain the normal values whereas the one obtained for α_2 contains the faulty value.

Case of a fault on parameter V_m*: In this simulation, we assume a fault on $V_m = 0.2$ at $t = 27s$. This fault is detected in $t = 0.02s$ after its occurence. Once the fault is detected, the estimation algorithm is initialized with $\gamma_1 = [0,\ 0.04]$, $\gamma_2 = [0,\ 0.007]$, $\gamma_3 = [0,\ 0.3]$, and we obtain in 33.43s the intervals $\alpha_1 = [0,\ 0.0150]$, $\alpha_2 = [0,\ 0.0248]$ and $V_m = [0.0242,\ 0.3]$.*
The intervals on α_1 and α_2 contain the normal values whereas the one for V_m contains the faulty value, hence confirming the fault.

Thus, through this example, different normal and faulty scenarios have been consid-

ered. For every scenario, the parameters have been estimated correctly with reasonable precision.
The proposed method consists of a fault detection and identification method for bounded uncertainty nonlinear models relying on an original parameter identifiability scheme. It takes benefit of a differential algebra based method for checking SM-identifiability and its operational counterpart μ-SM-identifiability. These notions provide a way to study different aspects of identifiability for uncertain bounded-error systems, in particular systems that represent an infinite family of nonlinear systems. By building the parameter estimation scheme on the analysis of identifiability, we guarantee that the solution set reduces to one connected set, avoiding this way the pessimism of SM methods. Identifiability is closely related to diagnosability as it provides the guaranty that two situations corresponding to different parameterized settings are distinguishable.

The following example concerns a benchmark used during the SIRASAS project. This work has been made in collaboration with R. Pons and L. Travé-Massuyès. It has been published in [99, 98].

6.2 Fault detection relying on fault model identification

6.2.1 Benchmark description

Our case study concerns the aerospace domain, and deals more specifically with the *electrical flight control systems* (EFCS) of a civil aircraft. Due to component malfunctions, an erroneous oscillating signal may propagate through the EFCS to the control surfaces (as shown in Figure 6.1), leading to an unwanted control surface oscillation [39]. This *oscillatory failure case* (OFC) must be detected because when it acts within the actuator bandwidth, it may consequently:

- generate load factors on the aircraft structure due to resonance phenomenon and aeroelasticity;
- stress actuators and reduce their lifetime;
- lower passengers comfort.

The OFC is assumed to be a sinus or triangle-shaped signal whose frequency, phase and range obey an uniform law. When this polluted signal adds up to the normal signal, it is called a *liquid failure*; when it replaces the original signal, it is then said to be a *solid failure* [39]. Figure 6.2 shows the real position of the control surface, its estimated position and the residual resulting from the difference between real and estimated positions, in the case of liquid and solid sinus shaped OFC.

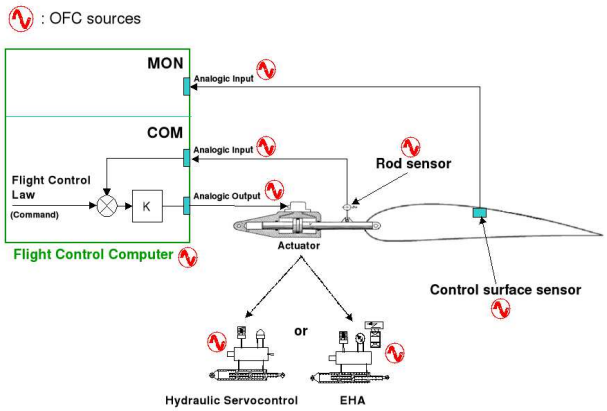

Figure 6.1: OFC source location in the control loop.

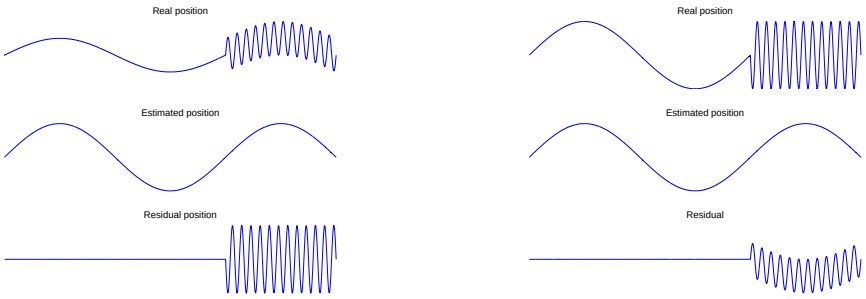

Figure 6.2: Residuals in the case of liquid (left) and solid (right) failure.

The goal of this work is to detect the OFC beyond a given amplitude in a given number of periods, whatever the frequency.

We should refer to [39] to get further details about the detection of OFCs in EFCS as well as its current implementation in A380 flight control computers.

In this case study, we run tests introducing oscillatory failures in the control loop. Two fault models, triangle shaped and sinus shaped, are used. Parameters are estimated over one period of the signal.

6.2.2 Sinus-shaped fault

A high noisy sinus-shaped liquid fault signal with a range $A = 1$ degree and a frequency of $f = 0.5$Hz is introduced in the control surface model. The initial parameter box is given by $A \times f = [0, 3] \times [0, 10]$.

Figure 6.3 shows the results provided by the algorithm SIVIA when the fault model is supposed to be sinus shaped. Range parameter A is shown on the horizontal axis while frequency f is on the vertical one. Red boxes have been rejected, yellow ones have a length inferior to the stop condition set in the algorithm. The green boxes represent the solution.

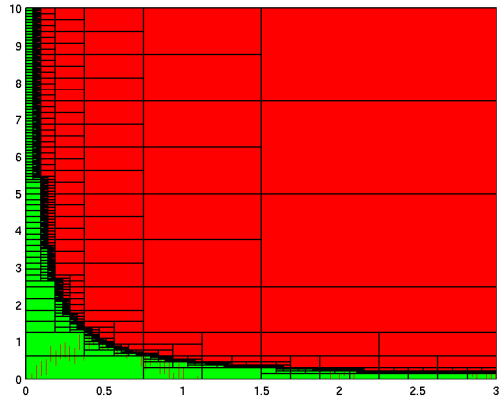

Figure 6.3: Sinus-shaped fault.

When the fault model is triangle-shaped, the algorithm stops after a few iterations and its conclusion is the non-existence of a solution.

6.2.3 Triangle-shaped fault

In this example, the fault is triangle-shaped with a range 2 degrees and a frequency $f = 0.5$Hz which gives a period $T = 2$s, with a still highly noisy signal. The inital parameter box is now $A \times T = [0, 3] \times [0, 5]$.

Figure 6.4 exhibits the obtained results with a triangle-shaped fault model. The parameter A is on the horizontal axis and the period T on the vertical axis. One can notice that the estimation results are fully in accordance with the injected fault.

With a sinus-shaped fault model, the algorithm concludes again to the non-existence of a solution.

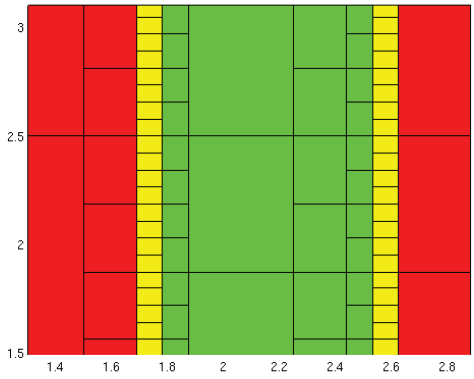

Figure 6.4: Triangle-shaped fault.

The tests show good results for confirming a fault. Now, the real advantage of the method with respect to others is that it is very efficient to prove the non-existence of the solution, that is to discard specific kinds of failures in the real system. In the two case study scenarios, the invalidation of the triangle-shaped (sinus-shaped) fault model is obtained within a few iterations. We notice that a stochastic method would not invalidate the non relevant fault model but it would conclude to the existence of a solution with a wide confidence range, which is much more difficult to interpret.

6.3 Fault detection relying on state estimation

The benchmark considered in this example is the same as the previous one. This work has been developped in collaboration with R. Pons and L. Travé-Massuyès [97].

In this subsection we propose a simplified version of the method based on Taylor serie expansion. This has been successfully used in a benchmark proposed in the SIRASAS project.

6.3.1 Control Surface Position Model

A simple model of the system is represented in Figure 6.5. The control surface is moved by an hydraulic actuator which has a moving rod linked to the control surface. The rod position is expressed in millimeters and can be converted into a control surface deflection in degrees.

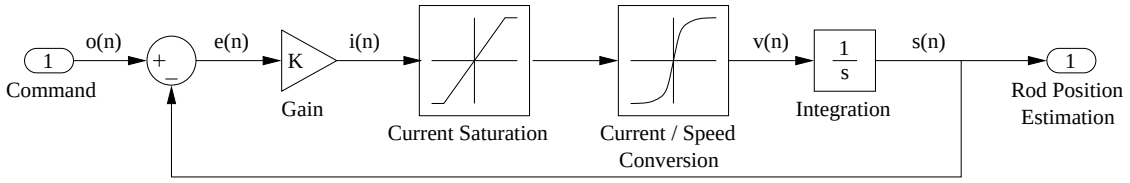

Figure 6.5: Control surface position estimation model.

In this model, $o(t_j)$ is the position control signal at time t_j. The control error ε is given by:

$$\varepsilon(t_{j+1}) = o(t_{j+1}) - \hat{s}(t_j). \tag{6.2}$$

Thus $\varepsilon(t_{j+1})$ is the difference between the position control o at time t_{j+1} and the estimated position $\hat{s}$ at time t_j. The estimated current $\hat{i}(t_j)$ is proportional to the error:

$$\hat{i}(t_j) = K\varepsilon(t_j), \tag{6.3}$$

where K is a constant control gain. A saturation is then applied to the current hence limiting its value within predefined bounds. It is then converted to speed $\hat{v}(t_j)$ by interpolation with data stored in a look-up table. Finally, the estimated control surface position $\hat{s}(t_j)$ at time t_j is computed by integration of the speed. This model can be given under the state space form where $x(t_j) = \hat{s}(t_j)$ and $u(t_j) = o(t_j)$ by the equation $\dot{x}(t) = Kg_1\left(u(t) - x(t)\right)$ where the nonlinear function $g_1(.)$ describes the saturation and conversion blocks [39].

6.3.2 Scheme for detection by state estimation

The presented approach uses a classical prediction-correction two steps approach (presented in Figure 6.6). The difference between the classical prediction step concerns the use of the mean value and intermediate value theorems.

6.3.2.1 Prediction Step

The proposed prediction step is based on the mean value and intermediate value theorems. To apply this method, some local monotonicity conditions are required. It is shown that this approach is successful in controlling the well-known and undesirable wrapping effect.

6.3.2.1.1 Mean value theorem Let $l_1 : I = [t_j, t_{j+1}] \to \mathbb{R}$ be a function of class C^1 on the interval $[t_j, t_{j+1}]$. Then there exists some ζ in $]t_j, t_{j+1}[$ such that:

$$l_1(t_{j+1}) = l_1(t_j) + h\frac{\mathrm{d}l_1}{\mathrm{d}t}(\zeta), \tag{6.4}$$

where $h = t_{j+1} - t_j$.

6.3.2.1.2 Intermediate value theorem Let $l_2 : I = [t_j, t_{j+1}] \to \mathbb{R}$ be a continuous function on an interval I. Then the image set $l_2(I)$ is also an interval, and either it contains $[l_2(t_j), l_2(t_{j+1})]$, or it contains $[l_2(t_{j+1}), l_2(t_j)]$ depending on the values of $l_2(t_j)$ and $l_2(t_{j+1})$; that is:

$$l_2(I) \supseteq [l_2(t_j), l_2(t_{j+1})] \text{ or } l_2(I) \supseteq [l_2(t_{j+1}), l_2(t_j)]. \tag{6.5}$$

If the function l_2 is monotonic on I then:

$$l_2(I) = [l_2(t_j), l_2(t_{j+1})] \text{ or } l_2(I) = [l_2(t_{j+1}), l_2(t_j)]. \tag{6.6}$$

These two theorems can be extended to a function from $[t_j, t_{j+1}]$ to $\mathbb{R}^n$.

In the proposed approach, we also extend these two theorems to interval analysis. In the mean value theorem, we replace the function l_1 by the state function $x(.)$ given in Equation (2.1), and then we apply the intermediate value theorem to the function $\dot{x}(.)$.

To estimate the state at t_{j+1}, knowing $x(t_j)$, the following equation is used:

$$x(t_{j+1}) = x(t_j) + h\dot{x}(\zeta), \tag{6.7}$$

where ζ belongs to $]t_j, t_{j+1}[$. This equation extended to interval analysis leads to:

$$[x(t_{j+1})] \subseteq [x(t_j)] + h[\dot{x}(\zeta)], \tag{6.8}$$

Under the assumption of local monotonicity of the function $\dot{x}(.)$ on $[t_j, t_{j+1}]$, we obtain from the intermediate value theorem an enclosure of $[\dot{x}(\zeta)]$, given by:

$$\left[\min(\underline{\dot{x}}(t_j), \underline{\dot{x}}(t_{j+1})), \max(\overline{\dot{x}}(t_j), \overline{\dot{x}}(t_{j+1}))\right]. \tag{6.9}$$

Note that local monotonicity is justified if h is small compared to the dynamics of the system, which is generally the case and which is especially true in this application.

An over estimate $[x^+(t_{j+1})]$ of the state vector $[x(t_{j+1})]$ is then computed, given by:

$$[x^+(t_{j+1})] = [x(t_j)] + h\left[\min(\underline{\dot{x}}(t_j), \underline{\dot{x}}(t_{j+1})), \max(\overline{\dot{x}}(t_j), \overline{\dot{x}}(t_{j+1}))\right]. \tag{6.10}$$

6.3.2.2 Correction Step

This step is classical and can be explained with Figure 6.6. At t_{j+1}, an output vector $[y(t_{j+1}, .)]$ is obtained, corresponding to:

$$[y(t_{j+1}, .)] = [z(t_{j+1}) - \overline{v}(t_{j+1}), z(t_{j+1}) - \underline{v}(t_{j+1})], \tag{6.11}$$

where $\underline{v}(t_{j+1})$ and $\overline{v}(t_{j+1})$ are given in Equation (2.2). The noise is generally symmetric and centered around zero. Equation (2.2) is then rewritten as follows:

$$[z(t_{j+1})] = [y(t_{j+1}, .) - V, y(t_{j+1}, .) + V], \tag{6.12}$$

where $V > 0$ is the maximum noise range.

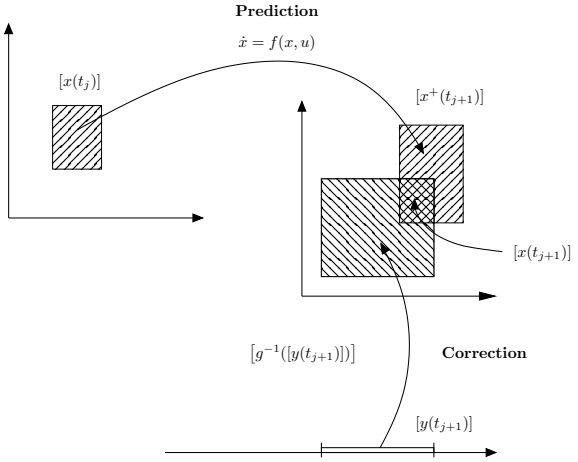

Figure 6.6: Prediction-correction step at time t_j.

Then, we compute the set $[g^{-1}([y(t_{j+1})])]$ by the algorithm SIVIA. The solution set at the sample time t_{j+1} is finally given by:

$$[x(t_{j+1})] = [x^+(t_{j+1})] \bigcap [g^{-1}([y(t_{j+1})])]. \tag{6.13}$$

Note that in this case study, a sensor measures the position of the rod moving the control surface from which the value of the control surface position is derived. The function g in Equations (2.1) and (6.13) being the identity function, the correction step described before is not necessary, thus saving significant computer time.

Thus, to conclude the presentation of the proposed approach, the behaviour of the OFC detection method can be tuned by setting two parameters noted η and ζ.

6.3.2.3 Introduction of η and ζ Parameters

η Parameter

With the integration method described above, a fault is detected when there is a discrepancy between the predicted value of a variable and its real value measured by a sensor. A discrepancy is characterized by an empty intersection between the envelope of the predicted value and measurement plus the sensor noise.

We stated earlier that we want to define a prediction $[x(t_j)]$ of the state vector $x(t_j)$ at time t_j. The predicted value $y_p(t_j)$ of the system output vector given by the observation equation of (2.1) is a box $[y_p(t_j)]$ such that:

$$[y_p(t_j)] = g([x(t_j)]). \tag{6.14}$$

If we raise an alarm at the first occurrence of an empty intersection, the consequence is to be very sensitive to high noisy measurements and/or error sensor reading. This is why we only generate an alarm when there are η *successive empty intersections*.

Proposition 6.3.1 *An alarm is raised at time* t_k *if and only if there exists an integer* $k \in [\eta, +\infty[$ *such that* $\forall j \in [k-\eta+1, k],\ [y_p(t_j)] \bigcap [z(t_{j+1}) - V, z(t_{j+1}) + V] = \emptyset$.

Since g is the identity function in our application, we obtain:

$$\exists\, k\ \in [\eta, +\infty[\quad \forall j \in [k-\eta+1, k],\ \ [x(t_j)] \bigcap [z(t_{j+1}) - V, z(t_{j+1}) + V] = \emptyset. \tag{6.15}$$

The drawback of this method is to delay the detection of a fault. The value of the parameter η has then to be chosen carefully, depending on the noise level, the quality of sensors and the length of step size with respect to the dynamics of the system.

At time $t = 402.23$s, we inject a triangle-shaped solid OFC with a frequency of 0.98Hz, a range of 14.37mm, a shift of 0.53mm and a phase of -0.16rad. Figure 6.7 displays the result of the simulation (left side) with a zoom on the beginning of the OFC (right side).

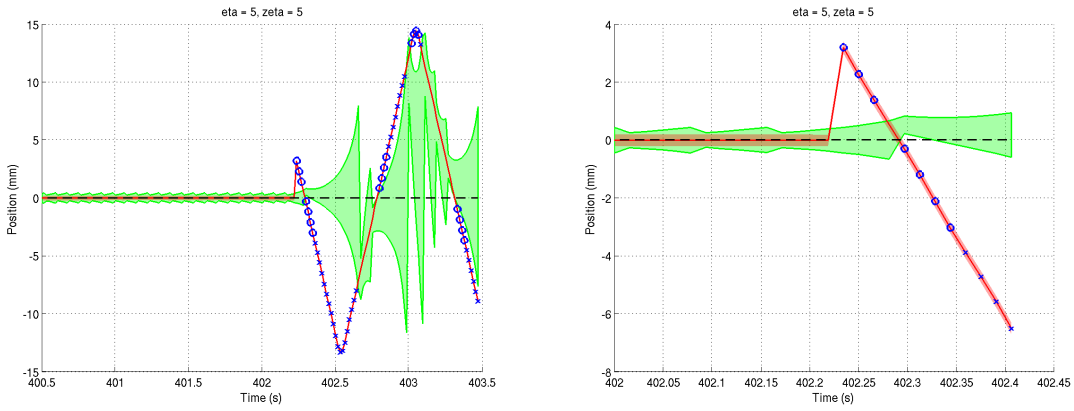

Figure 6.7: Occurrence of an OFC.

At the first time step, the algorithm detects an empty intersection between the measure and the prediction, it sends a warning signal represented by a circle on the measurement plot. There are three consecutive warnings. Since the OFC is periodic, its range decreases and then intersects the prediction again. The warning signal then stops. But the OFC still decreases and goes out of the predicted envelope again, thus generating the warning signal again. The warning signal is turned into an alarm signal (represented by crosses on the measure plots) when there are η consecutive empty intersections. On Figure 6.7 as we have $\eta = 5$, the alarm is emitted in this example at the 5th empty intersection between measure and prediction.

A point to notice is that, because of the periodic nature of an OFC, the alarm signal appears and disappears depending on the range of the OFC. This does not affect the robustness of the method since reconfiguration actions are taken at the *first* occurrence of the alarm signal.

With $\eta = 5$ the alarm signal is emitted only at the 10th iteration after the OFC occurred; taking a value of $\eta = 1$ would reduce this detection delay. In fact, taking high values for η allows us to avoid false alarms. As a matter of fact, the considered control loop system acts like a first order system. Hence there is a delay between a change in the command and its consequence on the system output value.

This delay has no consequence when the system is in steady state but it generates false alarms in transient state when η is chosen small. Figure 6.8 shows a test without any occurrence of OFC. When the slope of the transient is high, there are empty intersections between measure and prediction that occur during very few consecutive iterations. When the η parameter is chosen small, this generates false alarms (left side of Figure 6.8). Using a higher η value, these false alarms are no longer emitted; only warning messages are raised (right side of Figure 6.8). This eventually delays the generation of the alarm, but only for a few iterations. This delay, because of the small step size, corresponds to a very small time delay with respect to the dynamics of the system.

ζ Parameter

This parameter is used to set the number of iterations between two successive resettings of the prediction on the measured value. At a given time step t_i, the prediction is computed using the *measured value* of the position. During the next $\zeta - 1$ steps, from time step t_{i+1} to $t_{i+\zeta-1}$, the prediction is computed using the *prediction computed on the previous step*. At step $t_{i+\zeta}$, the computation of the prediction uses again the measurement. Since g in (6.14) is the identity function, the second equation of the system (6.14) can be rewritten in discrete time:

$$y(t_i, .) = x(t_i, .). \tag{6.16}$$

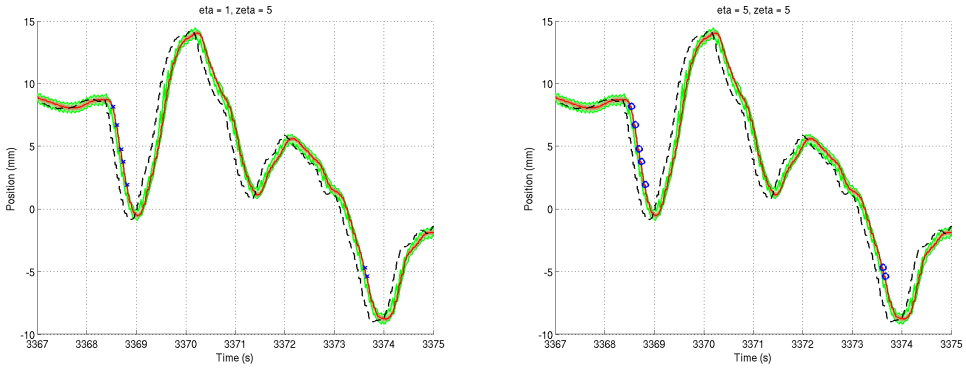

Figure 6.8: Simulation without OFC with $\eta = 1$ (left side) and $\eta = 5$ (right side).

The first equation of the system (2.1) becomes:

$$x(t_{i+1}) = \begin{cases} f\left(z(t_i), u(t_i)\right) & \text{if } mod(i, \zeta) = 0, \\ f\left(y(t_i), u(t_i)\right) & \text{if } mod(i, \zeta) \neq 0, \end{cases} \tag{6.17}$$

where $z(t_i)$ is the measured value of the control surface position.

Examples of different settings of these parameters and their consequences on the results of the simulation are shown in the next subsection.

As seen previously, ζ is used to control how often the computation of the predicted control surface position is reset to the measure of this position.

Figure 6.9 shows an example of such a reset of the predicted value to the measured value every $\zeta = 6$ iterations. The two plots show the same data labeled by time on the left side and by the number of iterations on the right side. This figure shows also that when there is no reset, the width of the predicted envelope grows at each iteration step, which is a well known effect due to the use of interval calculus.

Figure 6.10 shows two results of the same test with a value of $\zeta = 2$ on the left side and $\zeta = 8$ on the right side (Figure 6.10).

We can see that the width of the predicted envelope grows with ζ. A large value generates a larger predicted envelope thus reducing warning and alarm signals. ζ can hence be seen as a way to filter out the measure especially when the measurement noise is important or when erratic measures happen. *A contrario*, a large envelope reduces the available information. Indeed, if we let the envelope width grow, it becomes so large that it does not contain any more information: the predicted envelope contains any possible value for the control surface position, and it is then impossible to detect any kind of fault. Figure 6.11 shows the same test as the one in Figure 6.10 but with $\zeta = 18$.

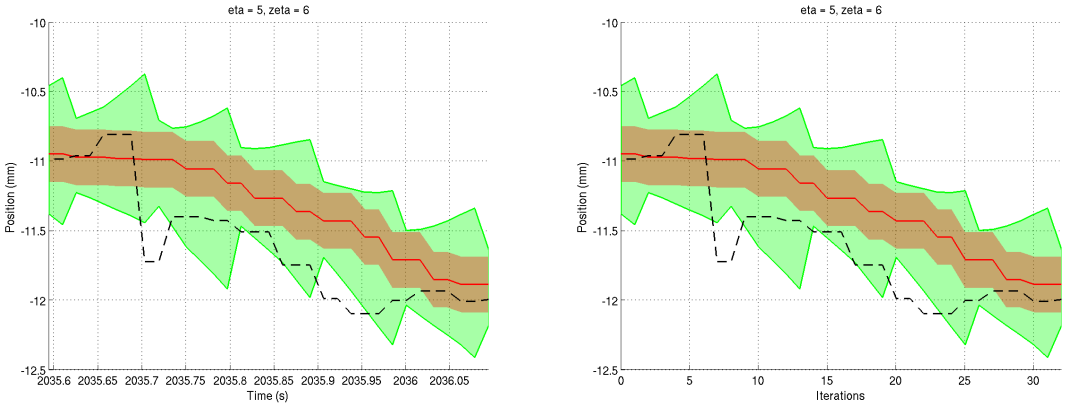

Figure 6.9: Reset of the prediction on the measure every $\zeta = 6$ iterations.

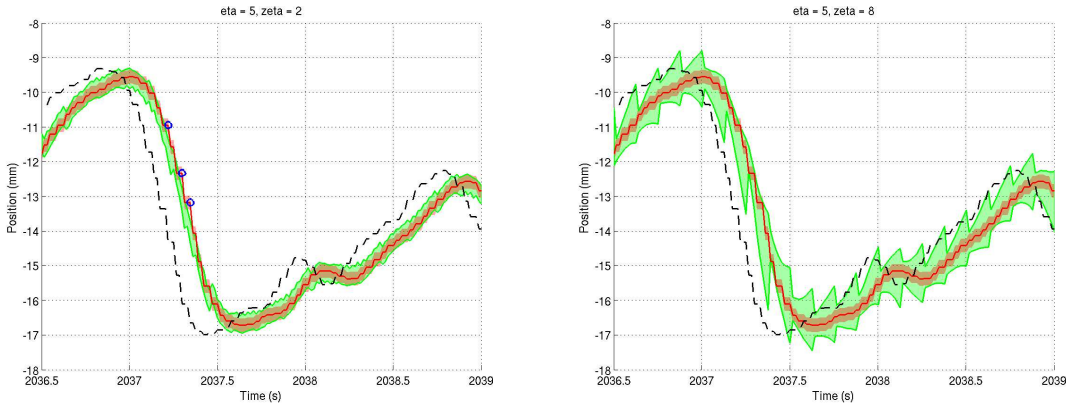

Figure 6.10: Same test with $\zeta = 2$ (left side) and $\zeta = 8$ (right side).

6.3.2.4 Test results

The tests have been performed using the MATLAB numerical computing environment and programming language [120] developed by The MathWorks, Inc. Interval calculus uses the INTerval LABoratory MATLAB toolbox version 5.5 [43] which is provided and developed by the Institute for Reliable Computing at the Hamburg University of Technology (TUHH), Germany.

The data used to perform simulation and to test the detection method was provided by Airbus France. It consists of two files with data recorded during flight tests. The recorded variables are the command for the position of the rod governing the control surface in

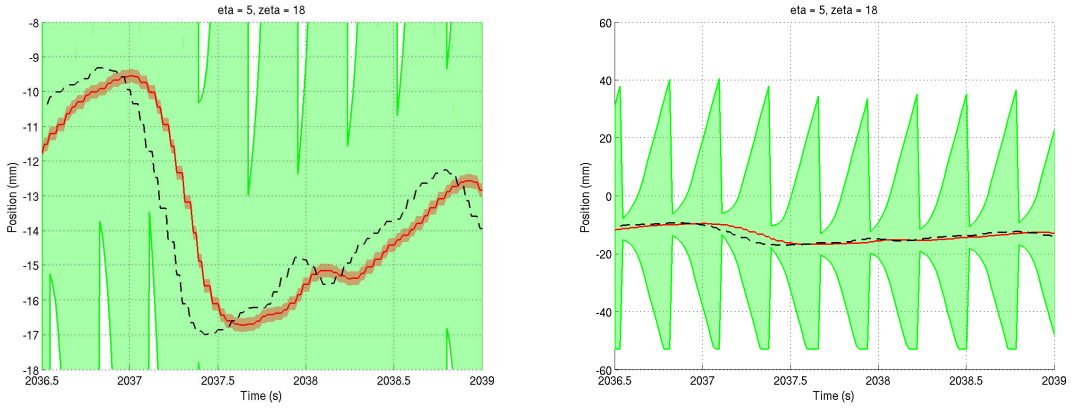

Figure 6.11: Test results with $\zeta = 18$ with different vertical scales on left and right sides.

mm and the measurement of the angular position of this control surface in degrees. This measure has been converted to the corresponding rod position in mm.

1) First test round

The recorded data starts at time $t = 0$s and ends at time $t = 4062.5$s i.e. for a duration of 1h 7min 42.5s representing 260,001 iterations with a 0.015625s step size. In this test, we randomly injected 51 faults in the data provided by Airbus. Characteristics of faults are given by a frequency belonging to $[0.25,\ 9.93]$ Hz, a range in $[1.42,\ 50.69]$ mm, shift and phase respectively in $[-26.69,\ 74.79]$ mm and $[-2.56,\ 3.05]$ rad. Figure 6.12 shows the command of the system. The bottom plot is a square wave that shows whether the simulation runs in normal mode (low value) or if a fault is present (high value).

We ran simulations on the whole data set with faults injected for values of η and ζ going from 1 to 20.

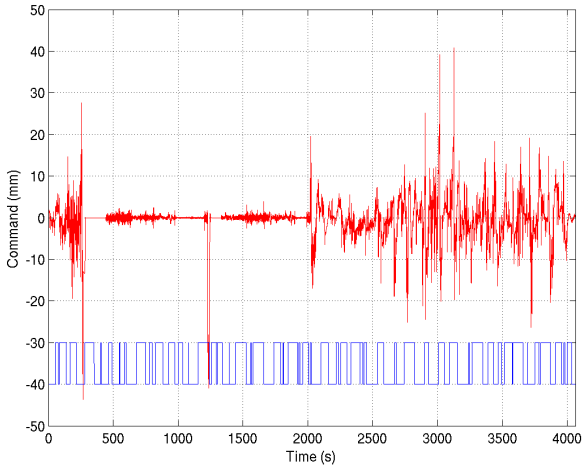

Figure 6.12: Command and injected faults - test no.1

No Detection Rate:
Figure 6.13 illustrates the no detection rate.

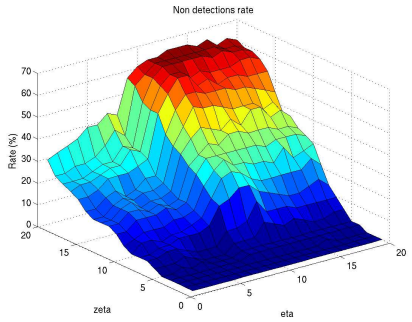

Figure 6.13: Fault no detection rate (test no.1)

The no detection is determined by considering only the iterations when an OFC is present. We then compute the ratio of the number of iterations in which an alarm is not emitted divided by the total number of iterations in which an alarm should have been emitted.

We can see that the parameter η does not affect the no detection rate. Oppositely, the rate relies strongly on ζ: the greater ζ is, the higher the non detections rate is. As it has

been stated previously, the width of the predicted position envelope grows with ζ, hence lowering the detection sensitivity of the algorithm.

If we choose $\zeta \leq 8$, whatever the value of η, we have a rate that stands below 10%, which is a good result if we consider the detection delay as seen previously.

False Alarm Rate:
Figure 6.14 illustrates the false alarm rate. The false alarm rate is the ratio of the number

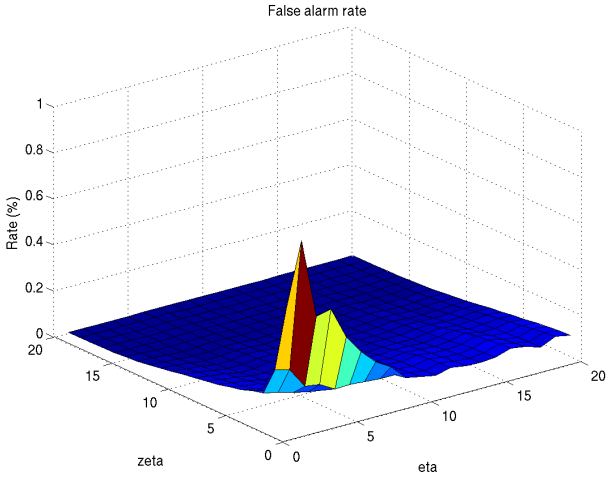

Figure 6.14: False alarm rate - test no.1

of iterations without occurrence of an OFC during which an alarm is emitted divided by the total number of iterations without OFC.

The first noteworthy result is that the worst rate (measured for $\eta = 2$ and $\zeta = 1$) is about 0.82% which is very low. When $\zeta \geq 4$, the rate falls to less than 0.1%. Here again, since ζ is chosen greater or equal to 4, the η parameter does not affect consequently the false alarm rate.

False Alarm Average Length:
Figure 6.15 shows the false alarm average length.

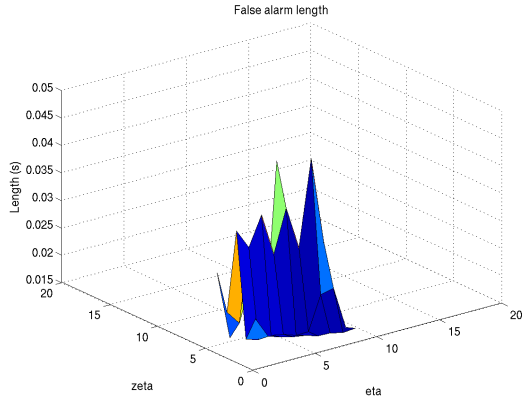

Figure 6.15: False alarm average length (test no.1)

False alarms exist for $\eta \leq 9$ and $\zeta \leq 5$. When such false alarm occurs, its duration is less than 47ms, i.e. less than 3 iteration steps.

Detection Delay
Figure 6.16 shows the false alarm average length.

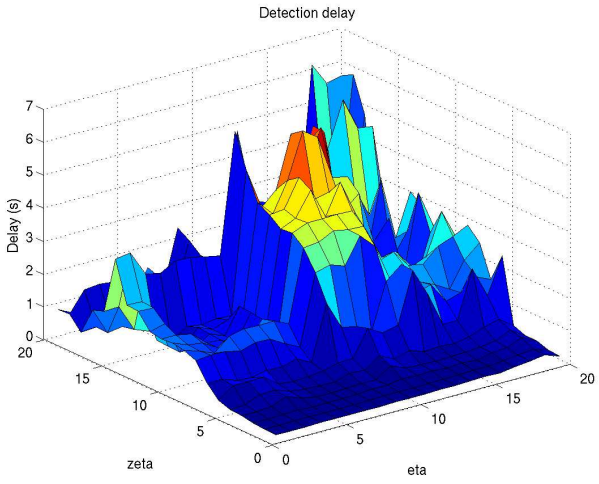

Figure 6.16: Detection delay - test no.1

We can see that whatever the value of η, we achieve good results for $\zeta \leq 5$. With this setting, the detection delay remains lower than 0.5s which corresponds to a maximum of 5 periods for OFC whose frequency is lower than 10Hz. This meets the requirements.

2) Second test round

The purpose of the second test round is to test the detection method against more constraining scenarios, i.e. OFC with higher frequency and smaller range. Each test has been performed in the following way: a random starting time is chosen within the data file. We run the simulation from this time point for a few iterations to initialize the algorithm and simulation data. Then we introduce an OFC in the data and we wait for an alarm. If the alarm is raised before the OFC starts, the simulation is stopped and we conclude to a false alarm. If the alarm is not raised after a time corresponding to ten periods of the OFC, we stop the simulation and the conclusion is a non detection. Otherwise, the detection delay, i.e. the difference between the time when the OFC started and the time it is detected, is recorded.

The data used to run this test are the same as the one used in the first test round (see Figure 6.12).

The difference with the first test round procedure is first that we did not run the simulation for the whole data file. Secondly we did not perform any test in normal situation, i.e. without any occurrence of an OFC, but kept normal data for a few iterations at the beginning of the simulation, in order to initialize data. Thirdly, we stopped the simulation as soon as an alarm is raised. If no alarm is raised, the simulation stops after ten OFC's periods. This scheme allowed us to drastically reduce the duration of a test and then run many more tests.

Fault characteristics:

1582 different OFCs were tested whose parameters follow a uniformly distributed random law. The OFC frequency is randomly chosen in the interval $[0.1, 10]$Hz, its range within $[0, 10]$mm, its shift within $[-10, 10]$mm and its phase within $[-\pi, \pi]$rad. Figure 6.17 shows the OFC parameter histograms. We can see that each OFC parameter is uniformly distributed on the interval given by its lower and upper bound.

Each OFC has been tested as a solid sinus-shaped fault, liquid sinus-shaped, solid triangle-shaped and liquid triangle-shaped. Parameters η and ζ have been tested for every value going from 1 to 20. The total number of performed tests is consequently 2,531,200.

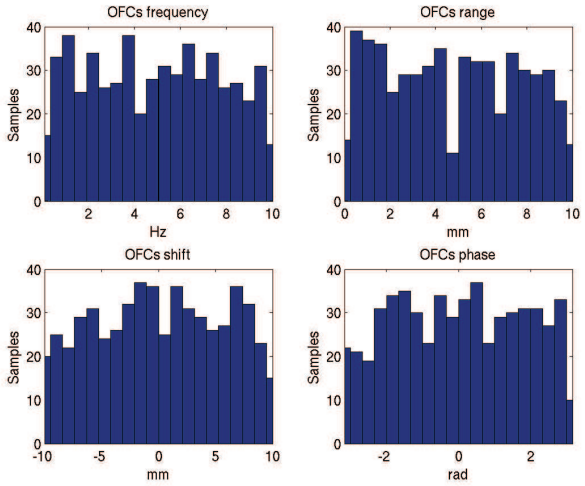

Figure 6.17: OFCs frequency, range, shift and phase histograms - test no.2

Results:
Figure 6.18 presents the non detection rate, the false alarms rate, and the detection delay given in seconds and in number of periods of the injected OFC.

The results are very similar to those obtained in the first test. For values of η and ζ around 5 to 7, the non detection rate and false alarms rate are low and the detection delay is below two periods of the injected OFC period. The non detection rate grows with η and ζ. False alarms occur only for small values of these parameters.

Figure 6.19 shows the characteristics of the non detected OFCs. This figure shows that no conclusion can be drawn about the influence of the OFCs parameters on the results since they are uniformly distributed.

Figure 6.20 confirms this conclusion. We can see that the detection delay grows slowly with the OFC frequency. It seems not to depend on the OFC range, shift and phase. It does not depend on the OFC delta, i.e. the difference between the last value before OFC is injected and the first value after injection. The delta value depends on the range, shift and phase of the OFC. Although we could have thought that the bigger this delta would be, the easier it would be detected, i.e. with a short delay, figure shows that it is not the case.

Last figure 6.21 shows the minimal range of the detected OFC for every values of η and ζ. For values of η and ζ around 5, the smallest detected OFC had a range of 0.022mm.

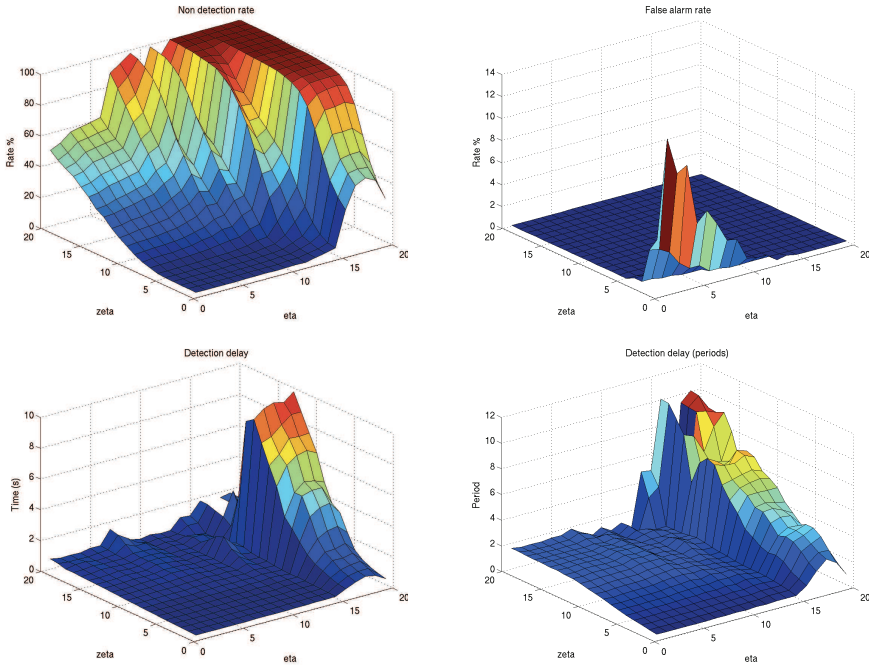

Figure 6.18: Results of test no.2

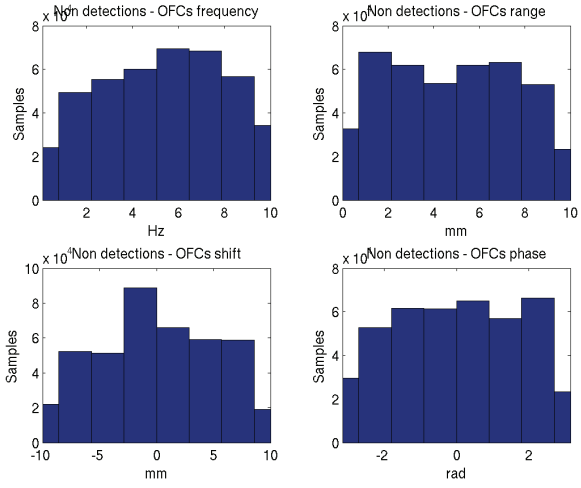

Figure 6.19: Non detections histograms - test no.2

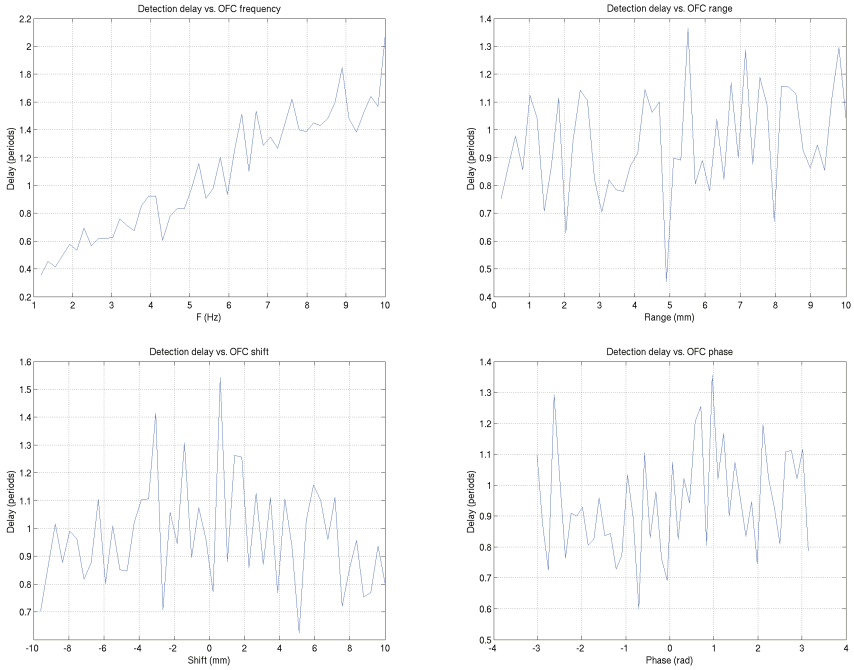

Figure 6.20: Detection delay vs. OFCs parameters - test no.2

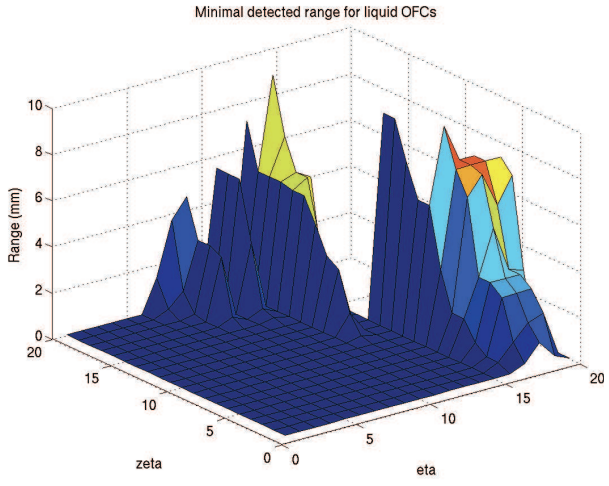

Figure 6.21: Smallest range of detected OFC - test no.2

6.3.2.5 Conclusion

The first noticeable point that can be drawn from the examination of these results is that the two test rounds exhibit the same achievement. These tests were performed differently and observing the same trends from one test to the other shows that the detection algorithm we used is correct and has been correctly implemented, since the results are reproducible.

The first test showed excellent results, especially for the false alarms rate, but the other test results proved that it was too optimistic. This overestimation is due to the way we computed the results. In fact, the rates were the results of the division of the iterations during which an event occurred (false alarms, detections, non detections) by the total number of iterations of the whole simulation. For example, if a false alarm occurs for n iterations and then disappears in a simulation that runs for m iterations, the false alarm rate is said to be n/m. In a real system, the occurrence of a false alarm generates an appropriate answer from the system (e.g. transferring the control from the master computer to the slave one). In order to better reflect the reality, we changed the way to compute the results. If a false alarm occurs during a simulation, we stop it and mark it as failed. The false alarm rate is then the ratio of the number of failed simulations divided by the total number of simulations. The same way of counting was applied to non detection rate and detection rate. This explains the difference between the first test round results and the other.

The simulation duration was not recorded but the observations made during the tests showed that the length of the simulation was mostly often lower than the time length of the data. There were some cases where the simulation time was greater, sometimes with a ratio up to 3, but these cases were minority. This is why we can assume that the method is compatible with real-time requirement. This is especially true if we consider running this method on a dedicated hardware rather than in an interpreted language environment such as Matlab.

The requirements were met for the non detection rate, the detection delay and the false alarm rate with values of the parameters around five and seven.

6.4 Fault detection relying on the iIKF

The example presented in this section is the same as in the previous chapter. This work has been developped during the thesis of J. Xiong.
We consider that system (5.1) can suffer additive faults on sensors and we adopt the single fault assumption. With the conventional Kalman filter, the principe of fault detection is to detect an abnormal change in the residual vector :

$$r_{k+1} = y_{k+1} - \hat{y}_{k+1|k}, \tag{6.18}$$

where y_{k+1} represents the measured output at time $k+1$. When y_{k+1} is not faulty and without measurement noise, the residual is statistically reduced to zero. When a fault occurs, the residual vector is expected to become non null and at least one of its components indicates the fault.

Like for the conventional Kalman filter, we can define a confidence interval $I^i_{[\hat{y}_{k+1|k}]}$ at 99.7% for each component $[\hat{y}^i_{k+1|k}]$, $i = 1, ..., m$, of $[\hat{y}_{k+1|k}]$ used for fault detection thresholding:

$$\left[\underline{\left([\hat{y}_{k+1|k}]^i - 3 * [\sigma_{k+1}]^i\right)}, \overline{\left([\hat{y}_{k+1|k}]^i + 3 * [\sigma_{k+1}]^i\right)}\right], \tag{6.19}$$

where $[\sigma_{k+1}]^i$ represents the standard deviation of $[\hat{y}_{k+1|k}]^i$. The confidence interval $I^i_{[\hat{y}_{k+1|k}]}$ is guaranteed in the sense that it includes all the confidence intervals of the candidate values belonging to the interval output estimate. In this respect, it is quite conservative.

Fault detection is achieved, at time $k+1$, by checking for consistency the confidence interval (at 99,7%) $I^i_{y_{k+1}}$ of y^i_{k+1} against the confidence interval $I^i_{[\hat{y}_{k+1|k}]}$ of $[\hat{y}_{k+1|k}]$, for $i = 1, \ldots, m$ [1]. Thus, we consider a binary variable τ_k indexed by the time instant which infers:

$$\tau_k = \begin{cases} 1 \text{ if } \exists i \text{ s.t., } I^i_{y_{k+1}} \cap I^i_{[\hat{y}_{k+1|k}]} = \emptyset \\ 0 \text{ otherwise.} \end{cases} \tag{6.20}$$

When a fault occurs, it corrupts the output measures, which is reinjected in the iIKF at the correction step. Hence, the output estimate is not reliable for representing the healthy system. Thus as soon as the fault is detected, the innovation step in the interval Kalman filter is halted until the system is restored healthy. A similar approach can be found in [7, 122], known as the *Semi-Closed Loop* (SCL) strategy.

Example 6.4.1 *To test the efficiency of the proposed iIKF based fault detection approach, a sensor fault affecting the system is introduced at time $k = 50$. This fault is persistent until time $k = 80$. The fault value is set to approximatively 4 standard deviations. We use confidence intervals at $99,7\%$.*

Figure 6.22 provides the output prediction and the real measured output together with the fault indicator τ_k. τ_k rightly concludes to the occurrence of a fault at time $k = 50$ and this fault is persistant until $k = 80$.

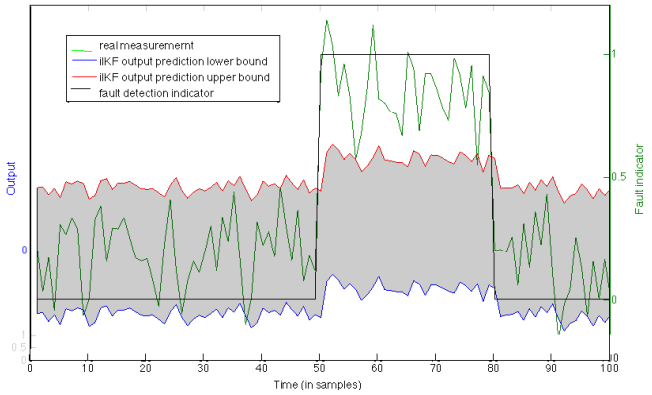

Figure 6.22: Fault detection using the iIKF and the SCL strategy

Figure 6.23 clearly shows that the iIKF output estimate produced without the SCL strategy "follows" the faulty measured output, preventing efficient fault detection. This is due to the correction in the innovation step of iIKF. The a posteriori state estimate is indeed compensated according to the measurement, independently on whether it is faulty or not.

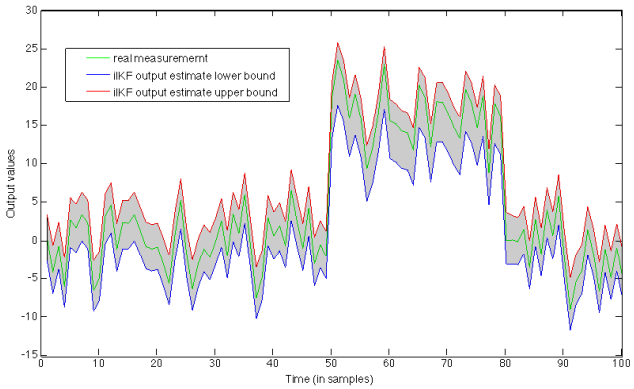

Figure 6.23: iIKF output estimate in the faulty situation without the SCL strategy

We should point out that in our scenario, no calibration takes place. But in more complex systems, it is likely to have singular interval matrices triggering the calibration.

The improved interval Kalman filter iIKF provides all the optimal estimates consistent with bounded-errors and achieves good control of the pessimism inherent to interval analysis. Through a set of simulations, the efficiency of the iIKF based Semi-Closed Loop fault detection algorithm that we propose is clearly demonstrated.

6.5 Conclusion

The first section of this chapter dealt with fault detection relying on SM-identifiability closely related to SM-diagnosability. SM-identifiability provides the guaranty that two situations corresponding to different parameterized settings are distinguishable which has potential in diagnosis. By building the parameter estimation scheme on the analysis of identifiability, we guarantee that the solution set reduces to one connected set, avoiding this way the pessimism of SM methods.

The second section dealt with fault detection by fault model identification. The tests showed good results for confirming a fault and this method is very efficient to prove the non-existence of the solution, that is to discard specific kinds of failures in the real system.

The third section concerned a fault detection scheme based on state estimation. The developped algorithm consists in a prediction-correction two steps approach in which the prediction step uses the mean value and intermediate value theorems. The correction step takes into account the parameter ζ; a wise choice of ζ combined with a wise choice of parameter η leads to good results in terms of false alarm rate, no detection rate and detection delay as seen on the benchmark.

To finish this chapter, a fault detection algorithm based on the iIKF has been developped. This algorithm has been applied to a system with additive faults on sensors; the obtained results showed the efficiency of this approach.

Thus, troughout this chapter, the potential of the concepts developped in this manuscript for fault detection and diagnosis are highlighted. These concepts can be applied to a large class of models with bounded-errors or mixed errors.

Chapter 7

Perspectives and research project

My perspectives in the short term focus on managing mixed uncertainties affecting dynamic systems and on the different paradigms presented in the fifth chapter. The first direction concerns the theoretical aspects and proofs related to the modeling with mixed uncertainties which is part of the thesis of Tuan Anh Tran (October 2014 to September 2017). An application of this work will be diagnosing such models.
Another perspective concerns the reduction of the complexity of the algorithms developped in the third chapter. In fact, it is known that the numerical complexity of the approaches proposed in the third chapter severely limits the applicability of these approaches. Thus a big effort must be devoted to this issue.
The last direction consists in extending to hybrid systems the main concepts developped in this manuscript such as SM-identifiability, SM-diagnosability, optimal input design and the case of mixed uncertainties. These directions are developped below.

7.1 Mixed uncertainties

As seen in previous chapters, models including the representation of bounded uncertainties are an interesting alternative to the stochastic approach. Indeed, the probability distributions of noises and disturbances of a dynamic system may be difficult to identify and some types of uncertainties are better represented by bounded errors. Many methods have been developed within a bounded-error framework. In the last decade, set-membership methods have significantly improved from a fundamental point of view, particularly regarding the integration of differential models (Taylor serie expansion, Müller Theorems), [59] and reachability computations [105]. They have been used for many problems like stability analysis, synthesis of control laws, validation, dependability, estimation, diag-

nosis, etc. These methods have been proposed as substitutes for stochastic approaches as all uncertainties (noise, disturbances, model errors, etc.) are assumed to be bounded. However, some types of uncertainties are well fitted to a statistical context. Furthermore, the advantages of both approaches show that they are complementary rather than opposite. Regarding the estimation in a set-membership framework, the advantage is that the results are guaranteed. However, they do not provide any detail related to the probability density values inside the sets and can lead to very conservative results when they are applied to real systems. For all these reasons, we have proposed to include the two types of uncertainties in the modeling of real systems. Considering uncertain stochastic systems, we have described an improvement of the interval Kalman Filtering [136] and in [44] an optimal input design procedure is proposed for such systems.
This line of research devoted to mixed uncertainties has been little explored in previous works and requires theoretical developments to define a unified formalism which should allow to deal with uncertain random variables and uncertain distribution laws. This is the first line for future works. I would like to properly develop the theoretical tools in order to combine these two types of uncertainties. This work will lead to a thorough investigation to propose a theoretical framework for the definition and manipulation of uncertain probability distributions. This unified framework should allow to provide relevant models for the estimation of dynamical systems and diagnosis applications.

To tackle this problem, I could take inspiration from some works, such as those on interval probabilities or p-boxes [14], [125], those on belief networks [25], or also from [111] where an uncertain expectation operator is proposed. This framework should allow to tackle correctly the problem of state or parameter estimation in the context of mixed uncertainties present in nonlinear uncertain stochastic systems. State and parameter estimation are two of the possible approaches to address fault detection and diagnosis, either in a stochastic framework (for example [35]) or in a set-membership framework [102].

In the thesis of Tuan Anh Tran, the following problems are investigated:

- Definition of a unified theoretical framework for modeling stochastic and bounded uncertainties,
- Design of filtering algorithms with mixed uncertainties (including generalization of the Kalman filter and the particle filter) for nonlinear dynamical models,
- Study of the properties of these filters (stability, convergence),
- Application to fault detection and isolation.

A comparative study between stochastic filters (Kalman filter, particle filter) and set-membership filter based on interval analysis in terms of convergence of state estimation,

quality of outer approximation (e.g. containing the real state) and computational complexity has been proposed in collaboration with Tuan Anh Tran, Françoise Le Gall and Louise Travé-Massuyès [121].

7.2 Analysis of algorithms

This line of research concerns the reduction of the complexity of the algorithms developped in the SM-identifiability framework. These algorithms are based on the elimination of non-measured states (in Differential Algebra) and it is known that the complexity of the involved algebraic manipulations often makes formal calculus too expensive, especially when the functions are not polynomial. They are also based on bisections. A severe restriction of the use of these algorithms is thus their computational complexity which is exponential. For example, concerning SIVIA, it is well-known that the need for an efficient implementation of this algorithm is driven by its high computational complexity due to its branch-and-bound nature, which in the worst case is exponential in the number of variables [51]. However, in [41], interval constraint propagation is used within the SIVIA algorithm to reduce its computational complexity by reducing the number of boxes to be bisected [49] and potentially reduces its computation time. Thus this work, based on a novel vector implementation, represents a first tentative to reduce the computational time of SIVIA.
Concerning the Differential Algebra approach, giving the complexity of the Rosenfeld-Gröebner algorithm is an open problem. In spite of this point, a first natural step towards estimating the complexity is obtaining a bound on the orders of derivatives in the polynomials computed by the Rosenfeld-Gröbner algorithm. In the particular cases of linear systems and systems with two differential polynomials in two differential indeterminates, relevant bounds are proposed in [113], [21]. More recently in [37], a bound holding for a set of ordinary differential polynomials F in n differential indeterminates is proposed and is given by $M(F) \leq (n-1)! \times M(F_0)$ where $M(F)$ is the sum of maximal orders of differential indeterminates occurring in F and F_0 is the initial set of generators of the radical ideal. Since regular ideals can be decomposed into characterizable components algebraically, the bound also holds for the orders of derivatives occurring in a characteristic decomposition of a radical differential ideal [38].
Based on these works, I propose to analyse and to reduce the complexity of the whole framework of SM-identifiability algorithms by:

- Evaluating the complexity of the algorithms used in the SM-identifiability framework, and if not possible, to give an upper bound of the complexity,
- Using [41] to reduce the computational complexity of bisection algorithms,

- Using the recent advances in Differential Algebra approach. Some algebraic algorithms have been proposed by O. Golubitsky [38] and it will be interesting to include these new algorithms in our approach. Maybe, it will be necessary to relax the whole problem of SM-identifiability analysis. Another idea is to exhibit some theorems linking SM-identifiability of linearized uncertain models (around an equilibrium point) and SM-identifiability of nonlinear dynamical uncertain models as it exists in the classical sense.

- Describing precisely the class of models for which this new work holds.

To finish this line of research, I plan to implement the tools to test SM-identifiability in a software presently developped in the DISCO Team of LAAS-CNRS that achieves estimation (state and/or parameter), prediction, simulation and reachability analysis for SM-dynamical continuous or hybrid models. This software results from the integration of the software Prognospice developped in the CORAC-EPICE project [124], the software developped within the MAGIC-SPS project ([78, 80]) and the software PSADE developped within the MICPAC project.

7.3 Extension to hybrid systems

Another perspective is to extend the concepts of SM-identifiability and optimal input design to hybrid systems with bounded errors (SM-hybrid models) without discrete control. A potential application of this extension is fault detection and diagnosis for such models by state or parameter estimation.
Hybrid systems include both discrete and continuous dynamics. The state of a hybrid system is defined by the values of the continuous variables and a discrete mode.

The state estimation of a hybrid system is generally divided into two parts: the estimation of the current mode and knowing the mode, the estimation of continuous state [5], [53]. Many contributions are only interested in the second part, for example [34]. From 2011 to 2015, the MAGIC-SPS project addressed the problem of health-monitoring for uncertain hybrid systems which are hybrid systems with bounded uncertainties. In this project, detection and fault localization for uncertain hybrid models are based on an estimate of the state including a set-estimation of the continuous component. It has been shown that it is possible to estimate the discrete configurations of a hybrid automaton through set-membership methods: [8, 81, 79, 78, 80]. In the recent thesis of M. Maïga [77], an effective method is proposed to cross the set-membership guard (SM-guard). This method consists in carrying out bisection in the time direction only and then several contractors are applied simultaneously to reduce the domain of state vectors located on the guard during the studied time slot. After this, a method for merging trajectories based on

zonotopic enclosures is proposed. To extend my works to SM-hybrid models, I propose the following ideas:

- my first idea is to design input (for the continuous part of the SM-hybrid model) allowing to cross a specific SM-guard and thus to put the model in a specific mode.
- Another idea relying on optimal input design is to obtain the input that produces data from which model parameters can be estimated accurately.
- Concerning SM-estimation, it is well-known that the set-membership guaranteed integration schemes are computationally stable only for some very small sizes of parameter boxes. The SIVIA algorithm like parameter estimation algorithms is hence particularly inefficient as it enumerates candidate parameter subspaces starting with the whole parameter space. This is why [124] proposes the Focused Recursive Partitioning (FRP) which consists in partitionning the parameter search space into small boxes and applying the SM-integration scheme on each candidate box. We then keep track of the parameters vectors for which the model outputs are consistent with the measurements for all sample times i.e. the unfeasible ones are discarded. Computing the convex hull then provides a minimal and maximal value for the admissible parameter vectors. Thus I think that the parameter SM-estimation scheme could be enhanced in the following way:
  - Analyse SM-identifiability of the parameter space and assume that the initial parameter search box is globally SM-identifiable which means that the solution set is a unique connected set,
  - Partition the initial parameter search space,
  - Choose randomly a box into the partition and launch the SM-integration scheme. Test the consistency of the model output with the measurements. Thus three cases are possible: the box is admissible, the box is uncertain or the box must be rejected. If the box is admissible, because the parameter search space is globally SM-identifiable, we know that it is enough to test the neighboring boxes. If the box is uncertain we can bisect it and test it again. If the box is rejected, we can randomly test another box.
- Another problem concerns crossing a guard when the guard is based on an uncertain parameter value. Then, in the set-membership framework, it is known that if the guard condition between two modes is based on a parameter value. For example if the guard condition is given by "the state $x(.)$ is such that $x(.) \geq p$", where p is a parameter, thus part of the futur state, after crossing the guard, can be in a specific

mode and the other part in another mode. If the value of p is unknown, testing SM-identifiability of p seems to be the first step. If p is globally SM-identifiable and not μ-SM-identifiable, there exist some situations in the set of all admissible values of p for which the futur mode will be the same. Thus using an FRP of the initial parameter search space for the guard condition to exhibit the box of parameters consistent with the measurements should allow to limit the parameter values of the guard. To my knowledge, this problem has never been studied.

To finish my research project proposal, my perspective on the long term is to consider uncertain stochastic hybrid systems. To achieve this perspective, the first aim will be to describe a theoretical framework based on the framework developped in the first line of perspectives. After this, it will be interesting to develop methods and algorithms to identify these models. Thus, based on the previously described results and the previous lines of perspectives, the development of uncertain stochastic hybrid systems will be an interesting extension with a lot of potential applications in engineering.

Bibliography

[1] O Adrot, H Janati-Idrissi, and D Maquin. Fault detection based on interval analysis. In *Proceedings of the 15th Triennial World Congress*, Barcelona, Spain, 2002.

[2] T. Alamo, J. Bravo, and E. Camacho. Guaranteed state estimation by zonotopes. *Automatica*, 41(6):1035–1043, 2005.

[3] R.C. Aster, B. Borchers, and C.H. Thurber. *Parameter estimation and inverse problems*. Academic Press, 2005.

[4] S. Audoly, G. Bellu, L. D'Angio, M. P. Saccomani, and C. Cobelli. Global identifiability of nonlinear models of biological systems. *IEEE Transactions on Biomedical Engineering*, 48:55–65, 2001.

[5] M. Babaali. *Switched linear systems : observability and observers*. PhD, School of Electrical and Computer Engineering, Georgia Institute of Technology, 2004.

[6] G. Belforte and P. Gay. Optimal worst case estimation for LPV-FIR models with bounded errors. In *Proceedings of the 39th IEEE Conference on Decision and Control (CDC)*, volume 5, pages 4573–4577, Sydney, NSW Australia, 2000.

[7] E. Benazera and L Travé-Massuyès. A diagnosis driven self-reconfigurable filter. *18th International Workshop on Principles of Diagnosis (DX-07)*, pages 21–28, 2007.

[8] E. Benazera and L. Travé-Massuyès. Set-theoretic estimation of hybrid configurations. *IEEE Transactions on Systems, Man and Cybernetics. Part B*, 39(5):1277–1291, 2009.

[9] M. Berz and K. Makino. Verified integration of odes and flows using differential algebraic methods on high-order Taylor models. *Reliable Computing*, 4:361 – 369, 1998.

[10] J. Blesa, F. Le Gall, C. Jauberthie, and L. Travé-Massuyès. State estimation and fault detection using box particle filtering with stochastic measurements. In *Proceedings of the 26th International Workshop on Principles of Diagnosis (DX)*, pages 67–73, Paris, France, 2015.

[11] F. Boulier, D. Lazard, F. Ollivier, and M. Petitot. Computing representation for radicals of finitely generated differential ideals. *Technical report, IT-306, Université Lille I, LIFL, 59655, Villeneuve d'Ascq*, 1997.

[12] N. Bourbaki. *Elements of Mathematics*. Springer-Verlag, 1989.

[13] I. Braems, L. Jaulin, M. Kieffer, and E. Walter. Guaranteed numerical alternatives to structural identiability testing. In *Proceedings of the 40th IEEE Conference on Decision and Control*, pages 3122–3127, Orlando, USA, 2001.

[14] L.M. De Campos, J.F. Huete, and S. Moral. Probability intervals: a tool for uncertain reasoning. *International Journal of Uncertainty, Fuzziness and Knowledge-Based Systems*, 2(2):167–198, 1994.

[15] G. Chabert and L. Jaulin. Contractor programming. *Artifical Intelligence*, 173:1079–1100, 2009.

[16] G. Chabert, L. Jaulin, and X. Lorca. A Constraint on the Number of Distinct Vectors with Application to Localization. In *Proceedings of the 15th International Conference of Principles and Practice of Constraint Programming*, volume 5732, pages 196–210, Lisbon, Portugal, 2009.

[17] M.J. Chapman, K.R. Godfrey, M.J. Chappell, and N.D. Evans. Structural identifiability of nonlinear systems using linear/nonlinear splitting. *International Journal of Control*, 76:209–216, 2003.

[18] M.J. Chappell and K.R. Godfrey. Structural identifiability of the parameters of a nonlinear batch reactor model. *Mathematical Biosciences*, 108:245–251, 1992.

[19] G. Chen, J. Wang, and S.L. Shieh. Interval Kalman filtering. *IEEE Transactions on Aerospace and Electronic Systems*, 33(1):250–259, Jan 1997.

[20] R.T.N. Chen. Input design for aircraft parameter identification: using time optimal control formulation. *AGARD-CP-172*, Paper 13, 1975.

[21] R. Cohn. *The Greenspan bound for the order of differential systems*. 79(4) American Mathematical Society, Providence, RI, 1980.

[22] C. Combastel. Merging Kalman filtering and zonotopic state bounding for robust fault detection under noisy environment. In *Proceedings of the 9th IFAC Symposium on Fault Detection, Supervision and Safety of Technical Processes (SAFEPROCESS)*. Paris, France, sep 2015.

[23] M.O. Cordier, L. Travé-Massuyès, and X. Pucel. Comparing diagnosability in continuous and discrete-event systems. In *Proceedings of the 17th International Workshop on Principles of Diagnosis (DX)*, pages 55–60, 2006.

[24] P. Coton, A. Bucharles, C. Jauberthie, T. Le Moing, and L. et Planckaert. Caire - identification des dérivées de stabilité dynamique. Technical report, ph.2. Rapport technique 1/05650, ONERA, 2001.

[25] F. G. Cozman. Credal networks. *Artificial Intelligence*, 120:199–233, 2000.

[26] JC. Cruz-Victoria, R. Martinez-Guerra, and JJ. Rincon-Pasaye. On linear systems diagnosis using differential and algebraic methods. *Journal of the Franklin Institute*, 345:102–118, 2008.

[27] M. Dao. *Caractérisation d'ensembles par des méthodes intervalles. Applications en automatique*. PhD thesis, Université d'Angers, December 2006.

[28] L. Denis-Vidal and G. Joly-Blanchard. Identifiability of some nonlinear kinetics. In *Proceedings of the 3rd Workshop on Modelling of Chemical Reaction Systems*, Heidelberg, Germany, 1996.

[29] L. Denis-Vidal, G. Joly-Blanchard, and C. Noiret. Some effective approaches to check identifiability of uncontrolled nonlinear systems. *Mathematics and Computers in Simulation*, 57:35–44, 2001.

[30] L. Denis-Vidal, G. Joly-Blanchard, C. Noiret, and M. Petitot. An algorithm to test identifiability of nonlinear systems. In *Proceedings of the 5th IFAC Symposium on Nonlinear Control Systems*, volume 7, pages 174–178, St Petersburg, Russia, 2001.

[31] S. Diop and M. Fliess. Nonlinear observability, identifiability, and persistent trajectories. In *Proceedings of the 30th Conference on Decision and Control*, pages 714–719, Brighton, UK, 1991.

[32] J.J. DiStefano III. Complete parameter bounds and quasi-identifiability conditions for a class of unidentifiable linear systems. *Mathematical Biosciences*, 65:51–68, 1983.

[33] C. Durieu and E. Walter. Estimation ellipsoidale à erreur bornée. In *Identification des systèmes*, Paris: Hermès, 2001.

[34] G. Ferrari-Trecate, D. Mignone, and M. Morar. Moving horizon estimation of hybrid systems. *IEEE Transactions on Automatic Control*, 47(10):1663–1676, 2002.

[35] P.M. Frank. *Fault diagnosis in dynamic systems via state estimation-a survey*, pages 35 – 98. Springer Netherlands, 1987.

[36] J. Gertler. Fault detection and isolation using parity relations. *Control Engineering Practice*, 5(5):653–661, May 1997.

[37] O. Golubitsky, M. Kondratieva, M. Moreno Maza, and A. Ovchinnikov. A bound for the Rosenfeld–Gröbner algorithm. *Journal of Symbolic Computation*, 43(8):582 – 610, 2008.

[38] O. Golubitsky, M. Kondratieva, M. Moreno Maza, and A. Ovchinnikov. *Bounds and algebraic algorithms in differential algebra: the ordinary case*. In: Decker, W., Dewar, M., Kaltofen, E., Watt, S. M. (Eds.), Challenges in Symbolic Computation Software. No. 06271 in Dagstuhl Seminar Proceedings. Internationales Begegnungs und Forschungszentrum für Informatik (IBFI), Schloss Dagstuhl, Germany, 2007.

[39] P. Goupil. Oscillatory failure case detection in A380 electrical flight control system by analytical redundancy. In *Proceedings of the 17th IFAC Symposium on Automatic Control in Aerospace (ACA)*, pages 681–686, Toulouse, France, 2007.

[40] P. Guerra, V. Puig, and A. Ingimundarson. Robust fault detection with state estimators and interval models using zonotopes. In *Proceedings of the 17th International Workshop on Principles of Diagnosis (DX)*, pages 109–116, Penaranda de Duero, Spain, 2006.

[41] P. Herrero, P. Georgiou, C. Toumazou, B. Delaunay, and L. Jaulin. An Efficient Implementation of SIVIA Algorithm in a High-Level Numerical Programming Language. *Reliable computing*, pages 239–251, 2012.

[42] A. Ingimundarson, J.M. Bravo, V. Puig, T. Alamo, and P. Guerra. Robust fault detection using zonotope-based set-membership consistency test. *International Journal of Adaptive Control And Signal Processing*, 23(4):311–330, 2009.

[43] Institute for Reliable Computing. INTLAB – INTerval LABoratory. `http://www.ti3.tuhh.de/rump/intlab/index.html`. Technische Universität Hamburg-Harburg.

[44] C. Jauberthie and E. Chanthery. Optimal input design for a nonlinear dynamical uncertain aerospace system. In *Proceedings of the 9th IFAC Symposium on Nonlinear Control Systems (NOLCOS)*, pages 469–474, Toulouse, France, 2013.

[45] C. Jauberthie, R. Pons, L. Travé-Massuyès, and P. Goupil. Detection of oscillatory failures by state estimation in a bounded-error context. Technical Report 09133, Toulouse, France, March 2009.

[46] C. Jauberthie, N. Verdière, and L. Travé-Massuyès. Set-membership identifiability: definitions and analysis. In *Proceedings of the 18th IFAC World Congress*, pages 12024–12029, Milan, Italie, 2011.

[47] C. Jauberthie, N. Verdière, and L. Travé-Massuyès. Fault detection and identification relying on set-membership identifiability. *Annual Reviews in Control*, 37, No. 1:129–136, 2013.

[48] L. Jaulin, M. Kieffer, I. Braems, and E. Walter. Guaranteed nonlinear estimation using constraint propagation on sets. *International Journal of Control*, 74(18):1772–1782, 2001.

[49] L. Jaulin, M. Kieffer, I. Braems, and E. Walter. Guaranteed nonlinear estimation using constraint propagation on sets. *International Journal of Control*, 74(18):1772–1782, 2001.

[50] L. Jaulin, M. Kieffer, O. Didrit, and E. Walter. *Applied Interval Analysis, with examples in parameter and state estimation, Robust control and robotics*. Springer, Londres, 2001.

[51] L. Jaulin and E. Walter. Set inversion via interval analysis for nonlinear bounded-error estimation. *Automatica*, 29(4):1053–1064, 1993.

[52] G. Joly-Blanchard and L. Denis-Vidal. Some remarks about identifiability of controlled and uncontrolled nonlinear systems. *Automatica*, 34:1151–1152, 1998.

[53] R. Kajdan, D. Aubry, and F. Kratz. Gauss-newton observers for mode and state estimation of nonlinear switched systems. In *Proceedings of the 46th IEEE Conference on Decision and Control (CDC)*, pages 3214–3220, New-Orleans, USA, 2007.

[54] R.E. Kalman. A new approach to linear filtering and prediction problems. *Transactions of the ASME–Journal of Basic Engineering*, 82(D):35–45, Jan 1960.

[55] R.B. Kearfott and V. Kreinovich. *Applications of interval computations*. Springer, 1996.

[56] M. Kieffer and E. Walter. Guaranteed estimation of the parameters of nonlinear continuous-time models: Contributions of interval analysis. *International Journal of Adaptive Control and Signal Processing*, 25(3):191–207, 2011.

[57] Michel Kieffer, Luc Jaulin, Éric Walter, and Dominique Meizel. Robust autonomous robot localization using interval analysis. *Reliable Computing*, 6(3):337–362, 2000.

[58] A. Kirsch. *An introduction to the Mathematical Theory of Inverse Problems, second edition*. Springer, New York, 2011.

[59] M. Kletting, M. Kieffer, and E. Walter. *Two approaches for guaranteed state estimation of nonlinear continuous-time models*, pages 199–220. In A. Rauh et E. Auer, Springer- Verlag, 2011.

[60] E.R. Kolchin. *Differential algebra and algebraic groups*. Academic Press, New York, 1973.

[61] V. Kreinovich, L. Longpre, S. Starks, G. Xiang, J. Beck, R. Kandathi, A. Nayak, S. Ferson, and J. Hajacos. Interval versions of statistical techniques with applications to environmental analysis, bioinformatics, and privacy in statistical databases. *Journal of Computational and Applied Mathematics*, 199(2):418–423, February 2007.

[62] V. Kreinovich and H.T. Nguyen. Interval-Valued Fuzzy Control in Space Exploration. *Bulletin for Studies and Exchanges on Fuzziness and its Applications*, (71):55–64, July 2011.

[63] S. Lagrange, N. Delanoue, and L. Jaulin. On sufficient conditions of injectivity, development of a numerical test via interval analysis. *Journal Reliable computing*, 13:409–421, 2007.

[64] S. Lagrange, N. Delanoue, and L. Jaulin. Injectivity analysis using interval analysis : Application to structural identifiability. *Automatica*, 44(11):2959–2962, 2008.

[65] S. Lesecq, A. Barraud, and K. Tran Dinh. Numerical accurate computations for ellipsoidal state bounding. In *Proceedings of the 1th IEEE Mediterranean Conference on Control and Automation (MED'03)*, Rhodes, Greece, 2003.

[66] A. Levant. Robust exact differentiation via sliding mode technique. *Automatica*, 34:379–384, 1998.

[67] A. Levant. Higher order sliding modes and arbitrary order exact robust differentiation. In *Proceedings of European Control Conference (ECC)*, pages 996–1001, Porto, Portugal, 2001.

[68] A. Levant. Higher-order sliding modes, differentiation and output-feedback control. *International Journal of Control*, 76:924–941, 2003.

[69] O. Lhomme. Consistency techniques for numeric CSPs. In *Proceedings of International Joint Conference on Artificial Intelligence*, pages 232–238, 1993.

[70] O. Lhomme, R. La Chantrerie, A. Gotlieb, and M. Rueher. Boosting the interval narrowing algorithm. In *Proceedings of the 1996 Joint International Conference and Symposium on Logic Programming*, pages 378–392, Bonn, Germany, 1996. The MIT Press.

[71] B. Li, C. Li, J. Si, and G.P. Abousleman. Interval least-squares filtering with applications to robust video target tracking. In *Proceedings of IEEE International Conference on the Acoustics, Speech and Signal Processing*, pages 3397–3400, 2008.

[72] Q. Li, C. Jauberthie, L. Denis-vidal, and Z. Cherfi. Guaranteed state and parameter estimation for nonlinear dynamical aerospace models. In *Proceedings of the 11th International Conference in Informatics in Control, Automation and Robotics (ICINCO)*, pages 519 – 527, Vienna, Austria, 2014.

[73] Q. Li, C. Jauberthie, L. Denis-vidal, and Z. Cherfi. Optimal initial state for fast parameter estimation in nonlinear dynamical systems. In *Proceedings of the 9th IFAC Symposium on Biological and Medical Systems (BMS)*, pages 556 – 562. Berlin, Germany, 2015.

[74] L. Ljung and T. Glad. On global identifiability for arbitrary model parametrizations. *Automatica*, 30:265–276, 1994.

[75] R.J. Lohner. Enclosing the solutions of ordinary initial and boundary value problems. In E.W. Kaucher, U.W. Kulisch, and C. Ullrich, editors, *Computer Arithmetic: Scientific Computation and Programming Languages*, pages 255 – 286, Stuttgart, 1987. Wiley-Teubner.

[76] S.T. Glad M. Fliess. An algebraic approach to linear and nonlinear control. In *Essays on Control: Perspectives in the Theory and its Application*, volume 14, pages 223–267, Cambridge, MA, Birkhaüser, 1993.

[77] M. Maïga. *Surveillance préventive des systèmes hybrides à incertitudes bornées*. PhD thesis, Université d'Orléans, 2015.

[78] M. Maïga, C. Combastel, N. Ramdani, and L. Travé-Massuyès. Nonlinear hybrid reachability using set integration and zonotope enclosures. In *Proceedings of the 17th IFAC European Control Conference (ECC)*, pages 234–239, Strasbourg, France, 2014.

[79] M. Maïga, N. Ramdani, and L. Travé-Massuyès. A fast method for solving guard set intersection in nonlinear hybrid reachability. In *Proceedings of the 52nd IEEE Conference on Decision and Control (CDC)*, pages 508–513, Firenze, Italy, 2013.

[80] M. Maïga, N. Ramdani, and L. Travé-Massuyès. Robust fault detection in hybrid systems using set-membership parameter estimation. In *Proceedings of the 9th IFAC Symposium on Fault Detection, Supervision and Safety of Technical Processes (SafeProcess)*, pages 296–301, Paris, France, 2015.

[81] M. Maïga, N. Ramdani, L. Travé-Massuyès, and C. Combastel. A comprehensive method for reachability analysis of uncertain nonlinear hybrid systems. *IEEE Transactions on Automatic Control*, PP(99):1–6, 2015.

[82] C. Masreliez and R. Martin. Robust bayesian estimation for the linear model and robustifying the Kalman filter. *IEEE Transactions on Automatic Control*, 22(3):361–371, 1977.

[83] R.K. Mehra and D.G. Lainiotis. *Synthesis of optimal inputs for Multiinput-Multioutput (MIMO) systems*. Academic press, 1976.

[84] G. Melquiond. Proving Bounds on Real-Valued Functions with Computations. *Journal of Automated Reasoning*, 5195:2–17, 2008.

[85] M. Milanese and C. Novara. Nonlinear Set Membership prediction of river flow. *Systems & Control Letters*, 53(1):31–39, September 2004.

[86] R.E. Moore. *Interval Analysis*. Prentice Hall, New Jersey, 1966.

[87] R.E. Moore and F. Bierbaum. *Methods and Applications of Interval Analysis*. SIAM Studies in Applied Mathematics 2, 1979.

[88] E.A. Morelli. Flight test of optimal inputs and comparison with conventional inputs. *Journal of aircraft*, 36:389 – 397, 1999.

[89] J. R. Munkres. *Topology a first course*. Prentice Hall, New Jersey, 1975.

[90] N.S. Nedialkov. VNODE-LP a validated solver for initial value problems in ordinary differential equations. Technical Report Tech. Report CAS-06-06-NN, Dept. of Computing and Software, McMaster University, Canada, 2006.

[91] N.S. Nedialkov. An interval solver for initial value problems in ordinary differential equations. *http://www.cas.mcmaster.ca/ nedialk/vnodelp*, 2010.

[92] N.S. Nedialkov, K.R. Jackson, and J.D. Pryce. An effective high-order interval method for validating existence and uniqueness of the solution of an IVP for an ODE. *Reliable Computing*, 7:449 – 465, 2001.

[93] A Neumaier. Taylor forms - use and limits. *Reliable Computing*, pages 9–43, 2003.

[94] F. Ollivier. *Le problème de l'identifiabilité structurelle globale : approche théorique, méthodes effectives et bornes de complexité*. PhD, Ecole Polytechnique, France, 1990.

[95] H. Pohjanpalo. System identifiability based on the power series expansion of the solution. *Mathematical Biosciences*, 41:21–33, 1978.

[96] P. Poignet and N. Ramdani. Robust Estimation of Parallel Robot with Interval Analysis. In *Proceedings of the 42nd IEEE Conference on Decision and Control (CDC)*, Maui, Hawaii (USA), 2003.

[97] R. Pons, C. Jauberthie, and L. Travé-Massuyès. Set-membership detection of oscillatory failure cases. Technical report, LAAS-CNRS, Report 10516. 47 pages, 2010.

[98] R. Pons, C. Jauberthie, L. Travé-Massuyès, and P. Goupil. Control surfaces oscillatory failures identification using interval analysis. In A. Grastien, W. Mayer, and M. Stumptner, editors, *Proceedings of the 19th International Workshop on Principles of Diagnosis (DX'08)*, pages 323–330, Blue Mountains, Australia, September 2008.

[99] R. Pons, C. Jauberthie, L. Travé-Massuyès, and P. Goupil. Interval analysis based learning for fault model identification. application to control surfaces oscillatory failures. In E. Bradley and L. Travé-Massuyès, editors, *Proceedings of the 22nd International Workshop on Qualitative Reasoning*, pages 115–122, Boulder, CO, USA, June 2008. University of Colorado.

[100] L. Pronzato and E. Walter. Robust experiment design via maximin optimization. *Mathematical Biosciences*, 89(2):161–176, 1988.

[101] T. Raïssi, N. Ramdani, and Y. Candau. Set membership state and parameter estimation for systems described by nonlinear differential equations. *Automatica*, 40:1771–1777, 2004.

[102] S. A. Raka and C. Combastel. Fault detection based on robust adaptive thresholds: a dynamic interval approach. *Annual Reviews in Control Journal*, 37(1):119–128, 2013.

[103] N. Ramdani. Computing reachable sets for uncertain nonlinear hybrid systems using interval constraint propagation techniques. *Nonlinear Analysis: Hybrid Systems*, pages 1–23, June 2010.

[104] N. Ramdani, N. Meslem, and Y. Candau. A hybrid bounding method for computing an over-approximation for the reachable set of uncertain nonlinear systems. *IEEE Transactions on Automatic Control*, 54(10):2352–2364, 2009.

[105] N. Ramdani, N. Meslem, and Y. Candau. Computing reachable sets for uncertain nonlinear monotone systems. *Nonlinear Analysis : Hybrid Systems*, 4(2):263–278, 2010.

[106] N. Ramdani and P Poignet. Robust Dynamic Experimental Identification of Robots With Set Membership Uncertainty. *IEEE/ASME Transactions on Mechatronics*, 10(2):253–256, April 2005.

[107] H. Ratschek. Inclusion functions and global optimization. *Mathematical Programming*, 33(3):300–317, 1985.

[108] A. Rauh, J. Minisini, and E. P. Hofer. Verification Techniques for Sensitivity Analysis and Design of Controllers for Nonlinear Dynamic Systems with Uncertainties. *International Journal of Applied Mathematics and Computer Science*, 19(3):425–439, September 2009.

[109] L. Ravanbod, N. Verdière, and C. Jauberthie. Determination of set-membership identifiability sets. *Mathematics in Computer Science Journal*, 8:391–406, 2014.

[110] P. Ribot, C. Jauberthie, and L. Travé-Massuyès. State estimation by interval analysis for a nonlinear differential aerospace model. In *Proceedings of the IFAC European Control Conference*, pages 4839–4844, Kos, Greece, 2007.

[111] A. Rico and O. Strauss. Imprecise expectations for imprecise linear filtering. *International Journal of Approximate Reasoning*, 51(8):933–947, 2010.

[112] R. Rihm. Interval methods for initial value problems in odes. In *IMACS-GAMM International Workshop on Validated Computations*, Amsterdam, 1994. Elsevier.

[113] J. Ritt. *Differential algebra*. American Mathematical Society, Providence, RI, 1950.

[114] J. Rohn. Inverse interval matrix. *SIAM Journal on Numerical Analysis*, 30(3):864–870, June 1993.

[115] J. Rohn. Positive Definiteness and Stability of Interval Matrices. *SIAM Journal on Matrix Analysis and Applications*, 15(1):175–184, 1994.

[116] C.R. Rojas, J.S. Welsh, G.C. Goodwin, and A. Feuer. Robust optimal experiment design for system identification. *Automatica*, 43(6):993–1008, 2007.

[117] S.M. Rump. INTLAB - INTerval LABoratory. In Tibor Csendes, editor, *Developments in Reliable Computing*, pages 77–104. Kluwer Academic Publishers, Dordrecht, 1999. `http://www.ti3.tu-harburg.de/rump/`.

[118] M.P. Saccomani, S. Audoly, and L. D'Angio. Parameter identifiability of nonlinear systems: the role of initial conditions. *Automatica*, 39:619–632, 2004.

[119] M. Staroswiecki and G. Comtet-Varga. Analytical redundancy relations for fault detection and isolation in algebraic dynamic systems. *Automatica*, 37:687–699, 2001.

[120] Inc. The MathWorks. MATLAB computing software. `http://www.mathworks.com`.

[121] T.A. Tran, F. Le Gall, C. Jauberthie, and L. Travé-Massuyès. Two stochastic filters and their extenxions using interval analysis. In *Proceedings of the 4th IFAC International Conference on Intelligent Control and Automation Sciences*, pages 49–54, Reims, France, 2016.

[122] L. Travé-Massuyeès, T. Escobet, R. Pons, and S. Tornil. The Ca-En diagnosis system and its automatic modelling method. *Computación i Sistemas, Revista Iberoamericana de Computación*, 5(2):128–143, 2001.

[123] L. Travé-Massuyès, T. Escobet, and X. Olive. Diagnosability analysis based on component-supported analytical redundancy relations. *IEEE Transactions on Systems, Man, and Cybernetics, Part A*, 36:1146–1160, 2006.

[124] L. Travé-Massuyès, R. Pons, P. Ribot, Y. Pencolé, and C. Jauberthie. Condition-based monitoring and prognosis in an error-bounded framework. In *Proceedings of the 26th International Workshop on Principles of Diagnosis (DX)*, pages 83–90, Paris, France, September 2015.

[125] L. Utkin and S. Destercke. Computing expectations with continuous p-boxes: Univariate case. *International Journal of Approximate Reasoning*, 50(5):778–798, 2009.

[126] S. Vajda, K.R. Godfrey, and H. Rabitz. Similarity transformation approach to structural identifiability of nonlinear models. *Mathematical Biosciences*, 93:217–248, 1989.

[127] S. Vajda, J.J. DiStefano III, K.R. Godfrey, and J. Fagarasan. Parameter space boundaries for unidentifiable compartmental models. *Mathematical Biosciences*, 97:27–60, 1989.

[128] P.P.J. Van Den Bosch and A.C. Van Der Klauw. *Modeling, Identification and Simulation of Dynamical Systems*. CRC-Press, 1994.

[129] N. Verdière, L. Denis-Vidal, G. Joly-Blanchard, and D. Domurado. Identifiability and estimation of pharmacokinetic parameters of ligands of macrophage mannose receptor. *International Journal of Applied Mathematics and Computer Science*, 15:101–110, 2005.

[130] N. Verdière, C. Jauberthie, and L. Travé-Massuyès. Functional diagnosability and detectability of nonlinear models based on analytical redundancy relations. *Journal of Process Control*, 35:1–10, 2015.

[131] E. Walter. *Identifiability of state space models*. Springer, Berlin, 1994.

[132] E. Walter and Y. Lecourtier. Global approaches to identifiability testing for linear and nonlinear state space models. *Mathematics and Computers in Simulation*, 24:472–482, 1982.

[133] E. Walter and L. Pronzato. *Identification de modèles paramétriques à partir de données expérimentales*. MASSON, 1994.

[134] E. Walter and P. Young. *Nonlinear Identification and Estimation*. 2003.

[135] G. Welch and G. Bishop. An Introduction to the Kalman Filter. Technical Report TR 95-041, University of North Carolina at Chapel Hill, Department of Computer Science, Los Angeles, California USA, 2001.

[136] J. Xiong. *Set-membership state estimation and application on fault detection*. PhD thesis, INP Toulouse, Université de Toulouse. 2013., september.

[137] J. Xiong, C. Jauberthie, and L. Travé-Massuyès. New computation aspects for existing interval Kalman filtering and application. In *Proceedings of the 15th IFAC Workshop on Control Applications of Optimization (CAO)*, 6p, Rimini, Italy, 2012.

[138] J. Xiong, C. Jauberthie, and L. Travé-Massuyès. Improvements in computational aspects of interval Kalman filtering enhanced by constraint propagation. In *Proceedings of the 11th IEEE International Workshop on Electronics, Control, Measurement, Signals and their application to Mechatronics (ECMSM) 2013*, 6p, Toulouse, France, 2013.